IDENTIFYING, MODELING AND TARGETING IGF-II OVEREXPRESSION IN ADRENOCORTICAL CARCINOMA

by

Ferdous M. Barlaskar

A dissertation submitted in partial fulfillment
of the requirements for the degree of
Doctor of Philosophy
(Cellular and Molecular Biology)
in The University of Michigan
2011

Doctoral Committee:

Associate Professor Gary D. Hammer, Chair
Professor Cunming Duan
Professor Ram K. Menon
Assistant Professor Dan A. Bochar
Assistant Professor Patrick J. Hu

TABLE OF CONTENTS

LIST OF FIGURES

ABSTRACT

IDENTIFYING, MODELING AND TARGETING IGF-II OVEREXPRESSION IN ADRENOCORTICAL CARCINOMA

by

Ferdous M. Barlaskar

Chair: Gary D. Hammer

Insulin-like growth factor-II (IGF-II) is a mitogenic growth factor that elicits cellular effects primarily through its downstream signaling pathway. The IGF signaling pathway is a critical cellular system for stimulating growth and preventing apoptosis and is implicated in development and progression of various cancers, including adrenocortical carcinoma (ACC). ACC is a rare endocrine malignancy that carries a poor clinical prognosis, and lacks effective treatment options. Recently, there is emerging data regarding the molecular determinants involved in ACC initiation and/or progression through examination of the gene expression profiles and of the familial ACC syndromes. From these data, one particular molecular alteration linked to ACC is the loss of imprinting (LOI) within the 11p15.5 chromosomal region, which results in overexpression of the gene encoding IGF-II (named *IGF2*).

We hypothesize that *IGF2* upregulation plays a critical role in ACC pathogenesis. We tested our hypothesis first by validating that our ACC samples possessed LOI-mediated *IGF2* upregulation with concomitant active IGF signaling and then identified which regulatory elements in the *IGF2* gene locus affect its expression. Next, we commenced modeling LOI to upregulate *IGF2* expression specifically in the mouse

adrenal cortex. Although, LOI did not result in ACC, we identified *IGF2*-mediated activation of canonical Wnt signaling, another molecular perturbation commonly associated with ACC pathogenesis. The activation of IGF and Wnt signaling pathways simultaneously in the mouse adrenal cortex resulted in a more dramatic dysplastic phenotype compared to both LOI adrenals and constitutive Wnt adrenals. Finally, we tested our hypothesis by targeting the IGF-1R (the receptor through which IGF-II elicits its effects) in H295 cells, a cell line derived from a human ACC and possessing constitutive IGF signaling. Targeting resulted in specific growth inhibition *in vitro* and also *in vivo* using mouse xenografts. We observed targeting IGF signaling inhibition in combination with mitotane, the only FDA approved drug for ACC treatment in patients, resulted in greater growth inhibition *in vitro* and *in vivo* when compared either agent alone. Taken together, this findings support our hypothesis that *IGF2* upregulation plays a critical role in ACC pathogenesis.

CHAPTER 1

INTRODUCTION

THE NORMAL ADRENAL CORTEX AND ADRENOCORTICAL CARCINOMAS

Perhaps the first written description pertaining to the existence of the adrenal gland dates back to the Old Testament in the story of the fraternal twins, Esau and Jacob. In this tale, Esau was described as remarkably large, strong and hairy (all symptoms consistent with congenital adrenal hyperplasia) while Jacob was completely normal (Leoutsakos and Leoutsakos, 2008). During the 2nd century AD, the great Roman physician and philosopher, Claudius Galens, clearly described the attachment of the left renal vein to the left adrenal vein, referring to it as "loose flesh", and as such, discovered the adrenal gland from his animal dissections (Leoutsakos and Leoutsakos, 2008). It wasn't until about 2000 years later in 1849, when Thomas Addison presented a paper on the clinical features of patients with adrenal disease and assigned this historically enigmatic tissue a physiological role (Pearce, 2004). Finally in 1886, Felix Frankel was credited as the first to describe a patient with an adrenal tumor, a pheochromocytoma (Whiting and Doogue, 2009).

Over a century later, the basic understanding of adrenal tumors has grown immensely. My specific interest and research resides in better understanding cancers arising from the adrenal cortex. Adrenocortical carcinoma (ACC) is a rare endocrine malignancy defined by a heterogeneous clinical presentation, dismal prognosis, and lack of effective therapeutic regimens. The incidence of ACC ranges from 0.5 to 2 cases per

million people per year, accounting for 0.02% of all reported cancers (Wajchenberg et al., 2000). Unfortunately, most patients with this cancer present with metastatic disease which reduces the 5 year survival rate to less than 10% (Icard et al., 2001). This introductory chapter aims to summarize normal adrenal anatomy and physiology, address adrenal development and maintenance in the context of tissue specific stem/progenitor cells, cover epidemiological aspects and clinical management of ACC, establish ACC in the framework of the cancer stem cell hypothesis, and finally, describe the genetic and molecular events implicated in the pathogenesis of ACC.

Adrenal Anatomy

The adrenal gland, a component of the hypothalamic-pituitary-adrenal (HPA) axis, is a major hormone-secreting organ. The gland is composed of two functionally distinct organs. The medulla, derived from neural crest cells of neuroectoderm lineage, synthesizes catecholamines that facilitate the acute mammalian stress or "fight-or-flight" response. The cortex, derived from the cells of the intermediate mesoderm, synthesizes steroid hormones that mediate body homeostasis and chronic stress responses. The cortex is organized into three concentric zones, zona glomerulosa (zG), zona fasciculata (zF), and zona reticularis (zR), each responsible for the production of different steroid hormones. In 1866. the first description of the zonal organization of the cortex was described with nomenclature that is still in use today (Arnold, 1866; Evelyn, 1927). The cells of the zG are organized in rounded clusters around capillary coils or "glomeruli" and synthesize mineralocorticoids. The cells of the zF synthesize glucocorticoids and are

arranged in radial rows separated by trabeculae and blood vessels. The cells of the zR are arranged in a uniform reticular net of connective tissue and blood vessels and synthesize a subset of sex steroid precursors, including the neurohormone dehydroepiandosterone (DHEAS). Although histological and functional differences exist between the adrenal cortices of various mammalian species (mainly the absence of zR and the presence of the fetal/X-zone in some rodents), common developmental principles appear to mediate the formation and homeostatic maintenance of the gland (Arnold, 1866; Evelyn, 1927; Keegan and Hammer, 2002).

Adrenal Gland Development and Establishiment of the Definitive (Adult) Cortex

Adrenal gland development in the mammal is defined by discrete histological events (Else and Hammer, 2005; Keegan and Hammer, 2002; Uotila, 1940). The first milestone is marked by the proliferation of the mesoderm-derived coelomic epithelia and underlying mesonephric mesenchymal cells, forming the embryonic adrenogonadal primordia (AGP) that reside between the primitive urogenital ridge and the dorsal mesentery (Hatano et al., 1996; Luo et al., 1994)(reviewed in Else and Hammer (Else and Hammer, 2005) and Kim and Hammer (Kim and Hammer, 2007)). Essential for the formation of the adrenogonadal primordium is expression of the orphan nuclear receptor, Sf1 (Nr5a1, Nuclear Receptor Subfamily 5, Group A, Member 1: or Ad4BP). Although Sf1 expression is critical, a variety of loss-of-function studies indicate that additional transcription factors including pre-B-cell leukemia homeobox 1(Pbx1), odd-skipped related 1 (Odd1, Osr1), and polycomb group protein M33 also participate in specification and/or expansion of the AGP (James et al., 2006; Katoh-Fukui et al., 2005; Schnabel et al., 2003). The bilateral AGP then divide into the adrenal primordia (adrenal blastema,

often referred to as the fetal adrenal or fetal zone) and the gonadal primordia. The molecular specification of the adrenal primordia is initiated through the upregulation of *Sf1* expression by Wilm's tumor 1 (Wt1) and Cbp/p300-interacting transactivator, with Glu/Asp-rich carboxy-terminal domain, 2 (Cited2) (Val et al., 2007). Upon separation of the adrenal primordia from the AGP, a different transcription complex containing the homeobox protein PKNOX1 (Pknox1, Prep1), homeobox gene 9b (Hox9b), and Pbx1 is recruited to maintain fetal zone expression of Sf1 through activation of a fetal zone specific Sf1 enhancer (FAdE). Subsequently, Sf1 itself provides feed forward activation of its own expression in this compartment (Zubair et al., 2006). Coincident with this transcriptional cascade is the coalescence of the mesenchymal capsule around the fetal cortex (Else and Hammer, 2005; Kim and Hammer, 2007). Once encapsulation is complete, the development of the definitive cortex (definitive zone or adult cortex) becomes evident between the capsule and fetal cortex.

Because the cells of the definitive cortex are continually renewed throughout life, a unified model for the formation and maintenance of this structure is paramount. In a previous review, we (the Hammer laboratory) provided two distinct possibilities for the developmental establishment and post-natal maintenance of the definitive cortex (Kim and Hammer, 2007). 1), The definitive cortex arises from the precursors within the mesenchymal capsule (i.e. the capsule contains the adrenal cortical stem cells) (Kim and Hammer, 2007). 2), The fetal cortex contains precursors, which gives rise to the adult cortex (i.e. capsule serves the role of stem cell "niche" (Kim and Hammer, 2007). Recent and emerging data allow for a reconciliation of these two models in the form of an adrenocortical stem/progenitor niche hypothesis.

In the burgeoning field of stem cell biology, the concept of stem cell residence is used to define the complex microenvironment composed of the stem cells and the supporting niche cells. The stem cell niche provides structural and trophic support, topographical information, and physiological cues to resident stem cells that govern stem cell fate (i.e., self-renewal and symmetric or asymmetric division) (Fuchs et al., 2004; Jones and Wagers, 2008; Sneddon and Werb, 2007). Data from organ systems such as the blood, gonad, and hair follicle reveal conserved niche components that include stromal support cells, extracellular matrix (ECM) and vasculature (Fuchs et al., 2004; Jones and Wagers, 2008). Multiple studies have characterized a complex network of capillary beds together with an enrichment of ECM components within the adrenal capsule (Bassett and West, 1997; Chamoux et al., 2001; Magennis and McNicol, 1998; Otis et al., 2007; Tokunaga, 1996; Virtanen et al., 2003) and we suggest that these components provide the needed structural and physiological support to the adrenocortical stem cells. The capsular niche would serve to both recruit stem cells during development and to regulate stem cell fate throughout the life of the organism (Fuchs et al., 2004; Whetton and Graham, 1999). We favor a model whereby the adrenocortical stem cells reside within the capsule itself (ie: the capsule serves as the physical site of adrenocortical stem cell as well as the niche) and give rise to the underlying definitive cortex in response to a variety of capsular/subcapsular morphogenic signals (Wnt, SHH, Notch). Indeed, circumstantial evidence comes from chimeric mouse studies that detail concordant clonality of patches of capsular cells and underlying cortical radial stripes (i.e. chimeric patches in capsule lined up with chimeric radial stripes in the cortex),

suggesting a shared origin (Iannaccone et al., 2003; Kiiveri et al., 2002; Landini and Iannaccone, 2000; Weinberg et al., 1985).

While these data are provocative, there remains no conclusive molecular or genetic evidence confirming whether the capsule serves as a stem/progenitor cell pool and/or as a niche for the subcapsular cells. Therefore, determining the lineage relationship between the fetal cortex (precursor population), capsule and definitive cortex is of paramount importance Recent data demonstrate that the definitive cortex is derived from the fetal adrenal cortex (Zubair et al., 2006; Zubair et al., 2008). The data suggest that the FAdE is first shut off (in fetal cells destined to become definitive cells) followed by the activation of a definitive Sf1 enhancer in the emerging definitive cells (Zubair et al., 2008). However, data emerging from our laboratory suggest that Sf1 expression is actively repressed in a subset of capsular cells by the capsule-specific HLH factor Pod-1 and that genetic loss of Pod-1 results in activation of Sf1 in a subset of capsular cells and an increased number of Sf1-expressing cells in the underlying cortex. Because the definitive cortex only becomes evident between the developing capsule (Sf1 negative) and fetal adrenal cells (Sf1 positive), we propose a model whereby the fetal precursor cells gives rise to Sf1 negative cells that participate in the formation of the capsule (stem cell residence). In such a model, mitogenic/morphogenic signals (endocrine and capsular paracrine/autocrine) activate the Sf1 negative capsular stem cells which exit from the capsular niche into the subcapsular environment, where they commence Sf1 expression. Current data suggest that this process requires the loss of capsular Pod-1 expression in the Sf1 negative cell, subsequent activation of the yet-to-be determined definitive Sf1

enhancer and ultimate expression of Sf1 in subcapsular rapidly amplifying progenitor cells. Data in support of these models are discussed throughout this review.

Anatomic Evidence in Support of Adrenocortical Stem/Progenitor Cells

What is the evidence for the existence of adrenocortical stem/progenitor cells? While the glomerulosa has been classically defined as a homogenous aldosterone-producing zone directly under the capsule, three observations suggest that the glomerulosa is composed of multiple cell types that participate in the homeostatic maintenance of the adrenal cortex. Early microscopic studies of the adrenal glands of different vertebrates suggested the presence of peripheral undifferentiated cells. For example, in the arctic seal (*Phoca vitulina vitulina*), clusters of rounded large cells, referred to as adrenocortical blastema, reside within both the capsule and trabeculae that arise from the capsule as perpendicular cords piercing into the outer cortex (Bragulla et al., 2004). These cells contain conspicuously large euchromatin-rich nuclei and have high ratios of both rough to smooth endoplasmic reticulum and cristae-type to tubulus-type mitochondria, all characteristic features of less-differentiated cells (Bragulla et al., 2004). Because these cells have the histologic appearance of progressive centripetal transition to the juxtaposed glomerulosa cells (Bragulla et al., 2004), it has been hypothesized that the blastema define a population of undifferentiated cells that undergo both proliferation and differentiation in response to homeostatic stimuli. Recent observational studies in the grass snake (*Natrix natrix L.*) suggest a similar peripheral pool of undifferentiated "transitional" cells that have the potential to differentiate into

steroidogenic adrenocortical cells (Rupik, 2002). The glomerulosa of other species exhibit variable thicknesses and tortuosity with a wide range of embedded, undifferentiated clusters that at times coalesce into circumferential zones of undifferentiated cells. The restricted circumferential expression of Pre-adipocyte factor 1 or Pref-1 (a factor that serves to inhibit differentiation in a variety of tissues) in the glomerulosa of the rat supports such a hypothesis that the glomerulosa layer is composed of cells of varying degrees of differentiation (i.e. progenitor cells). Specifically, an outer layer expresses both Pref-1 and aldosterone synthase; a middle inner layer expresses only Pref-1 and an inner layer above the fasciculata zone expresses no Pref-1, aldosterone synthase, or 11beta-hydroxylase (Halder et al., 1998). In the rat, the two inner aldosterone synthase negative zones of the glomerulosa are referred to as the zona undifferentiated (zU) or zona intermedia (zI) (Vinson et al., 1992). In the mouse adrenal, where a defined undifferentiated zone is not observable, such cells might be scattered between differentiated glomerulosa cells. The paucity of expression of certain steroidogenic enzyme genes (Cyp11b1 and Cyp11b2) in these cells has fueled the hypothesis that these cells undergo a morphological transition into differentiated steroidogenic cells of the zG (Mitani et al., 1999, 2003; Mitani et al., 1994).

Indeed, early histological studies place "new" adrenocortical cells in the most peripheral position of cellular columns/projections arising from the capsule (Baker, 1952). It has been proposed that the slowly proliferating cells in the capsule generate daughter cells that eventually are centripetally displaced to populate the adrenal cortex (Beuschlein et al., 2002; Pignatelli et al., 2002). The robust mitosis and proliferation in the subcapsular region (Race and Green, 1955; Zajicek et al., 1986) is more consistent

with transiently amplifying progenitor population. Results of experiments employing radioactive-thymidine, BrdU pulse chase and PCNA staining are consistent with this notion and indicate that subcapsular cells of the rat adrenal replenish the neighboring steroidogenic zones, suggesting this population provides a pool of progenitors that serve to maintain the functional capacity of the cortex (Mitani et al., 1999; Mitani et al., 1994; Ogishima et al., 1992; Vinson et al., 1992; Wright et al., 1973; Zajicek et al., 1986).

Epidemiology and Clinical Management of Adrenocortical Carcinomas

Adrenal neoplasms are routinely uncovered during medical imaging studies (e.g. abdominal CT scans) performed for other health concerns. Post-mortem studies reveal that approximately 3-9% of autopsy cases of patients over 50 years old (Brunt and Moley, 2001; Kloos et al., 1995) harbor adrenocortical neoplasms. In the vast majority of cases, these 'incidentalomas' are benign adenomas rather than the rare and deadly ACC. Physicians encountering these tumors must always be wary of the potential but unlikely scenario of ACC, particularly when confronting a necrotic or hemorrhagic lesion or a mass with irregular borders or signs of invasion. While size is considered a reliable predictor of malignancy (greater than 5-6 cm^3 considered an high risk of malignancy), even small lesions presumed benign are routinely followed by CT or MRI, as adrenocortical carcinomas less than 5 cm^3 have already metastasized in ~14% of cases (Barnett et al., 2000).

ACC has been characterized as having a bimodal age distribution with an increased incidence in the first and fifth decades of life (Wooten and King, 1993). In

addition, ACC is slightly more common in women (Latronico and Chrousos, 1997). The vast majority of pediatric ACCs are uncovered by signs and symptoms of hormone excess stemming from the steroidogenic activity of the tumor - most common symptom being virilization secondary to androgen hypersecretion (Latronico and Chrousos, 1997). Although ACC in children may manifest in the context of a familial cancer syndrome (such as Li-Fraumeni or Beckwith-Wiedemann syndromes discussed below), the majority of pediatric ACCs, and nearly all adult cases, arise sporadically (Kirschner, 2002).

The prognosis for ACC is largely dependent on the grade of tumor and stage of diagnosis, with the most dismal scenario held for those presenting with distant metastases. Pediatric patients generally have a favorable prognosis due to the early detection because of their functional tumor symptoms. Unfortunately, the majority of adult ACCs are hormonally silent (Latronico and Chrousos, 1997), making early diagnosis extremely uncommon. Most adult ACC patients present incidentally or with constitutional symptoms or pain secondary to abdominal mass effects (Ahlman et al., 2001). The hormonal excess observed in pediatric ACCs but not often encountered in adult ACCs implies they may arise from different molecular perturbations and therefore, may be different diseases. However, studies comparing the gene expression profiles of pediatric and adult ACCs have a remarkably similar gene signature and thus, suggest that adult and childhood ACCs may utilize common pathogenic genetic/epigenetic alterations (West et al., 2007).

Surgical resection is the treatment of choice for patients with resectable primary and even metastatic lesions. Additionally, adjuvant mitotane (1,1-dichloro-2-(o-chlorophenyl)-2-(p-chlorophenyl) ethane) treatment, following radical ACC resection,

may prolong recurrence-free survival by 17 to 32 months (Terzolo et al., 2007). Although only a limited number of small therapeutic trials have been initiated for ACC, the International Consensus Conference on Adrenal Cancer, held at the University of Michigan in 2003 formally endorsed two "best practice" regimens for advanced disease (Schteingart et al., 2005). The EDP schedule, etoposide, doxorubicin, cisplatin plus mitotane boasts a response rate of approximately 50% with a median survival time of 2 years (Berruti et al., 1998). Alternatively, a regimen of streptozotocin plus mitotane has induced response rates of approximately 35% with a median survival of 16 months (Khan et al., 2000). Current efforts include an evaluation of these regimens head-to-head in an international randomized control trial (FIRM-ACT.ORG) and investigations by a number of groups into the molecular genetics of the disease in search of unique signaling defects that can be exploited in a targeted therapeutic approach.

Adrenocortical Carcinomas in the Context of Cancer Stem Cells

The cancer stem cell theory hypothesizes that a distinct subpopulation of cancer cells maintain the stem-cell potential (Lobo et al., 2007). These cells, termed 'cancer stem cells', are uniquely endowed with the ability to self-renew and differentiate into multiple different cell types within a cancer, analogous to normal tissue stem cells. Cancer stem cells have been identified in blood, breast, brain, colon and pancreatic cancers and the list is expanding (Lobo et al., 2007). Furthermore, evidence is mounting that aberrant epigenetic reprogramming of stem/progenitor cells is another level of dysregulation contributing to the pathogenesis in human cancers (Feinberg et al., 2006).

While cancer stem cells are predicted to be the only cells within a tumor that can give rise to new tumor cells, they are also predicted to be the only cells that are not responsive to standard chemotherapeutic protocols. This theory challenges current dogma of cancer therapeutics that all tumor cells possess equal malignant potential. Thus, drug discovery is challenged to shift treatment paradigms towards targeting this tumorigenic subpopulation of cancer stem cells for a potential cure. A myriad of questions arise from applying this new perspective of oncology to adrenocortical carcinoma. Are there adrenal cancer stem cells? Can they be isolated from human ACC samples like other cancers? Can therapeutics target these cells and lead to relapse-free survival?

Genetic and Molecular Events Implicated in the Pathogenesis of Adrenocortical Carcinoma

Armed with emerging data on adrenocortical stem/progenitor cells and our data describing the important molecular mechanisms regulating adrenocortical organ maintenance, we began to examine the biology of genes known to be mutated in hereditary ACC syndromes such as Beckwith-Wiedemann Syndrome (BWS), Familial Adenomatous Polyposis (FAP) and Li-Fraumeni Syndrome. Because these genes are known to play various roles in the regulation of somatic stem cell fate in a variety of systems (Barlaskar and Hammer, 2007; Libe et al., 2007), we hoped to gain insights into both the normal and pathologic roles of these factors in adrenocortical stem and/or progenitor cells.

Beckwith-Wiedemann Syndrome and IGF-II:

Beckwith-Wiedemann Syndrome (BWS) is a rare embryonic overgrowth disorder that manifests with macrosomia, macroglossia, abdominal wall defects, renal abnormalities, cleft palate and an increase in a variety of childhood cancers, including ACC. It has a frequency in the United States of about 1/14000 and about 10-15% of cases are familial (Weksberg et al., 2005). Approximately 85% of BWS patients have causative defects in the genomic imprinting of five genes located in two chromosomal clusters within the 11p15.5 region (Enklaar et al., 2006). The two genes comprising the distal cluster are the *IGF2* (insulin-like growth factor 2) and *H19* (an untranslated mRNA) genes. The proximal cluster includes the *CDKN1C* (cyclin-dependent kinase inhibitor $p57^{kip2}$), *KCNQ1* (potassium voltage-gated channel) and *KCNQ1OT1* (KCNQ1 overlapping transcript) genes. Several studies have demonstrated the association of *IGF2* expression with malignant versus benign adrenal tumors (Gao et al., 2002; Liu et al., 1995) and DNA microarray expression analysis implicates *IGF2* as the single highest expressed gene in the majority of sporadic ACCs (Giordano et al., 2003). Mouse models have also confirmed that overexpression of the *IGF2* gene results in a BWS-like syndrome (Sun et al., 1997) that includes adrenal hyperplasias and cytomegaly (Weber et al., 1999).

The IGF signaling system consists of two secreted ligands (IGF-I and IGF-II), three membrane-bound receptors (IGF-1R, IGF-2R and insulin receptor) and six high affinity extracellular IGF ligand binding proteins (IGFBP-1 through -6). IGF-I and IGF-II are homologous in 62% of their amino acids and also have a 40% sequence homology with their namesake ligand, insulin (Furstenberger and Senn, 2002). Similarities in the

ligands' primary protein structure underlie their comparable affinities for IGF1R, with IGF-I possessing a ~four-fold higher binding affinity *in vitro* (Forbes et al., 2002). Additionally, their sequence homology to insulin imparts the capacity to bind and activate the insulin receptor, though at a lower affinity than insulin (Forbes et al., 2002). The differences in IGF-I/II sequence homology account for IGF-II's exclusive binding to IGF-2R. This non-signaling molecule serves to decrease extracellular levels of IGF-II through ligand binding, complex internalization through receptor-mediated endocytosis and subsequent lysosomal degradation (Killian et al., 2000). IGF-II is often described as a key growth factor employed during early fetal development while postnatal IGF-I expression is utilized for maintaining normal growth as a downstream effector of growth hormone (GH) stimulation. As such, IGF-II levels are ~5 times higher than IGF-I in the human fetus, but intriguingly, it is still ~3.5 times higher than IGF-I in adult sera (Bennett et al., 1983). The physiologic basis of higher adult IGF-II serum concentrations without concomitant IGF-II-mediated activity has yet to be determined. Extracellular ligand binding causes IGF-1R autophosphorylation of its intracellular domain. Subsequently, the MAPK and PI3-K/Akt signaling pathways are activated to induce expression of numerous genes that regulate pro-growth/survival pathways in the cell (Nakae et al., 2001).

Because in the adrenal gland IGF-II is uniquely expressed in the capsule (http://www.GenePaint.org; ID MH523) (Han et al., 1992) and has recently been shown to be a critical mediator of the embryonic and tissue stem/progenitor cell niche (Bendall et al., 2007), the prediction that abnormal imprinting of the *IGF2* locus in the capsule/subcapsular unit serves as an initiator of the disease becomes a testable

hypothesis and a the IGF-II pathway a possible target for therapeutic intervention in ACC. Supporting and extending similar findings of others (Almeida et al., 2008), we have shown that antagonizing this pathway with two different pharmacologic agents that target IGF1R leads to a potent inhibition of growth of ACC cells in culture and in human ACC xenografts. We also demonstrated that the addition of mitotane (currently the only FDA approved therapy for ACC), increased the cytostatic effects of either compound on human ACC xenografts in mice (Barlaskar et al., 2008). The above data support the testable hypothesis that aberrant epigenetic reprogramming of 11p15.5 and potentially other loci in stem/progenitor cells participates in the etiology of a subset of cancers including ACC. These studies have led to successful Phase I trials of IGF1R inhibition in refractory ACC patients. The observation of stabilization of disease in 8 of 14 patients (57%) (Haluska et al.) has fueled a multi-institutional Phase II trial using this targeted approach as up-front therapy in stage 4 ACC.

Familial Adenomatous Polyposis:

Familial adenomatous polyposis (FAP) is a hereditary disorder in which patients typically present with innumerable colonic polyps and ultimate colonic cancer. This disorder is characterized by mutations in the adenomatous polyposis coli (APC) gene on chromosome 5q21-q22 that result in a truncated and/or non-functional APC protein (Groden et al., 1991; Kinzler et al., 1991). These patients also have increased risks of other cancers in the extracolonic organs including the pancreas, thyroid, and adrenal glands (Fearnhead et al., 2001; Naylor and Gardner, 1981; Naylor and Lebenthal, 1980; Painter and Jagelman, 1985).

The molecular mechanism of tumorigenesis resulting from APC gene mutations has been widely characterized (Aoki and Taketo, 2007; Fearnhead et al., 2001; Groden et al., 1991; Kinzler et al., 1991). The product of the APC gene functions as a tumor suppressor mainly through regulation of β-catenin protein stability and hence β-catenin-mediated transcription. Inactivating mutations of APC result in upregulation of the β-catenin target genes, subsequent unablated growth and ultimate tumor formation. Although recent evidence suggests additional functions of APC in cell adhesion, cell polarity and migration, chromosome segregation, and mitochondria-mediated apoptosis, this review addresses the role of APC only as a member of the β-catenin degradation complex (Aoki and Taketo, 2007). Predicated on the known role of APC in the regulation of the canonical Wnt signaling pathway in tissue development and homeostasis, our lab and others began analyzing the status of β-catenin in sporadic adrenocortical tumors. In earlier work the Bertherat laboratory had observed an increase in the nuclear/cytoplasmic ratio of β-catenin in sporadic ACC (Tissier et al., 2005). In collaboration with the Giordano laboratory, we began screening a panel of ACC samples for stabilization of β-catenin and observed a subset of carcinoma samples with strong nuclear accumulation of β-catenin indicative of active signaling. Utilizing expression array profiling, we compared carcinomas with strong nuclear β-catenin staining to carcinomas with only membranous β-catenin staining. In the analysis, we observed marked upregulation of classical β-catenin-mediated transcription targets, but only in ACC samples did we observe increased nuclear β-catenin. Such results support a potential role of active β-catenin signaling in a subset of patients with adrenocortical carcinoma.

To further test a hypothesis that active β-catenin signaling may initiate adrenocortical carcinogenesis through aberrant activation in adrenocortical subcapsular cells, we utilized a conditional knockout mouse approach. Employing the technology outlined in the Wnt section of this review, we began mating transgenic mice harboring floxed alleles in the *Apc* gene with the *Sf1-Cre*^{low} or *Sf1-Cre*^{high} transgenic mice. The initial analysis of the *Sf1-Cre*^{low}-mediated knockout mice revealed the presence of aberrant clusters of undifferentiated adrenocortical cells at the cortical-medullary apoptotic boundary and even within the adrenal medulla. The gene expression profile of these adrenals at 9 weeks of age revealed an expansion of cells with active β-catenin signaling but with diminished steroidogenic capacity as evidenced by robust Dax1 expression and decreased expression of steroidogenic enzymes (manuscript in preparation). With increase in age of the mouse, however, the cells begin to undergo differentiation as evidenced by a substantially upregulated steroidogenic gene profile. Lastly, at 45 weeks of age, these mice present with tumors that are histologically comparable to ACC. As such, we hypothesize that canonical Wnt signaling regulates the proliferation and undifferentiated state of adrenocortical stem/progenitor cells. With constitutive activation of the canonical Wnt pathway, expansion of this population is followed by ultimate cancer formation.

The additional mutations and signaling pathways contributing to these phenotypes are areas of active investigation. IGF and Wnt ligands are two such signals generated in the adrenal capsule that have been shown to be essential in the regulation of stem cell niches and/or the communication with neighboring stem/progenitor cells in multiple organ systems. Specifically, IGF is a critical mediator of the embryonic and tissue

stem/progenitor cell niche, while Wnt signaling is essential for stem/progenitor cell self-renewal in multiple systems (Bendall et al., 2007; Huelsken and Birchmeier, 2001).

Li-Fraumeni Syndrome:

This familial syndrome arises from mutations in the p53 tumor suppressor gene and is associated with breast cancer, soft tissue sarcomas, brain tumors, osteosarcoma, leukemia, and adrenocortical carcinoma (Sidhu et al., 2003). The LFS mutations in *p53* are most commonly located in exons 5 to 8 containing the highly conserved DNA binding domain of *p53 (Malkin, 2001)*. The *p53* gene, located on the 17p13.1 chromosomal segment, encodes the 393 amino acid tumor suppressor protein situated in the center of a network of signaling pathways that are essential for cell growth regulation and apoptosis induced by a diverse array of cellular stresses. In normal unstressed cells, the level of p53 protein is tightly regulated via binding of proteins such as MDM2 that promote p53 degradation via the ubiquitin/proteasome pathway. After sensing genotoxic or non-genotoxic stress, p53 protein levels increase by inhibition of its interactions with negative regulators and concomitant p53 activation by several kinases and acetylases. This results in p53-dependent transactivation of a large series of genes that trigger DNA repair mechanisms, sustain cell cycle arrest in G1/S phase, and initiate growth arrest or apoptosis if DNA damage is not repaired (Ljungman, 2000).

It is no surprise that p53's guardian function, which protects against unbridled proliferation, is bypassed in the vast majority of human cancers by direct and indirect inactivating mutations. Individuals carrying germline *p53* mutations develop cancers early in life, with carriers afflicted with tumors originating from multiple tissues in an

autosomal dominant fashion. Tumor suppressor genes, such as p53, generally must have alterations in both alleles to cause a loss of function. Loss of heterozygosity (LOH), where a deletion or other mutational event within the remaining normal allele renders the cell homozygous for the deleterious allele, has been demonstrated in ACC at the 17p13.1 locus (Gicquel et al., 2001; Yano et al., 1989). In fact, LOH at this locus has been reported to occur in 85% of carcinomas and 0% of adenomas, suggesting a possible marker for malignancy (Gicquel et al., 2001). It is not surprising therefore that the most frequently inherited p53 mutations associated with LFS are also found in sporadic cases of ACC (Zambetti, 2007).

Two mutations in *p53* that are implicated in LFS and result in an increased incidence of ACC are noteworthy. One of the most common p53 point mutants, Arg 175 to His, fails to bind DNA and therefore results in complete loss of p53 transcriptional activity. While this mutation manifests with a classic LFS cancer spectrum including ACC, it actually accounts for 6% of the missense mutations identified in all human cancers (Liu et al., 2000). On the contrary, in the southern region of Brazil where the rate of pediatric ACC is 10-15 times greater than worldwide incidence (Sandrini et al., 1997), virtually all patients have an identical germ-line point mutation of p53 encoding an Arg 337 to His amino acid substitution in exon 10 (Ribeiro et al., 2001). This particular mutation led to ACC development with a paucity of the other tumor types seen in LFS. This R337H polymorphism leads to a destabilization of p53 tetramerization in a pH dependent manner, providing a mechanism for loss of p53 transcriptional activity and adrenocortical-specific tumor formation (DiGiammarino et al., 2002). From a therapeutic standpoint, *in vivo* restoration of a lost tumor suppressor such as p53 has been a long

sought after goal. Recent research has shown restoration of endogenous p53 expression led to a prompt and impressive tumor regression of established *in situ* mouse tumors (Martins et al., 2006; Ventura et al., 2007; Xue et al., 2007). Thus renewing efforts to use pharmacological reactivation of p53 must be explored further as a potential therapeutic target for human cancers like ACC.

Conclusions

ACC remains a difficult disease to treat despite recent advances elucidating several mutations that contribute to the dysregulated adrenocortical growth in the disease. Transgenic mouse models that validate the importance of these molecular defects are active areas of investigation that will facilitate preclinical testing of novel therapeutic strategies and targeted chemotherapeutics. The need for larger multi-institutional registries and international clinical trials is paramount and will assure a more rapid and unified pursuit of these goals.

Bibliography

Leoutsakos, B., Leoutsakos, A., 2008. The adrenal glands: a brief historical perspective. Hormones (Athens) 7, 334-6.

Pearce, J.M., 2004. Thomas Addison (1793-1860). J R Soc Med 97, 297-300.

Whiting, M.J., Doogue, M.P., 2009. Advances in Biochemical Screening for Phaeochromocytoma using Biogenic Amines. Clin Biochem Rev 30, 3-17.

Wajchenberg, B.L., Albergaria Pereira, M.A., Medonca, B.B., Latronico, A.C., Campos Carneiro, P., Alves, V.A., Zerbini, M.C., Liberman, B., Carlos Gomes, G., Kirschner, M.A., 2000. Adrenocortical carcinoma: clinical and laboratory observations. Cancer 88, 711-36.

Icard, P., Goudet, P., Charpenay, C., Andreassian, B., Carnaille, B., Chapuis, Y., Cougard, P., Henry, J.F., Proye, C., 2001. Adrenocortical carcinomas: surgical trends and results of a 253-patient series from the French Association of Endocrine Surgeons study group. World J Surg 25, 891-7.

Arnold, J., 1866. Ein Beitrag zur feineren Struktur und dem Chemismus der Nebennieren.

Evelyn, H.-M., 1927. A transitory zone in the adrenal cortex which shows age and sex relationships. American Journal of Anatomy 40, 251-293.

Keegan, C.E., Hammer, G.D., 2002. Recent insights into organogenesis of the adrenal cortex. Trends Endocrinol Metab 13, 200-8.

Else, T., Hammer, G.D., 2005. Genetic analysis of adrenal absence: agenesis and aplasia. Trends Endocrinol Metab 16, 458-68.

Uotila, U.U., 1940. The early embryological development of the fetal and permanent adrenal cortex in man. The Anatomical Record 76, 183-203.

Hatano, O., Takakusu, A., Nomura, M., Morohashi, K., 1996. Identical origin of adrenal cortex and gonad revealed by expression profiles of Ad4BP/SF-1. Genes Cells 1, 663-71.

Luo, X., Ikeda, Y., Parker, K.L., 1994. A cell-specific nuclear receptor is essential for adrenal and gonadal development and sexual differentiation. Cell 77, 481-90.

Kim, A.C., Hammer, G.D., 2007. Adrenocortical cells with stem/progenitor cell properties: recent advances. Mol Cell Endocrinol 265-266, 10-6.

James, R.G., Kamei, C.N., Wang, Q., Jiang, R., Schultheiss, T.M., 2006. Odd-skipped related 1 is required for development of the metanephric kidney and regulates formation and differentiation of kidney precursor cells. Development 133, 2995-3004.

Katoh-Fukui, Y., Owaki, A., Toyama, Y., Kusaka, M., Shinohara, Y., Maekawa, M., Toshimori, K., Morohashi, K., 2005. Mouse Polycomb M33 is required for splenic vascular and adrenal gland formation through regulating Ad4BP/SF1 expression. Blood 106, 1612-20.

Schnabel, C.A., Selleri, L., Cleary, M.L., 2003. Pbx1 is essential for adrenal development and urogenital differentiation. Genesis 37, 123-30.

Val, P., Martinez-Barbera, J.P., Swain, A., 2007. Adrenal development is initiated by Cited2 and Wt1 through modulation of Sf-1 dosage. Development 134, 2349-58.

Zubair, M., Ishihara, S., Oka, S., Okumura, K., Morohashi, K., 2006. Two-step regulation of Ad4BP/SF-1 gene transcription during fetal adrenal development: initiation by a Hox-Pbx1-Prep1 complex and maintenance via autoregulation by Ad4BP/SF-1. Mol Cell Biol 26, 4111-21.

Fuchs, E., Tumbar, T., Guasch, G., 2004. Socializing with the neighbors: stem cells and their niche. Cell 116, 769-78.

Jones, D.L., Wagers, A.J., 2008. No place like home: anatomy and function of the stem cell niche. Nat Rev Mol Cell Biol 9, 11-21.

Sneddon, J.B., Werb, Z., 2007. Location, location, location: the cancer stem cell niche. Cell Stem Cell 1, 607-11.

Bassett, J.R., West, S.H., 1997. Vascularization of the adrenal cortex: its possible involvement in the regulation of steroid hormone release. Microsc Res Tech 36, 546-57.

Chamoux, E., Bolduc, L., Lehoux, J.G., Gallo-Payet, N., 2001. Identification of extracellular matrix components and their integrin receptors in the human fetal adrenal gland. J Clin Endocrinol Metab 86, 2090-8.

Magennis, D.P., McNicol, A.M., 1998. Vascular patterns in the normal and pathological human adrenal cortex. Virchows Arch 433, 69-73.

Otis, M., Campbell, S., Payet, M.D., Gallo-Payet, N., 2007. Expression of extracellular matrix proteins and integrins in rat adrenal gland: importance for ACTH-associated functions. J Endocrinol 193, 331-47.

Tokunaga, H., 1996. Postnatal development of the blood vasculature in the rat adrenal gland: a scanning electron microscope study of microcorrosion casts. Arch Histol Cytol 59, 305-15.

Virtanen, I., Korhonen, M., Petajaniemi, N., Karhunen, T., Thornell, L.E., Sorokin, L.M., Konttinen, Y.T., 2003. Laminin isoforms in fetal and adult human adrenal cortex. J Clin Endocrinol Metab 88, 4960-6.

Whetton, A.D., Graham, G.J., 1999. Homing and mobilization in the stem cell niche. Trends Cell Biol 9, 233-8.

Iannaccone, P., Morley, S., Skimina, T., Mullins, J., Landini, G., 2003. Cord-like mosaic patches in the adrenal cortex are fractal: implications for growth and development. Faseb J 17, 41-3.

Kiiveri, S., Liu, J., Westerholm-Ormio, M., Narita, N., Wilson, D.B., Voutilainen, R., Heikinheimo, M., 2002. Differential expression of GATA-4 and GATA-6 in fetal and adult mouse and human adrenal tissue. Endocrinology 143, 3136-43.

Landini, G., Iannaccone, P.M., 2000. Modeling of mosaic patterns in chimeric liver and adrenal cortex: algorithmic organogenesis? Faseb J 14, 823-7.

Weinberg, W.C., Howard, J.C., Iannaccone, P.M., 1985. Histological demonstration of mosaicism in a series of chimeric rats produced between congenic strains. Science 227, 524-7.

Zubair, M., Parker, K.L., Morohashi, K., 2008. Developmental links between the fetal and adult zones of the adrenal cortex revealed by lineage tracing. Mol Cell Biol 28, 7030-40.

Bragulla, H., Hirschberg, R.M., Schlotfeldt, U., Stede, M., Budras, K.D., 2004. On the structure of the adrenal gland of the common seal (Phoca vitulina vitulina). Anat Histol Embryol 33, 263-72.

Rupik, W., 2002. Early development of the adrenal glands in the grass snake Natrix natrix L. (Lepidosauria, Serpentes). Adv Anat Embryol Cell Biol 164, I-XI, 1-102.

Halder, S.K., Takemori, H., Hatano, O., Nonaka, Y., Wada, A., Okamoto, M., 1998. Cloning of a membrane-spanning protein with epidermal growth factor-like repeat motifs from adrenal glomerulosa cells. Endocrinology 139, 3316-28.

Vinson, G.P., Whitehouse, B., Hinson, J., 1992. The Adrenal Cortex. Prentice Hall Inc.
.

Mitani, F., Mukai, K., Miyamoto, H., Suematsu, M., Ishimura, Y., 1999. Development of functional zonation in the rat adrenal cortex. Endocrinology 140, 3342-53.

Mitani, F., Mukai, K., Miyamoto, H., Suematsu, M., Ishimura, Y., 2003. The undifferentiated cell zone is a stem cell zone in adult rat adrenal cortex. Biochim Biophys Acta 1619, 317-24.

Mitani, F., Suzuki, H., Hata, J., Ogishima, T., Shimada, H., Ishimura, Y., 1994. A novel cell layer without corticosteroid-synthesizing enzymes in rat adrenal cortex: histochemical detection and possible physiological role. Endocrinology 135, 431-8.

Baker, B.L., 1952. A comparison of the histological changes induced by experimental hyperadrenocorticalism and inanition. Recent Prog Hormone Res 7, 331.

Beuschlein, F., Mutch, C., Bavers, D.L., Ulrich-Lai, Y.M., Engeland, W.C., Keegan, C., Hammer, G.D., 2002. Steroidogenic factor-1 is essential for compensatory adrenal growth following unilateral adrenalectomy. Endocrinology 143, 3122-35.

Pignatelli, D., Ferreira, J., Vendeira, P., Magalhaes, M.C., Vinson, G.P., 2002. Proliferation of capsular stem cells induced by ACTH in the rat adrenal cortex. Endocr Res 28, 683-91.

Race, G.J., Green, R.F., 1955. Studies on zonation and regeneration of the adrenal cortex of the rat; effects of sodium restriction, potassium intoxication, corticotropin, and orchiectomy when studied with colchicine. AMA Arch Pathol 59, 578-86.

Zajicek, G., Ariel, I., Arber, N., 1986. The streaming adrenal cortex: direct evidence of centripetal migration of adrenocytes by estimation of cell turnover rate. J Endocrinol 111, 477-82.

Ogishima, T., Suzuki, H., Hata, J., Mitani, F., Ishimura, Y., 1992. Zone-specific expression of aldosterone synthase cytochrome P-450 and cytochrome P-45011 beta in rat adrenal cortex: histochemical basis for the functional zonation. Endocrinology 130, 2971-7.

Wright, N.A., Voncina, D., Morley, A.R., 1973. An attempt to demonstrate cell migration from the zona glomerulosa in the prepubertal male rat adrenal cortex. J Endocrinol 59, 451-9.

Brunt, L.M., Moley, J.F., 2001. Adrenal incidentaloma. World J Surg 25, 905-13.

Kloos, R.T., Gross, M.D., Francis, I.R., Korobkin, M., Shapiro, B., 1995. Incidentally discovered adrenal masses. Endocr Rev 16, 460-84.

Barnett, C.C., Jr., Varma, D.G., El-Naggar, A.K., Dackiw, A.P., Porter, G.A., Pearson, A.S., Kudelka, A.P., Gagel, R.F., Evans, D.B., Lee, J.E., 2000. Limitations of size as a criterion in the evaluation of adrenal tumors. Surgery 128, 973-82;discussion 982-3.

Wooten, M.D., King, D.K., 1993. Adrenal cortical carcinoma. Epidemiology and treatment with mitotane and a review of the literature. Cancer 72, 3145-55.

Latronico, A.C., Chrousos, G.P., 1997. Extensive personal experience: adrenocortical tumors. J Clin Endocrinol Metab 82, 1317-24.

Kirschner, L.S., 2002. Signaling pathways in adrenocortical cancer. Ann N Y Acad Sci 968, 222-39.

Ahlman, H., Khorram-Manesh, A., Jansson, S., Wangberg, B., Nilsson, O., Jacobsson, C.E., Lindstedt, S., 2001. Cytotoxic treatment of adrenocortical carcinoma. World J Surg 25, 927-33.

West, A.N., Neale, G.A., Pounds, S., Figueredo, B.C., Rodriguez Galindo, C., Pianovski, M.A., Oliveira Filho, A.G., Malkin, D., Lalli, E., Ribeiro, R., Zambetti, G.P., 2007. Gene expression profiling of childhood adrenocortical tumors. Cancer Res 67, 600-8.

Terzolo, M., Angeli, A., Fassnacht, M., Daffara, F., Tauchmanova, L., Conton, P.A., Rossetto, R., Buci, L., Sperone, P., Grossrubatscher, E., Reimondo, G., Bollito, E., Papotti, M., Saeger, W., Hahner, S., Koschker, A.C., Arvat, E., Ambrosi, B., Loli, P., Lombardi, G., Mannelli, M., Bruzzi, P., Mantero, F., Allolio, B., Dogliotti, L., Berruti, A., 2007. Adjuvant mitotane treatment for adrenocortical carcinoma. N Engl J Med 356, 2372-80.

Schteingart, D.E., Doherty, G.M., Gauger, P.G., Giordano, T.J., Hammer, G.D., Korobkin, M., Worden, F.P., 2005. Management of patients with adrenal cancer: recommendations of an international consensus conference. Endocr Relat Cancer 12, 667-80.

Berruti, A., Terzolo, M., Pia, A., Angeli, A., Dogliotti, L., 1998. Mitotane associated with etoposide, doxorubicin, and cisplatin in the treatment of advanced adrenocortical carcinoma. Italian Group for the Study of Adrenal Cancer. Cancer 83, 2194-200.

Khan, T.S., Imam, H., Juhlin, C., Skogseid, B., Grondal, S., Tibblin, S., Wilander, E., Oberg, K., Eriksson, B., 2000. Streptozocin and o,p'DDD in the treatment of adrenocortical cancer patients: long-term survival in its adjuvant use. Ann Oncol 11, 1281-7.

Lobo, N.A., Shimono, Y., Qian, D., Clarke, M.F., 2007. The biology of cancer stem cells. Annu Rev Cell Dev Biol 23, 675-99.

Feinberg, A.P., Ohlsson, R., Henikoff, S., 2006. The epigenetic progenitor origin of human cancer. Nat Rev Genet 7, 21-33.

Barlaskar, F.M., Hammer, G.D., 2007. The molecular genetics of adrenocortical carcinoma. Rev Endocr Metab Disord 8, 343-8.

Libe, R., Fratticci, A., Bertherat, J., 2007. Adrenocortical cancer: pathophysiology and clinical management. Endocr Relat Cancer 14, 13-28.

Weksberg, R., Shuman, C., Smith, A.C., 2005. Beckwith-Wiedemann syndrome. Am J Med Genet C Semin Med Genet 137C, 12-23.

Enklaar, T., Zabel, B.U., Prawitt, D., 2006. Beckwith-Wiedemann syndrome: multiple molecular mechanisms. Expert Rev Mol Med 8, 1-19.

Gao, Z.H., Suppola, S., Liu, J., Heikkila, P., Janne, J., Voutilainen, R., 2002. Association of H19 promoter methylation with the expression of H19 and IGF-II genes in adrenocortical tumors. J Clin Endocrinol Metab 87, 1170-6.

Liu, J., Kahri, A.I., Heikkila, P., Ilvesmaki, V., Voutilainen, R., 1995. H19 and insulin-like growth factor-II gene expression in adrenal tumors and cultured adrenal cells. J Clin Endocrinol Metab 80, 492-6.

Giordano, T.J., Thomas, D.G., Kuick, R., Lizyness, M., Misek, D.E., Smith, A.L., Sanders, D., Aljundi, R.T., Gauger, P.G., Thompson, N.W., Taylor, J.M., Hanash, S.M., 2003. Distinct transcriptional profiles of adrenocortical tumors uncovered by DNA microarray analysis. Am J Pathol 162, 521-31.

Sun, F.L., Dean, W.L., Kelsey, G., Allen, N.D., Reik, W., 1997. Transactivation of Igf2 in a mouse model of Beckwith-Wiedemann syndrome. Nature 389, 809-15.

Weber, M.M., Fottner, C., Schmidt, P., Brodowski, K.M., Gittner, K., Lahm, H., Engelhardt, D., Wolf, E., 1999. Postnatal overexpression of insulin-like growth factor II in transgenic mice is associated with adrenocortical hyperplasia and enhanced steroidogenesis. Endocrinology 140, 1537-43.

Furstenberger, G., Senn, H.J., 2002. Insulin-like growth factors and cancer. Lancet Oncol 3, 298-302.

Forbes, B.E., Hartfield, P.J., McNeil, K.A., Surinya, K.H., Milner, S.J., Cosgrove, L.J., Wallace, J.C., 2002. Characteristics of binding of insulin-like growth factor (IGF)-I and IGF-II analogues to the type 1 IGF receptor determined by BIAcore analysis. Eur J Biochem 269, 961-8.

Killian, J.K., Byrd, J.C., Jirtle, J.V., Munday, B.L., Stoskopf, M.K., MacDonald, R.G., Jirtle, R.L., 2000. M6P/IGF2R imprinting evolution in mammals. Mol Cell 5, 707-16.

Bennett, A., Wilson, D.M., Liu, F., Nagashima, R., Rosenfeld, R.G., Hintz, R.L., 1983. Levels of insulin-like growth factors I and II in human cord blood. J Clin Endocrinol Metab 57, 609-12.

Nakae, J., Kido, Y., Accili, D., 2001. Distinct and overlapping functions of insulin and IGF-I receptors. Endocr Rev 22, 818-35.

Han, V.K., Lu, F., Bassett, N., Yang, K.P., Delhanty, P.J., Challis, J.R., 1992. Insulin-like growth factor-II (IGF-II) messenger ribonucleic acid is expressed in steroidogenic cells of the developing ovine adrenal gland: evidence of an autocrine/paracrine role for IGF-II. Endocrinology 131, 3100-9.

Bendall, S.C., Stewart, M.H., Menendez, P., George, D., Vijayaragavan, K., Werbowetski-Ogilvie, T., Ramos-Mejia, V., Rouleau, A., Yang, J., Bosse, M., Lajoie, G., Bhatia, M., 2007. IGF and FGF cooperatively establish the regulatory stem cell niche of pluripotent human cells in vitro. Nature 448, 1015-21.

Almeida, M.Q., Fragoso, M.C., Lotfi, C.F., Santos, M.G., Nishi, M.Y., Costa, M.H., Lerario, A.M., Maciel, C.C., Mattos, G.E., Jorge, A.A., Mendonca, B.B., Latronico, A.C., 2008. Expression of insulin-like growth factor-II and its receptor in pediatric and adult adrenocortical tumors. J Clin Endocrinol Metab 93, 3524-31.

Barlaskar, F.M., Spalding, A.C., Heaton, J.H., Kuick, R., Kim, A.C., Thomas, D.G., Giordano, T.J., Ben-Josef, E., Hammer, G.D., 2008. Preclinical Targeting of the Type 1 Insulin-like Growth Factor Receptor in Adrenocortical Carcinoma. J Clin Endocrinol Metab.

Haluska, P., Worden, F., Olmos, D., Yin, D., Schteingart, D., Batzel, G.N., Paccagnella, M.L., de Bono, J.S., Gualberto, A., Hammer, G.D., Safety, tolerability, and pharmacokinetics of the anti-IGF-1R monoclonal antibody figitumumab in patients with refractory adrenocortical carcinoma. Cancer Chemother Pharmacol 65, 765-73.

Groden, J., Thliveris, A., Samowitz, W., Carlson, M., Gelbert, L., Albertsen, H., Joslyn, G., Stevens, J., Spirio, L., Robertson, M., et al., 1991. Identification and characterization of the familial adenomatous polyposis coli gene. Cell 66, 589-600.

Kinzler, K.W., Nilbert, M.C., Su, L.K., Vogelstein, B., Bryan, T.M., Levy, D.B., Smith, K.J., Preisinger, A.C., Hedge, P., McKechnie, D., et al., 1991. Identification of FAP locus genes from chromosome 5q21. Science 253, 661-5.

Fearnhead, N.S., Britton, M.P., Bodmer, W.F., 2001. The ABC of APC. Hum Mol Genet 10, 721-33.

Naylor, E.W., Gardner, E.J., 1981. Adrenal adenomas in a patient with Gardner's syndrome. Clin Genet 20, 67-73.

Naylor, E.W., Lebenthal, E., 1980. Gardner's syndrome. Recent developments in research and management. Dig Dis Sci 25, 945-59.

Painter, T.A., Jagelman, D.G., 1985. Adrenal adenomas and adrenal carcinomas in association with hereditary adenomatosis of the colon and rectum. Cancer 55, 2001-4.

Aoki, K., Taketo, M.M., 2007. Adenomatous polyposis coli (APC): a multi-functional tumor suppressor gene. J Cell Sci 120, 3327-35.

Tissier, F., Cavard, C., Groussin, L., Perlemoine, K., Fumey, G., Hagnere, A.M., Rene-Corail, F., Jullian, E., Gicquel, C., Bertagna, X., Vacher-Lavenu, M.C., Perret, C., Bertherat, J., 2005. Mutations of beta-catenin in adrenocortical tumors: activation of the Wnt signaling pathway is a frequent event in both benign and malignant adrenocortical tumors. Cancer Res 65, 7622-7.

Huelsken, J., Birchmeier, W., 2001. New aspects of Wnt signaling pathways in higher vertebrates. Curr Opin Genet Dev 11, 547-53.

Sidhu, S., Gicquel, C., Bambach, C.P., Campbell, P., Magarey, C., Robinson, B.G., Delbridge, L.W., 2003. Clinical and molecular aspects of adrenocortical tumourigenesis. ANZ J Surg 73, 727-38.

Malkin, D., 2001. The role of p53 in human cancer. J Neurooncol 51, 231-43.

Ljungman, M., 2000. Dial 9-1-1 for p53: mechanisms of p53 activation by cellular stress. Neoplasia 2, 208-25.

Gicquel, C., Bertagna, X., Gaston, V., Coste, J., Louvel, A., Baudin, E., Bertherat, J., Chapuis, Y., Duclos, J.M., Schlumberger, M., Plouin, P.F., Luton, J.P., Le Bouc, Y., 2001. Molecular markers and long-term recurrences in a large cohort of patients with sporadic adrenocortical tumors. Cancer Res 61, 6762-7.

Yano, T., Linehan, M., Anglard, P., Lerman, M.I., Daniel, L.N., Stein, C.A., Robertson, C.N., LaRocca, R., Zbar, B., 1989. Genetic changes in human adrenocortical carcinomas. J Natl Cancer Inst 81, 518-23.

Zambetti, G.P., 2007. The p53 mutation "gradient effect" and its clinical implications. J Cell Physiol 213, 370-3.

Liu, G., McDonnell, T.J., Montes de Oca Luna, R., Kapoor, M., Mims, B., El-Naggar, A.K., Lozano, G., 2000. High metastatic potential in mice inheriting a targeted p53 missense mutation. Proc Natl Acad Sci U S A 97, 4174-9.

Sandrini, R., Ribeiro, R.C., DeLacerda, L., 1997. Childhood adrenocortical tumors. J Clin Endocrinol Metab 82, 2027-31.

Ribeiro, R.C., Sandrini, F., Figueiredo, B., Zambetti, G.P., Michalkiewicz, E., Lafferty, A.R., DeLacerda, L., Rabin, M., Cadwell, C., Sampaio, G., Cat, I., Stratakis, C.A., Sandrini, R., 2001. An inherited p53 mutation that contributes in a tissue-specific manner to pediatric adrenal cortical carcinoma. Proc Natl Acad Sci U S A 98, 9330-5.

DiGiammarino, E.L., Lee, A.S., Cadwell, C., Zhang, W., Bothner, B., Ribeiro, R.C., Zambetti, G., Kriwacki, R.W., 2002. A novel mechanism of tumorigenesis involving pH-dependent destabilization of a mutant p53 tetramer. Nat Struct Biol 9, 12-6.

Martins, C.P., Brown-Swigart, L., Evan, G.I., 2006. Modeling the therapeutic efficacy of p53 restoration in tumors. Cell 127, 1323-34.

Ventura, A., Kirsch, D.G., McLaughlin, M.E., Tuveson, D.A., Grimm, J., Lintault, L., Newman, J., Reczek, E.E., Weissleder, R., Jacks, T., 2007. Restoration of p53 function leads to tumour regression in vivo. Nature 445, 661-5.

Xue, W., Zender, L., Miething, C., Dickins, R.A., Hernando, E., Krizhanovsky, V., Cordon-Cardo, C., Lowe, S.W., 2007. Senescence and tumour clearance is triggered by p53 restoration in murine liver carcinomas. Nature 445, 656-60.

CHAPTER 2

IDENTIFYING MECHANISMS OF *IGF2* UPREGULATION IN ADRENOCORTICAL CARCINOMA

ABSTRACT

Transcriptional profiling data derived from DNA microarray analysis of human adrenal tumors indicate locus dysregulation of the 11p15.5 chromosomal region and implicate the insulin-like growth factor-II (*IGF2*) gene as the single highest upregulated gene in the majority of adrenocortical carcinomas (ACCs). In contrast, two other genes within this locus (*H19* and *CDKN1C*) are reciprocally downregulated, suggesting a possible locus-specific epigenetic dysregulation within the ACC samples. Additionally, the majority of human ACC tissue samples and ACC cell lines tested display evidence of constitutive IGF ligand production and concomitant activation of downstream effector pathways. We utilized a technique called pyrosequencing to further analyze the gene locus to determine the methylation status of regulatory regions that may affect *IGF2* expression. This analysis revealed DMR2 is significantly hypomethylated in the ACC samples and this change is associated with increasing *IGF2* expression levels. This chapter provides evidence of aberrant epigenetic changes in ACCs may lead to *IGF2* upregulation and activated IGF signaling.

INTRODUCTION

Adrenocortical carcinomas (ACCs) are rare, accounting for ~0.05% of all reported cancers with a prevalence of ~2 cases/million/year, but are fatal in most cases (Latronico and Chrousos, 1997). The small number of diagnosed cases and its aggressive nature has made this cancer particularly difficult to study; however, its association with several familial tumor syndromes has shed some light on its pathogenesis. A few of these (namely *p53*, *APC* and *IGF2*) have been implicated in the pathogenesis of the more common sporadic form of ACC and lend credence that this cancer may arise from a select few of these molecular perturbations (Koch et al., 2002; Libe and Bertherat, 2005). For instance, the molecular basis of Beckwith-Wiedemann Syndrome (BWS), an overgrowth disorder with increased ACC incidence, has been mapped to 11p15.5, where expression of several genes (including *IGF2*) are regulated by differential DNA methylation (Enklaar et al., 2006; Weksberg et al., 2005).

Methylation of DNA is an epigenetic mechanism employed by cells to regulate gene expression, which is dictated by the methylation of the 5' carbon of cytosine adjacent to a guanine (denoted CpG) in a DNA strand. In particular, gene promoter regions contain a higher frequency of these CpGs (CpG islands) than would be expected due to random chance and play a role in directing the transcriptional output of these genes. Methylation of CpG islands in these promoter regions results in gene silencing. In contrast, absence of methylation of CpG islands results in increased gene expression, by permitting the transcriptional machinery access to critical regions of the promoter (Feinberg, 2007; Tost). Numerous studies implicated abnormal promoter hypermethylation of important tumor suppressor genes, suggesting that gene silencing

through methylation marks may contribute to the pathogenesis of human cancer (Garinis et al., 2002; Hoebeeck et al., 2009). Other studies have suggested promoter hypomethylation can play a reciprocal role in activating oncogene expression (Hatada et al., 2006; Scelfo et al., 2002).

DNA methylation is also involved in genomic imprinting, a mechanism that regulates the expression of a small subset of genes, which is determined by the inheritance of the parental allele. Other regulatory regions of the genome that contain a high concentration of CpG islands which are methylated on one allele (maternal or paternal) and are referred to as differentially methylated regions (DMRs). DMRs that participate in functionally maintaining this monoallelic mark at a chromosomal locus are designated as imprinting control regions (ICRs) (Gebert et al., 2009).

The imprinted *H19* and *IGF2* genes are located on the distal end of chromosome 11 in humans and on chromosome 7 in mice (Yoshimizu et al., 2008). Imprinting at this locus is controlled by an ICR located in between these two genes that results in *H19* expression from the maternally inherited chromosome, while *IGF2* is expressed from the paternal chromosome (**Fig. 2.1A**). This monoallelic expression pattern is regulated through the following mechanism: On the maternal allele, a chromatin insulator protein, CTCF, binds to specific sites on the unmethylated ICR. The CTCF/DNA complex blocks the *IGF2* promoter's ability to interact with distal enhancer elements shared with *H19*. This allows the promoter region of the *H19* gene exclusive access to these enhancers and results in maternal-allele specific expression of *H19*. Conversely, on the paternal allele, the ICR is methylated and this prevents CTCF binding. The *IGF2* promoter can now interact with the enhancers and is expressed from this chromosome. Studies examining

the potential mechanism of this paternal allele insulation by the ICR suggest that it is the physical interaction of the shared enhancers with the paternal promoters of the *IGF2* gene, through chromosomal looping, that allow the distal enhancers to activate paternal *IGF2* transcription (Thorvaldsen et al., 1998). Also, DNA methylation on the paternal ICR leads to secondary methylation of the H19 promoter and H19 becomes silenced on the paternal chromosome (Bartolomei, 2009). The means by which the ICR on the maternal allele represses *IGF2* expression is still contentious. Studies have suggested CTCF binding at the ICR mediates chromosomal looping at a silencer element within the *IGF2* gene that restricts the *IGF2* promoter's access to the shared enhancers, or that CTCF-mediated looping permits the enhancers to interact exclusively with the *H19* gene (Kurukuti et al., 2006; Murrell et al., 2004a; Yoon et al., 2007). More studies are necessary to determine the precise CTCF insulator mechanism employed on the maternal allele.

Adding another layer of complexity, studies have characterized the *IGF2* gene as containing 3 DMRs (DMR0 located within the P0 promoter, DMR1 located downstream of the P0 promoter, and DMR2 spanning the peptide-coding exons) (Bell and Felsenfeld, 2000; Eden et al., 2001; Moore et al., 1997; Murrell et al., 2004b) (**Fig. 2.1B**). All of these regulatory elements act combinatorially to precisely regulate *IGF2's* spatial and temporal expression levels (Bartolomei, 2009).

Overexpression of *IGF2* and aberrant imprinting of *IGF2* at these regulatory elements is known to play a role in congenital growth disorders such as BWS but also in various cancers such as Ewing's sarcoma, Wilm's tumor and colorectal cancer (Cui et al., 2003; Steenman et al., 1994; Zhan et al., 1995). In ACC, close to 90% of these cancers

exhibit IGF overexpression. These ACCs express greater than 100 fold higher levels of *IGF2* mRNA when compared to benign adenomas or normal adrenal tissues (de Fraipont et al., 2005; Giordano et al., 2009; Giordano et al., 2003). Whether *IGF2* upregulation is active and results in downstream signaling remains unknown. Moreover, the mechanism by which loss of imprinting at this locus leads to *IGF2* overexpression is not known.

In this chapter, we characterize the role and mechanism of *IGF2* upregulation and IGF signaling in ACC. Transcriptional profiling data derived from DNA microarray analysis of human adrenal tumors indicate locus dysregulation of the 11p15.5 chromosomal region, with the *IGF2* gene as the single highest upregulated transcript, while two other genes within this locus (*H19* and *CDKN1C*) are reciprocally downregulated in the vast majority of carcinomas. RT-PCR for *IGF1/2* transcripts showed most of the human ACC tissue samples and ACC cell lines tested display evidence of constitutive IGF transcript production. Immunohistochemistry and immunoblotting demonstrate most of these ACC samples also possess activation of downstream effector pathways. To explore the possible epigenetic changes that may account for *IGF2* upregulation, we utilized the pyrosequencing technology. This luminometric technique quantifies the degree of methylation of each individual CpG within an island sequentially through 'the sequencing by synthesis' principle. The enzymatically produced luminescence is directly proportional to the amount of pyrophosphate that is released upon nucleotide incorporation by DNA polymerase. Therefore the luminescence is used to quantitate the amount of methylated or unmethylated cytosine in a sample (Colella et al., 2003). Pyrosequencing analyses to determine the methylation status of regulatory regions reveal hypomethylated DMR1 in

all adrenal tissues. However, DMR2 is significantly hypomethylated in ACC samples and the level of hypomethylation is associated with increasing *IGF2* levels. This data provides evidence in support of aberrant epigenetic changes in ACCs resulting in *IGF2* upregulation and activated IGF signaling.

MATERIALS AND METHODS

DNA microarray analysis

The full details of the DNA microarray analysis were reported previously (Giordano et al., 2009). The Affymetrix array data was deposited into GEO (Gene Expression Omnibus) as series GSE10927. All adrenocortical tissues were derived from surgical specimens at the University of Michigan Health System (UMHS) and subsequently processed by the Tissue Procurement Service of the University of Michigan Comprehensive Cancer Center. The UMHS Institutional Review Board approved the laboratory studies using these samples. DNA samples were isolated by following manufacturer's protocols using a DNEasy tissue kit (Qiagen). Concentrations and purity were determined using a spectrophotometer.

Human adrenal tissue microarray

An adrenal-specific tissue array was constructed using human formalin-fixed, paraffin-embedded tissues that correspond to the tissues used for DNA microarray analysis and was stained with either phospho-Akt^{Ser473} (Zymed) or phospho-IGF-1R$^{Tyr1158/62/63}$ (Millipore). Immunoreactivity was scored blindly by a four-tier (negative, low (1+), medium (2+) and high (3+) positive) grading scheme. Due to the limited number of slides available for this type of analysis, we chose to only stain for the phosphorylated forms of Akt and IGF-IR as antibodies directed towards these phospho-moieties have been characterized in several published studies to be very specific for this post-translational event on each particular protein.

Cell lines and cell culture

All standard cell culture reagents were purchased from Invitrogen Life Technologies. The cell lines NCI-H295 (Gazdar et al., 1990), Y1 (Yasumura et al., 1966), and SW13 (Leibovitz et al., 1973) were obtained from American Type Culture Collection. The NCI-H295 and the SW13 cell lines were established from primary invasive human ACCs while the Y1 cell line was established from a spontaneous primary ACC in a LAF1 mouse. The RL251 cell line (Schteingart et al., 2001) cell line was previously described as a cell line generated from a primary human ACC and was generously provided by Dr. David Schteingart (University of Michigan). The ST5 cell line (Mellon et al., 1994) was generated from adrenal tumors in transgenic mice expressing SV40 T-antigen under the control of the promoter for the adrenal-specific human P450 cholesterol side-chain cleavage (P450scc) gene and was generously provided by Dr. Synthia Mellon (University of California at San Francisco). The Y1 and ST5 cell lines were maintained in DMEM supplemented with 7.5% horse serum and 2.5% calf serum. H295 cells were cultured DMEM/F12 media containing 2.5% calf serum supplemented with transferrin, insulin and selenium. RL251 and SW13 cells were maintained in DMEM with 10% FCS. Log phase cells were treated and analyzed as described above and were maintained for no longer than 15 weeks after recovery from frozen stocks.

Immunoblot analysis

Protein extracts from cells and snap frozen xenograft tissues were harvested in lysis buffer (40 mM HEPES, 120 mM sodium chloride, 10 mM sodium pyrophosphate,

10 mM sodium glycerophosphate, 1 mM EDTA, 50 mM sodium fluoride, 0.5 mM sodium orthovanadate, 1% Triton X-100 and Sigma protease inhibitor cocktail) and dissociated using brief sonication pulses on ice. Lysates were cleared by high speed centrifugation, and protein concentrations were determined by Bradford protein assay (BioRad). Proteins (15-30 micrograms per lane) were separated by standard SDS-PAGE and transferred to nitrocellulose. Membranes were incubated overnight with appropriate antibodies, incubated with HRP-labeled secondary antibodies (Roche), and antigens were detected with West Dura ECL Reagent (Pierce Biotechnology). IGF-1R tyrosine phosphorylation levels were assessed by overnight incubation of 500 μg cell lysate with 5 μg IGF-1Rβ antibody, immunoprecipitation with 50 μL Protein A-Agarose (Invitrogen), three lysis buffer washes and SDS-PAGE/immunoblotting with anti-phospho-tyrosine antibody.

RNA extraction and RT-PCR

Total RNA was isolated from tissue culture cells and snap frozen xenograft tissues using TRIzol reagent (Invitrogen) as detailed in the manufacturer's protocol. Following UV quantification of RNA, one microgram was subjected to *iScript* (BioRad) cDNA synthesis and final purification with PCR purification columns (Qiagen). RT-PCR for mRNA expression for *IGF2* and *GAPDH* genes was carried out in a standard thermocycler with species-specific primer sequences as follows: m*IGF2* Fwd TTCTCATCTCTTTGGCCTTCGCCT, m*IGF2* Rev ACGATGACGTTTGGCCTCTCTGAA, h*IGF2* Fwd TGGCATCGTTGAGGAGTGCTGTTT, h*IGF2* Rev GTTTGAAGATGCTGCTGTGCTTCCTC, mIGF1 Fwd ACCTCAGACAGGCATTGTGGATGA, mIGF1 Rev

AGCTTAGTGAGGACTGCCTTGCTT, hIGF1 Fwd GCCTGCGCAATGGAATAAAGTCCT, hIGF1 Rev TGCACTCCCTCTACTTGCGTTCTT. Quantitative RT-PCR analyses with species-specific intron-spanning primers were performed with SYBR Green PCR mix and ABI 7300 q-PCR system (Applied Biosystems). Primer sequences for h*IGF2* Fwd GCTGGCAGAGGAGTGTCC, h*IGF2* Rev GCTGGCAGAGGAGTGTCC, hGAPDH Fwd CCAACCGCGAGAAG, hGAPDH Rev TCCATCACGATGCC. It should be noted that *IGF* transcript levels do not necessarily reflect actual protein levels as post-transcriptional modifications may augment the translational output of these transcripts. After attempts to blot or stain specifically for IGF-II protein were unsuccessful, we used transcript quantitation (i.e., RT-PCR or q-PCR) and immunoblotting/immunostaining for downstream effector pathway members known to be activated by IGF signaling (e.g., phospho-Akt).

Bisulfite conversion and pyrosequencing

DNA samples were isolated by following manufacturer's protocols using a DNEasy tissue kit (Qiagen). Concentrations and purity were determined using a spectrophotometer. Sample DNA was bisulphite converted using EZ-DNA Methylation-Gold kit (Zymo Research) by following manufacturer's protocols. Bisulfite converted DNA was PCR amplified and pyrosequenced using previously published primers (Boissonnas et al., ; Dejeux et al., 2007; Dupont et al., 2004). PCR amplification was carried out with appropriate forward primer and 5'-biotinylated reverse primer using HotStarTaq Master Mix (Qiagen) with annealing temperatures of 50° C for DMR1 and 60° C for DMR2. Amplification for all samples was confirmed with agarose gel

electrophoresis. Pyrosequencing with appropriate sequencing primers were performed on PSQ HS 96 System/PyroMark MD System using Pyro Gold Reagent kits (Biotage) following manufacturer's protocols.

Statistical analysis

Tests between pairs of groups were performed with two-sided two sample T-tests. For more than two groups, two-way ANOVA models were used. Pyrosequencing data was compiled and R^2 values were calculated using Microsoft Excel.

RESULTS

Expression profile of *IGF2* and downstream signaling in human ACC tissues

Using DNA microarray technology, we analyzed mRNA derived from 10 normal adrenal cortices, 22 adrenocortical adenomas (ACAs), and 33 ACCs to reveal gene expression profiles (Giordano et al., 2009). We then generated a heatmap consisting of three genes (*IGF2*, H19, and CDKN1C) located in the 11p15.5 chromosomal region as there is LOH of this locus in 85% of ACCs (Gicquel et al., 2001). As shown in (**Fig. 2.2 A**), the vast majority of ACCs display very specific overexpression of *IGF2* gene transcripts, and concomitant reduced expression of *H19* (a noncoding RNA) and *CDKN1C* (encoding the cell cycle dependent kinase inhibitor, $p57^{kip2}$) genes, suggesting an imprinting defect of this chromosomal region. To validate these microarray results, quantitative RT-PCR (q-PCR) was performed on RNA isolated from three randomly selected ACAs and three ACCs (**Fig. 2.2 B**). Unfortunately, more human samples for this validation step were not available, as most have been processed for histology. Further analysis of active IGF signaling with the six human tumor samples from Fig 2.2 B was performed by immunoblotting for levels of total IGF-1R protein and phosphorylated Akt^{Ser473}, a downstream mediator of active IGF signaling (**Fig. 2.2 C**). Expression of IGF-1R was observed in all six tissues while two ACC samples possessed far greater levels of the receptor. Immunoblotting for phospho-Akt^{Ser473} suggested active IGF signaling in all three ACC samples and in only one ACA sample, but does not rule out activation from other signaling pathways. Interestingly, all six of these tumor samples had varying levels of total Akt compared to their levels of β-actin loading control. One particular adenoma sample (ACA 40) surprisingly displayed no appreciable

levels of Akt. Although immunoblotting revealed more Akt signaling in the ACC samples (all 3 in ACCs vs. 1 ACA sample), the lack of more available samples for this analysis along with the variable expression of IGF-1R and Akt proteins solicited further investigation to determine the extent of IGF-mediated signaling in normal and neoplastic tissues. Thus, we utilized a tissue microarray assay in which slides containing tissues from 24 ACCs, 22 ACAs and 4 normal adrenocortices. These slides were immunostained and scored blindly for phospho-IGF-1R and phospho-Akt^{Ser473} (**Fig. 2.2 D**). Higher intensities of phospho-IGF-1R were observed in ACC samples over ACA and normal adrenal tissue. Positive staining for phospho-Akt^{Ser473} was also observed in the majority of ACCs. However, knowing that approximately 90% of ACC samples possess very high levels of *IGF2* mRNA, the immunohistochemistry should reflect stronger staining intensities of phospho-IGR-1R and phospho-Akt^{Ser473} in a larger proportion of these tumor samples. This, along with data showing variable IGF-1R and Akt expression by immunoblotting, led us to consider possible genomic changes in copy number (e.g., amplifications, deletions, etc.) of the genes encoding IGF-1R and Akt. These types of mutations are a common finding in many types of cancers for both genes (Armengol et al., 2000; Liu et al., 2007). Presence these mutations may account for the protein expression variability observed in these tumor samples. Therefore, we analyzed our microarray data by graphing the mRNA expression of *IGF1R* and *Akt1* for each individual sample (**Fig. 2.2 E)**. We did not observe any significant quantitative change in the levels of either of these two transcripts across all adrenal samples, suggesting these types of genomic changes are not present in ACCs. This does not rule out, however, post-transcriptional changes that may affect the translational productivity of these

transcripts. In summary, molecular profiling of human adrenal tumors demonstrated overexpression of two critical components (*IGF2* by qRT-PCR and IGF-1R by immunoblotting) and coincident active IGF signaling. These results suggest a critical role of the IGF pathway in ACC pathogenesis.

Expression of IGF pathway members and downstream signaling in ACC cell lines

In order to determine the biologic relevance of IGF-1R in ACC, we first assessed the endogenous expression profiles of IGF ligands, IGF-1R, and downstream effectors of IGF-mediated signaling in five ACC cell lines (**Fig. 2.3**). We chose two mouse-derived lines, the Y1 (Cohen et al., 1957) and ST5 (Mellon et al., 1994), and three human lines derived from invasive primary adrenocortical carcinomas, NCI-H295 (Gazdar et al., 1990), SW13 (Leibovitz et al., 1973), and RL251 (Schteingart et al., 2001). Using RNA purified from cells maintained in overnight serum-starved or serum-containing media, semi-quantitative reverse transcriptase PCR was performed to detect *IGF1* and *IGF2* gene expression. The two mouse cell lines expressed *IGF1* while the H295 cells expressed *IGF2* transcript, in agreement with a previous study describing an autocrine role of IGF-II in H295 cells (Logie et al., 1999). Culture conditions, namely the presence of serum, did not appreciably affect *IGF* transcript levels, indicating constitutive expression of these ligands. To assess protein expression, IGF-1Rβ was immunoprecipitated from whole cell lysates, and immunoblotting was carried out. As shown in Fig 2.3, we observed only minimal levels of IGF-1R protein in RL251 cells compared with the four other cell lines. However, there was also variable protein expression observed between the four IGF-1R positive cell lines. Immunoprecipitates were also probed for phospho-tyrosine (a mark of autophosphorylation of the receptor)

and demonstrated receptor activation in all cell lines except RL251. Pathway activation was further confirmed by immunoblotting for phospho-Akt^{Ser473}. Interestingly, the SW13 cells possessed phosphorylated IGF-1R but without activation of Akt, suggesting that receptor activation does not result in downstream signaling activation. This indicates there may be an inactivating mutation in IGF-1R or a mediator of its signaling that uncouples receptor activation from its downstream Akt pathway signaling. As would be predicted, the RL251 cells lacked any response to serum stimulation presumably due to its lack of IGF-1R expression. The two ACC mouse lines (Y1 and ST5) displayed receptor and Akt activation in response to serum stimulation. The H295 cells also responded efficiently to serum stimulation with increased IGF-1R phosphorylation and phospho-Akt. Immunoblots for total protein levels of Akt were used as a loading control. Loading was also confirmed with immunoblotting for β-actin (data not shown). When comparing the molecular profiling of human ACC tumors in Fig. 2.2 (where we observed overexpression of *IGF2* and active IGF signaling) to these results, only the H295 cell line displayed both constitutive overexpression of *IGF2* and active IGF signaling. Although the ST5 and Y1 cell lines displayed active IGF signaling, this may be explained by their constitutive expression of *IGF1*. Taken together, we suggest the H295 cell line displayed characteristics that best recapitulated human ACC *in vitro*. Therefore, we utilized H295 for further experiments described in Chapter 4.

IGF2 DMR1 methylation status in human ACC tissues

As methylation regulates the gene expression of *IGF2* in normal and pathologic states, we examined the DMR regions of this gene. The DMR0, DMR2 and the *IGF2/H19* ICR regions within this locus are homologous between mouse and human

(Boissonnas et al.). There are conflicting reports in regards to whether the human DMR1 CpG islands are involved in regulating the gene expression of *IGF2*, although this homologous region is differentially methylated in the mouse (Dejeux et al., 2007; Murrell et al., 2004b). This element is located between the placental P0 promoter and mesodermal P1 promoter of *IGF2* in both species (Constancia et al., 2000). To investigate whether this region was epigenetically active in human ACC samples, we analyzed the potential methylation marks within this region with pyrosequencing. We examined the methylation status of three separate regions of CpG islands located within DMR1 in DNA purified from 2 normal adrenals, 9 adrenal adenomas and 16 adrenocortical carcinomas. These samples were also used in the DNA microarray analysis discussed above. Each CpG methylation percentage obtained through pyrosequencing for each tissue sample was first averaged within each sample and then compiled into three groups (Normal, ACA, and ACC) to compare combined values to one another (**Fig. 2.4 A-C**). Evaluation of the combined average methylation levels between normal, ACA, and ACC tissues across all three regions of DMR1 revealed no statistically significant difference between tissue types. Additionally, considering 5% methylation is below the methylation detection threshold (i.e. there is no methylation) we conclude this potential DMR is not a functional region of differential methylation in adrenocortical DNA (Colella et al., 2003).

IGF2 DMR2 methylation status in human ACC tissues

The intragenic *IGF2* DMR2 region is located across exon 8 and 9 in the human, where the peptide-coding region of IGF-II protein is encoded (Boissonnas et al., ; Feil et al., 1994). This region is paternally methylated in tissues expressing *IGF2* in both mouse

and human (Murrell et al., 2001). In the mouse, methylation of DMR2 increases expression of a LacZ reporter, implying DMR2 methylation is associated with active *IGF2* expression (Murrell et al., 2001). Thus, we were interested in comparing the methylation status of this region within our human adrenal samples. Pyrosequencing the *IGF2* DMR2 region in adrenal samples revealed a significant decrease in methylation when comparing adenomas and carcinomas to normal adrenal tissue DNA (**Fig 2.5 A**). Plotting each adrenal sample methylation percentage versus their respective *IGF2* transcript level (determined from DNA microarray analysis) revealed a weak inverse relationship between methylation and *IGF2* expression (R^2 value = 0.543) (**Fig 2.5 B**). This result suggests a role for *IGF2* DMR2 methylation in augmenting expression of *IGF2* in adrenal tissues. Interestingly, the adenomas samples had a statistically significant decrease in DMR2 methylation compared to normal tissue or ACCs without a subsequent increase in *IGF2* expression ($P<0.05$). This result suggests a stepwise progression of events may be occurring in which adenomas first acquire loss of DMR2 methylation. As these adenomas theoretically proliferate and progress towards a more malignant phenotype, this continual loss of DMR2 methylation reaches a 'hypomethylation threshold' that can now affect and increase *IGF2* expression. This conjecture is consistent with the progression model of ACC where a clonal expansion of cells acquiring more epigenetic/genetic defects over time causes a more malignant phenotype. However, further experimentation with a larger sample size will be necessary to determine if this is a bona fide pathologic mark in ACCs.

DISCUSSION

Several studies have established high *IGF2* expression as a dominant finding associated with ACC (Gicquel et al., 2001; Gicquel et al., 1997; Giordano et al., 2003; Ilvesmaki et al., 1993; Slater et al., 2006). In this study, we first validated this finding using DNA microarray analysis of our own samples. We then took these observations further by associating *IGF2* overexpression with higher IGF signaling activity in ACC samples to functionally validate IGF-II's activity through downstream signaling activation. As shown in the locus heatmap, *H19* and *CDKN1C* are consistently downregulated within the ACC population, suggesting these two genes may have tumor suppressive roles that are lost with the epigenetic change in the locus. Additionally, *H19* and *CDKN1C* are both paternally imprinted and maternally expressed, whereas *IGF2* is maternally imprinted and paternally expressed (Bartolomei, 2009). This finding supports the hypothesis that aberrant epigenetic changes in the 11p15.5 region of ACC result in the distinct locus signature observed in the microarray analysis. We tested this hypothesis by identifying an epigenetically active DMR2 that is hypomethylated in ACCs in comparison to adenomas and carcinomas.

Distinguishing localized adrenocortical lesions as either benign or malignant remains a critical clinical issue in the management of patients presenting with adrenal masses. This is especially important for patients with excised tumors as they have a high risk of reoccurrence. More prognostic ACC studies are limited by the rarity of these tumors and thus, only a handful of studies have molecularly compared benign and malignant adrenocortical tumors. Although *IGF2* overexpression is widely acknowledged to be important in ACC pathogenesis, the loss of heterozygosity of the

entire 11p15.5 locus has a higher prognostic value than *IGF2* expression alone (11p15 LOH relative risk ratio = 9 vs. *IGF2* overexpression relative risk ratio = 5) (Gicquel et al., 2001). This indicates additional genes within this locus, namely *H19* and *CKDN1C*, play more than a bystander role in ACC and merits further molecular and transgenic studies as to how these three specific genes, in concert, participate in the initiation, maintenance and/or progression of adrenal tumorigenesis.

The *H19* gene is functionally enigmatic as it encodes an RNA that is not translated into protein. Though it is as highly expressed as β-actin transcripts in the developing embryo (Gabory et al., 2006), its overexpression is associated with perinatal lethality (Yoshimizu et al., 2008). This suggests tight control of its expression is necessary for proper development. Interestingly, *H19* has been convincingly described as a tumor suppressor and an oncogene in several different cancer models (Matouk et al., 2007; Yoshimizu et al., 2008). Although uncharacteristic of prototypical cancer promoting or suppressing gene, this may allude to the cellular context in which *H19* expression is dysregulated. *IGF2* is almost always expressed in same tissues as *H19* through their monoallelic expression pattern. Interestingly, transgenic mice designed to disrupt this normal expression through a deleted maternal *H19* gene had an overgrowth phenotype while the reciprocal deletion of the paternal *IGF2* gene led to somatic undergrowth. This suggests *H19* expression affects *IGF2* repression in *cis* and that this *IGF2* overexpression (through maternal *H19* gene deletion) is responsible for the overgrowth phenotype. There is also a recent characterization of a microRNA (miR-675) within the *H19* gene that represses target gene translation (Cai and Cullen, 2007).

How *H19* potentially contributes to ACC pathogenesis has yet to be defined. As Fig. 2.2 A shows, *H19* is expressed at median levels in normal adrenals and ACAs while *IGF2* expression is very low in most samples. This expression pattern may be a reflection of *H19*-mediated suppression of *IGF2* expression in these tissues while in the carcinomas samples, the significant decrease in *H19* expression leads to the loss of this *IGF2* suppressor function and can subsequently enhance *IGF2* expression. Additionally, miR-675 has been recently shown to directly inhibit the tumor suppressor retinoblastoma (RB) in colorectal cancer, a cancer in which *H19* is upregulated (Tsang et al.). If the *IGF2* transcript is also shown to be a direct target of this particular microRNA, downregulation of H19 would further potentiate *IGF2* upregulation through loss of this post-transcriptional regulation. All these conjectured functions of *H19* will require more attention and experimentation in adrenal tumors to more accurately define the role of this non-coding RNA.

The tumor suppressor gene *CDKN1C* encodes the $p57^{kip2}$ protein that functions to negatively regulate cell cycle progression. This imprinted gene lies 800 kilobases upstream of the *IGF2* gene, is part of another ICR in the centromeric 11p15.5, is methylated on its paternal allele and is maternally expressed (Pateras et al., 2009). It is also frequently lost (through LOH) in several human cancers (Enklaar et al., 2006). Inactivating mutations of this imprinted gene are one of the causative defects identified in BWS in humans and modeled in mice (Zhang et al., 1997). Other than its loss of expression, very little is known about the role of this gene in adrenal tumorigenesis. No mutations were found in the *CDKN1C* coding regions of adrenal tumors, suggesting this ACC-specific loss of expression was not likely to come from genetic lesions (although

non-coding regions of the gene were not examined). Also, no studies to date have addressed the epigenetic status of this locus in ACCs. One could easily posit aberrant methylation could lead to loss of this monoallelic expression. In a very interesting study, MEFs treated *in vitro* with exogenous IGF-II displayed a dose-dependent decrease in $p57^{Kip2}$ expression. The protein's expression is also decreased in mice with high serum levels of IGF-II (Grandjean et al., 2000). This suggests that increased IGF-II may be, in part, mediating the decrease in *CDKN1C* gene expression in ACCs. Determining whether direct epigenetic changes at its locus, IGF-II-mediated expression changes, or perhaps the interplay of both would be very insightful in uncovering the mechanism by which *CDKN1C* is participating in ACC pathogenesis.

Research into the control of 11p15.5 imprinting has revealed a complicated regulatory mechanism that involves multiple enhancers, promoters, boundary elements, insulators, histone modifications, DNA looping structures, and other elements which are all allele-specific, and sometimes tissue-, development-, and species-specific (Bartolomei, 2009). For instance, there are three different 11p15.5 epigenetic profiles for three diseases mapped to this locus (BWS, Silver-Russell Syndrome and Wilm's Tumor) (Murrell et al., 2008). Therefore, the finding that the absence of DMR1 methylation in our samples suggest this region is a functionally inactive domain (Dupont et al., 2004). Based on our results, it is plausible that this domain has no functional role in adrenal biology or pathology. The decreased methylation in human DMR2 ACC samples was unexpected. This region has been characterized as a paternally methylated region in *IGF2*-expressing tissues and projected to act as an activator of transcription through the recruitment of transcription complexes (Murrell et al., 2001). If this hypothesis was

assumed to be true for our system and DMR2 was functionally participating in the overexpression of *IGF2*, we would predict increased methylation in the tumors possessing high *IGF2* levels. In most studies, however, it is the methylated DNA that attracts methyl CpG binding proteins that are repressive for transcription (Bird and Wolffe, 1999). Our observation does not necessarily refute this previous study but adds to the difficulty of conceptualizing a general paradigm for *IGF2* imprinting control when confounding factors preclude direct comparisons (i.e., mouse DMR2 versus human DMR2, cell line versus human tissue, normal versus cancer). To fully understand the complex regulation of these imprinted regions and their pathologic significance in ACC, a methylomic analysis throughout all CpG regions (i.e. promoters, DMRs, ICRs) of the locus needs to be conducted in parallel to each sample's *IGF2*, *H19*, and *CDKN1C* gene expression profile. Additionally, evaluating the methylation percentage at each individual CpG is necessary, as this could uncover a potential dominant mark(s) that may direct/regulate the methylation of other CpG regions.

In summary, we generated transcriptional profiling data, which reveal locus dysregulation of the 11p15.5 chromosomal region. This shows *IGF2* upregulation in addition to a reciprocal downregulation of *H19* and *CDKN1C* in human ACC samples. ACC tissues and cell lines show activation of downstream effector pathways. DMR2 is significantly hypomethylated in ACC samples and this change is associated with increasing *IGF2* levels. These data support our hypothesis that epigenetic changes in ACCs can upregulate *IGF2*, activate IGF signaling, and play a role in the pathogenicity of ACC.

ACKNOWLEDGEMENTS

Author Contributions: Ferdous Barlaskar is the first author on this study, conducted the majority of experiments and wrote the manuscript represented in this chapter. Rork Kuick generated the microarray heatmap and analyzed data. Daffyd Thomas performed the human tissue array staining and Thomas Giordano scored the tissue array staining and provided human tumor lysates. Gary Hammer directed the project and revised the manuscript. This work was published in *The Journal of Clinical Endocrinology and Metabolism*, 2009 Jan;94(1):204-12.

The authors acknowledge funding support from the U.S. National Institutes of Health/NIDDKD DK 062027 (Gary Hammer) and the American Cancer Society RSG-04-236 (Gary Hammer). Ferdous Barlaskar is supported through a pre-doctoral fellowship from NIH/Training Program for Organogenesis, T-32-HD007505. We thank Dr. David E. Schteingart and Kristen Stevens for technical support.

Figure 2.1. The imprinted 11p15.5 locus. (**A**) A schematic of genomic imprinting to regulate the monoallelic expression pattern of *H19* and *IGF2*. On the maternal allele, CTCF binds to specific sites on the unmethylated ICR. The CTCF/DNA complex blocks the *IGF2* promoter's ability to interact with distal enhancer elements shared with *H19*. This allows the promoter region of the *H19* gene exclusive access to these enhancers and results in maternal-allele specific expression of *H19*. On the paternal allele, the ICR is methylated and this prevents CTCF binding. The *IGF2* promoter can now interact with the enhancers and is expressed from this chromosome. (**B**) A schematic depicting the general location of the DMRs within the *IGF2* gene.

A

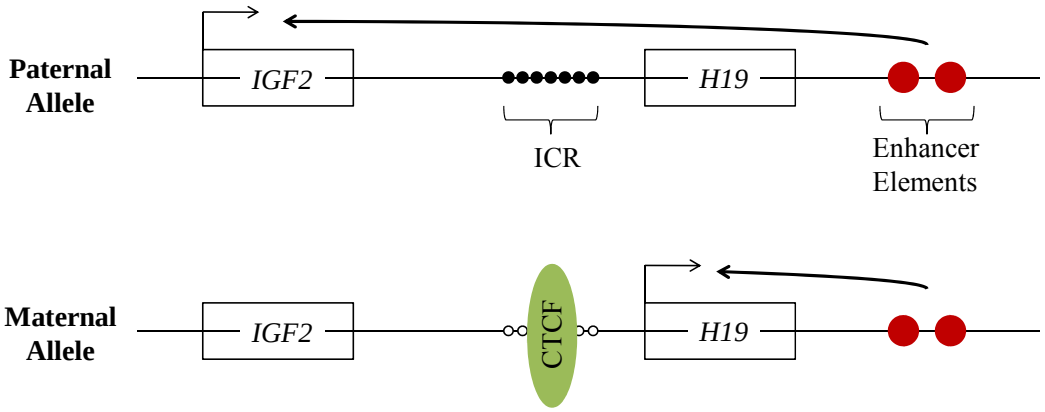
Paternal Allele
IGF2
H19
ICR
Enhancer Elements
Maternal Allele
IGF2
CTCF
H19

B

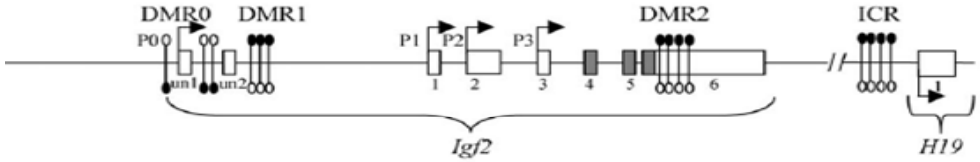
DMR0
DMR1
DMR2
ICR
P0
P1
P2
P3
un1
un2
1
2
3
4
5
6
Igf2
H19

Figure 2.2 Upregulation of *IGF2*, overexpression of IGF-1R and active IGF signaling in human adrenocortical carcinomas in comparison to normal and adenoma tissues. (**A**) Snapshot heatmap of the 11p15.5 chromosomal region generated from Affymetrix U133A 2.0 Plus oligonucleotide array. Shown are the imprinted genes *IGF2*, *H19*, and *CDKN1C* of 65 patient samples consisting of 10 normal adrenal tissues, 22 adrenal adenomas, and 33 sporadic adrenocortical carcinomas. Shades of red indicate increased expression of gene indicated on the right while shades of green reveal decreased expression levels. Numbers below heatmap represent location of tumor samples used for quantitative RT-PCR and immunoblotting. (**B**) Quantitative RT-PCR of three adrenocortical carcinomas and three adenomas for human *IGF2* transcript. The y-axis represents relative *IGF2* message levels normalized to glyceraldehyde 3-phosphate dehydrogenase (GAPDH) transcript levels. Data shown represent the mean +/- S.D. of triplicate samples of one representative experiment. (**C**) Immunoblot analysis of tumor samples described above for IGF-1R expression, Akt, and activated phosho-Akt^{Ser473} as readout for active IGF signaling. Immunoblotting of β-actin is shown as a protein loading control. (**D**) Histologically graded human tissue microarray staining for phospho-IGF-1R and phospho-Akt with results depicted as percentage pie charts. Immunoreactivity was scored blindly by a four-tier (negative, low (1+), medium (2+) and high (3+) positive) grading scheme of 24 ACCs, 22 ACAs, and 4 normal adrenal tissue. (**E**) Graphical representation of the *IGF1R* and *Akt1* gene expression profile for each human adrenal sample. Each sample is grouped into its own cohort (Normal, ACA, and ACC) and plotted for its relative mRNA expression on a base-10 log scale.

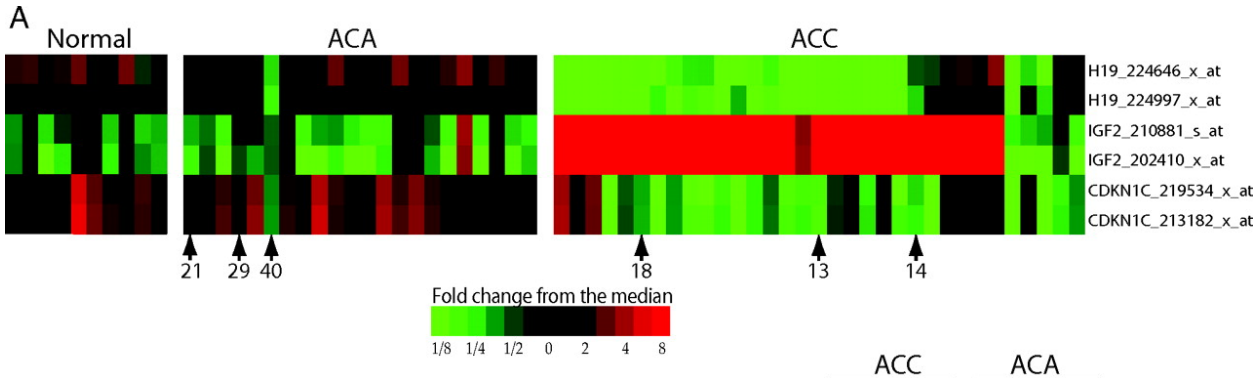
A
Normal
ACA
ACC
H19_224646_x_at
H19_224997_x_at
IGF2_210881_s_at
IGF2_202410_x_at
CDKN1C_219534_x_at
CDKN1C_213182_x_at
21
29
40
18
13
14
Fold change from the median
1/8 1/4 1/2 0 2 4 8

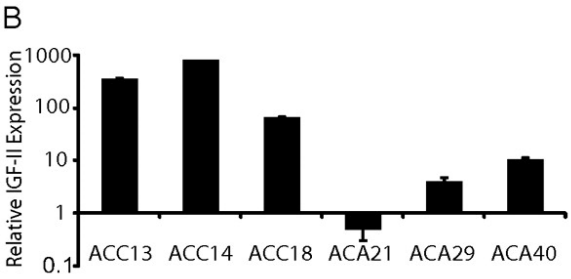
B
Relative IGF-II Expression
1000
100
10
1
0.1
ACC13
ACC14
ACC18
ACA21
ACA29
ACA40

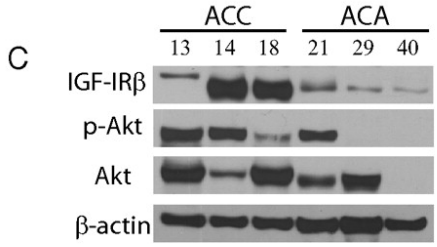
C
ACC
ACA
13 14 18 21 29 40
IGF-IRβ
p-Akt
Akt
β-actin

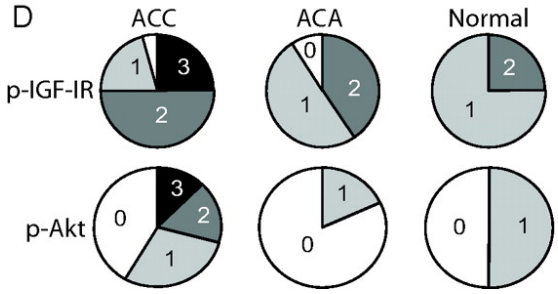
D
ACC
ACA
Normal
p-IGF-IR
p-Akt

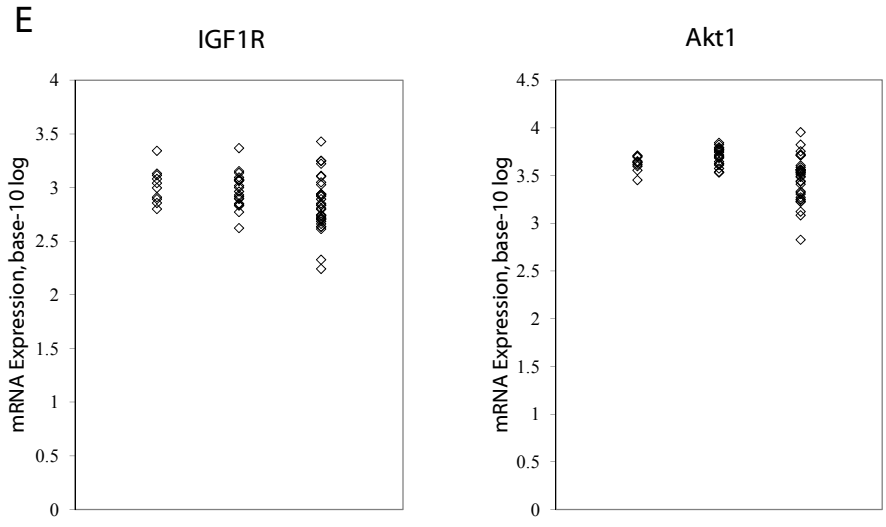
E
IGF1R
Akt1
mRNA Expression, base-10 log

Figure 2.3 Endogenous IGF signaling in a panel of adrenocortical carcinoma cell lines. A panel of mouse (Y1 and ST5) and human (H295, SW13, and RL251) ACC cell lines cultured in serum-free (-) or serum-containing (+) media assessed for endogenous transcript expression of *IGF1* or *IGF2* by gel based RT-PCR (top two panels). Whole cell lysates were immunoprecipitated for the IGF-1Rβ and subsequently immunoblotted for IGF-1Rβ and phospho-tyrosine (middle two panels). Lower two panels show immunoblots from whole cell lysates for phospho-Akt^{Ser473} and total Akt for protein loading control.

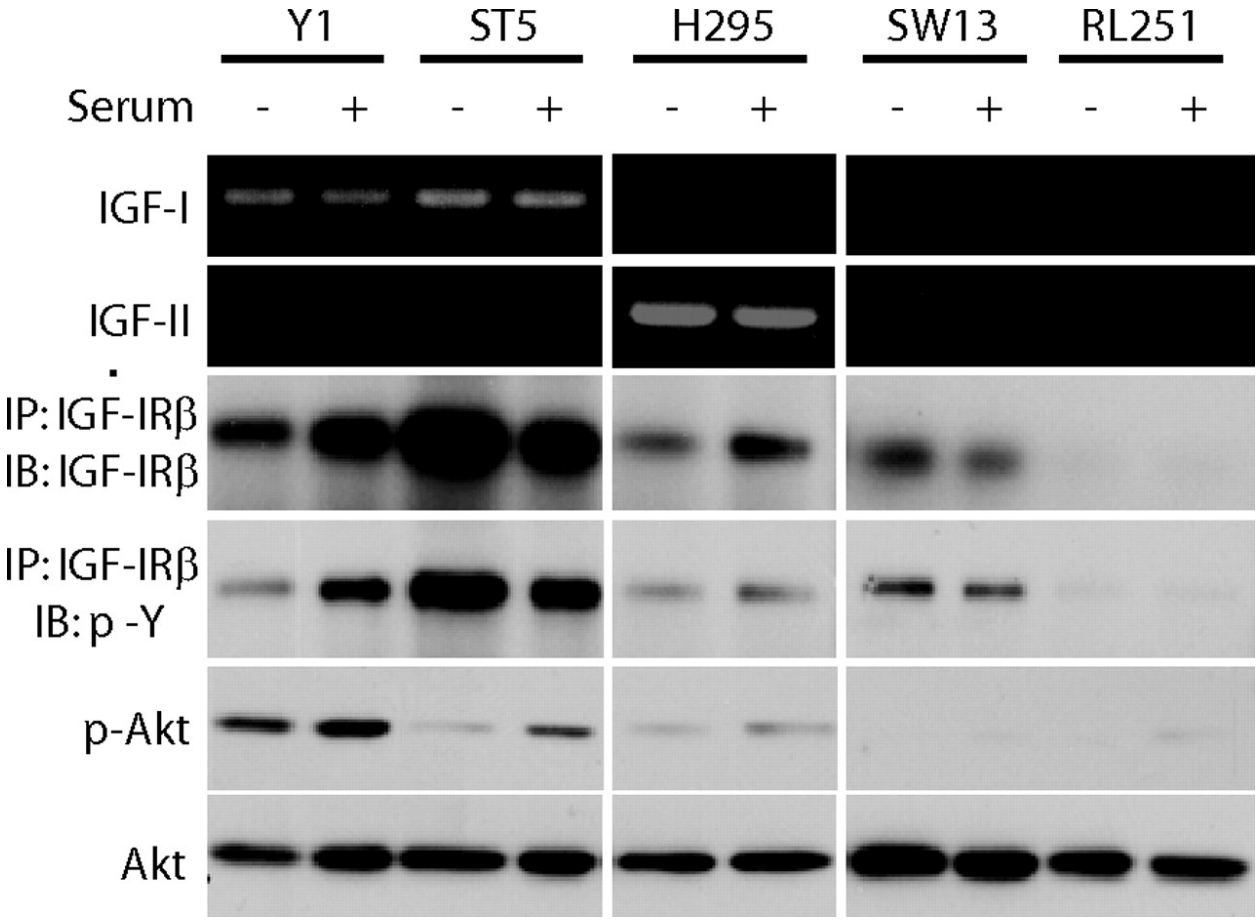
Y1
ST5
H295
SW13
RL251
Serum - + - + - + - + - +
IGF-I
IGF-II
IP: IGF-IRβ
IB: IGF-IRβ
IP: IGF-IRβ
IB: p -Y
p-Akt
Akt

Figure 2.4 DMR1 methylation analysis. Comparison of average methylation percentages from normal adrenal tissues (n=2), adrenal adenomas (n=9) and adrenal carcinomas (n=16) in DMR1 region 1 (**A**), region 2 (**B**) and region 3 (**C**). Error bars represent standard error of the mean.

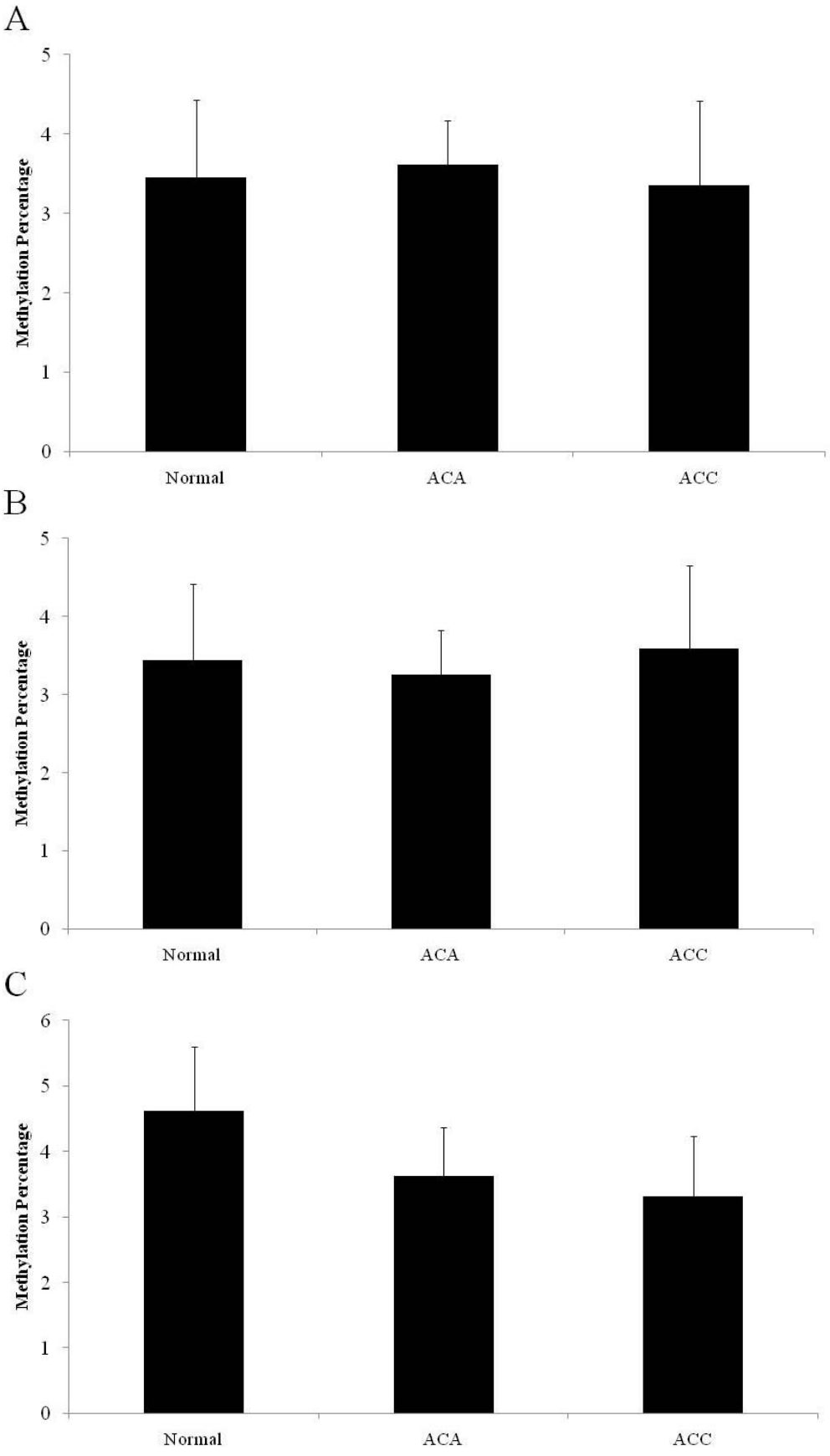
A
Methylation Percentage
0
1
2
3
4
5
Normal
ACA
ACC
B
Methylation Percentage
0
1
2
3
4
5
Normal
ACA
ACC
C
Methylation Percentage
0
1
2
3
4
5
6
Normal
ACA
ACC

Figure 2.5 DMR2 methylation analysis. (**A**) Comparison of average methylation percentages from normal adrenal tissues (n=2), adrenal adenomas (n=9) and adrenal carcinomas (n=16) in DMR2. Error bars represent standard errors of the mean. (**B**) Scatter plot of adrenal sample methylation percentages versus their *IGF2* transcript levels determined from DNA microarray analysis. R^2 value represents the square of the correlation coefficient from linear regression of the data points.

A

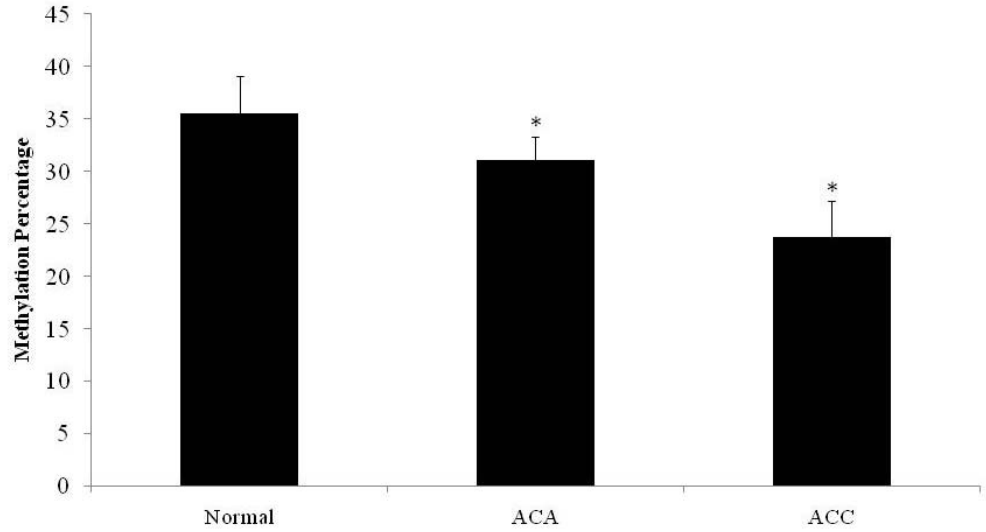
45
40
35
30
25
20
15
10
5
0
Methylation Percentage
*
*
Normal
ACA
ACC

B

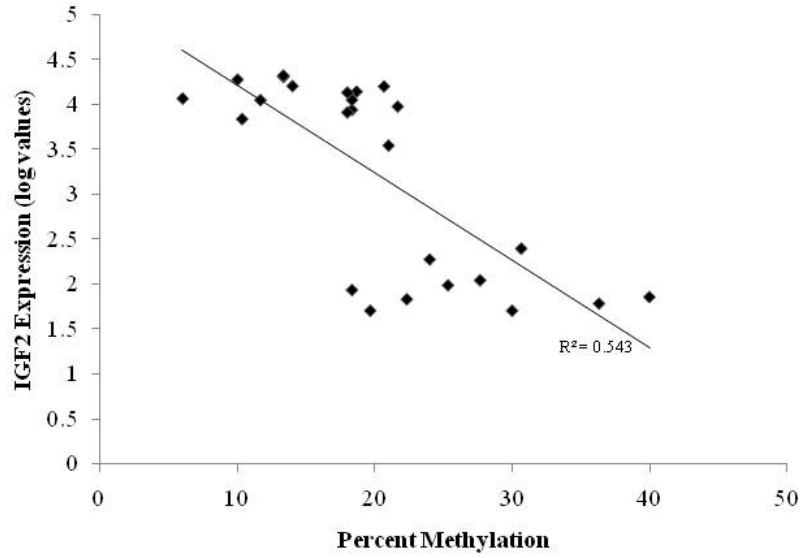
5
4.5
4
3.5
3
2.5
2
1.5
1
0.5
0
IGF2 Expression (log values)
R² = 0.543
0
10
20
30
40
50
Percent Methylation

BIBLIOGRAPHY

Latronico, A.C., Chrousos, G.P., 1997. Extensive personal experience: adrenocortical tumors. J Clin Endocrinol Metab 82, 1317-24.

Koch, C.A., Pacak, K., Chrousos, G.P., 2002. The molecular pathogenesis of hereditary and sporadic adrenocortical and adrenomedullary tumors. J Clin Endocrinol Metab 87, 5367-84.

Libe, R., Bertherat, J., 2005. Molecular genetics of adrenocortical tumours, from familial to sporadic diseases. Eur J Endocrinol 153, 477-87.

Enklaar, T., Zabel, B.U., Prawitt, D., 2006. Beckwith-Wiedemann syndrome: multiple molecular mechanisms. Expert Rev Mol Med 8, 1-19.

Weksberg, R., Shuman, C., Smith, A.C., 2005. Beckwith-Wiedemann syndrome. Am J Med Genet C Semin Med Genet 137C, 12-23.

Feinberg, A.P., 2007. Phenotypic plasticity and the epigenetics of human disease. Nature 447, 433-40.

Tost, J., DNA methylation: an introduction to the biology and the disease-associated changes of a promising biomarker. Mol Biotechnol 44, 71-81.

Garinis, G.A., Patrinos, G.P., Spanakis, N.E., Menounos, P.G., 2002. DNA hypermethylation: when tumour suppressor genes go silent. Hum Genet 111, 115-27.

Hoebeeck, J., Michels, E., Pattyn, F., Combaret, V., Vermeulen, J., Yigit, N., Hoyoux, C., Laureys, G., De Paepe, A., Speleman, F., Vandesompele, J., 2009. Aberrant methylation of candidate tumor suppressor genes in neuroblastoma. Cancer Lett 273, 336-46.

Hatada, I., Fukasawa, M., Kimura, M., Morita, S., Yamada, K., Yoshikawa, T., Yamanaka, S., Endo, C., Sakurada, A., Sato, M., Kondo, T., Horii, A., Ushijima, T., Sasaki, H., 2006. Genome-wide profiling of promoter methylation in human. Oncogene 25, 3059-64.

Scelfo, R.A., Schwienbacher, C., Veronese, A., Gramantieri, L., Bolondi, L., Querzoli, P., Nenci, I., Calin, G.A., Angioni, A., Barbanti-Brodano, G., Negrini, M., 2002. Loss of methylation at chromosome 11p15.5 is common in human adult tumors. Oncogene 21, 2564-72.

Gebert, C., Wrenzycki, C., Herrmann, D., Groger, D., Thiel, J., Reinhardt, R., Lehrach, H., Hajkova, P., Lucas-Hahn, A., Carnwath, J.W., Niemann, H., 2009. DNA methylation in the IGF2 intragenic DMR is re-established in a sex-specific manner in bovine blastocysts after somatic cloning. Genomics 94, 63-9.

Yoshimizu, T., Miroglio, A., Ripoche, M.A., Gabory, A., Vernucci, M., Riccio, A., Colnot, S., Godard, C., Terris, B., Jammes, H., Dandolo, L., 2008. The H19 locus acts in vivo as a tumor suppressor. Proc Natl Acad Sci U S A 105, 12417-22.

Thorvaldsen, J.L., Duran, K.L., Bartolomei, M.S., 1998. Deletion of the H19 differentially methylated domain results in loss of imprinted expression of H19 and Igf2. Genes Dev 12, 3693-702.

Bartolomei, M.S., 2009. Genomic imprinting: employing and avoiding epigenetic processes. Genes Dev 23, 2124-33.

Kurukuti, S., Tiwari, V.K., Tavoosidana, G., Pugacheva, E., Murrell, A., Zhao, Z., Lobanenkov, V., Reik, W., Ohlsson, R., 2006. CTCF binding at the H19 imprinting control region mediates maternally inherited higher-order chromatin conformation to restrict enhancer access to Igf2. Proc Natl Acad Sci U S A 103, 10684-9.

Murrell, A., Heeson, S., Reik, W., 2004a. Interaction between differentially methylated regions partitions the imprinted genes Igf2 and H19 into parent-specific chromatin loops. Nat Genet 36, 889-93.

Yoon, Y.S., Jeong, S., Rong, Q., Park, K.Y., Chung, J.H., Pfeifer, K., 2007. Analysis of the H19ICR insulator. Mol Cell Biol 27, 3499-510.

Bell, A.C., Felsenfeld, G., 2000. Methylation of a CTCF-dependent boundary controls imprinted expression of the Igf2 gene. Nature 405, 482-5.

Eden, S., Constancia, M., Hashimshony, T., Dean, W., Goldstein, B., Johnson, A.C., Keshet, I., Reik, W., Cedar, H., 2001. An upstream repressor element plays a role in Igf2 imprinting. Embo J 20, 3518-25.

Moore, T., Constancia, M., Zubair, M., Bailleul, B., Feil, R., Sasaki, H., Reik, W., 1997. Multiple imprinted sense and antisense transcripts, differential methylation and tandem repeats in a putative imprinting control region upstream of mouse Igf2. Proc Natl Acad Sci U S A 94, 12509-14.

Murrell, A., Heeson, S., Cooper, W.N., Douglas, E., Apostolidou, S., Moore, G.E., Maher, E.R., Reik, W., 2004b. An association between variants in the IGF2 gene and Beckwith-Wiedemann syndrome: interaction between genotype and epigenotype. Hum Mol Genet 13, 247-55.

Cui, H., Cruz-Correa, M., Giardiello, F.M., Hutcheon, D.F., Kafonek, D.R., Brandenburg, S., Wu, Y., He, X., Powe, N.R., Feinberg, A.P., 2003. Loss of IGF2 imprinting: a potential marker of colorectal cancer risk. Science 299, 1753-5.

Steenman, M.J., Rainier, S., Dobry, C.J., Grundy, P., Horon, I.L., Feinberg, A.P., 1994. Loss of imprinting of IGF2 is linked to reduced expression and abnormal methylation of H19 in Wilms' tumour. Nat Genet 7, 433-9.

Zhan, S., Shapiro, D.N., Helman, L.J., 1995. Loss of imprinting of IGF2 in Ewing's sarcoma. Oncogene 11, 2503-7.

de Fraipont, F., El Atifi, M., Cherradi, N., Le Moigne, G., Defaye, G., Houlgatte, R., Bertherat, J., Bertagna, X., Plouin, P.F., Baudin, E., Berger, F., Gicquel, C., Chabre, O., Feige, J.J., 2005. Gene expression profiling of human adrenocortical tumors using complementary deoxyribonucleic Acid microarrays identifies several candidate genes as markers of malignancy. J Clin Endocrinol Metab 90, 1819-29.

Giordano, T.J., Kuick, R., Else, T., Gauger, P.G., Vinco, M., Bauersfeld, J., Sanders, D., Thomas, D.G., Doherty, G., Hammer, G., 2009. Molecular classification and prognostication of adrenocortical tumors by transcriptome profiling. Clin Cancer Res 15, 668-76.

Giordano, T.J., Thomas, D.G., Kuick, R., Lizyness, M., Misek, D.E., Smith, A.L., Sanders, D., Aljundi, R.T., Gauger, P.G., Thompson, N.W., Taylor, J.M., Hanash, S.M., 2003. Distinct transcriptional profiles of adrenocortical tumors uncovered by DNA microarray analysis. Am J Pathol 162, 521-31.

Colella, S., Shen, L., Baggerly, K.A., Issa, J.P., Krahe, R., 2003. Sensitive and quantitative universal Pyrosequencing methylation analysis of CpG sites. Biotechniques 35, 146-50.

Gazdar, A.F., Oie, H.K., Shackleton, C.H., Chen, T.R., Triche, T.J., Myers, C.E., Chrousos, G.P., Brennan, M.F., Stein, C.A., La Rocca, R.V., 1990. Establishment and characterization of a human adrenocortical carcinoma cell line that expresses multiple pathways of steroid biosynthesis. Cancer Res 50, 5488-96.

Yasumura, Y., Buonassisi, V., Sato, G., 1966. Clonal analysis of differentiated function in animal cell cultures. I. Possible correlated maintenance of differentiated function and the diploid karyotype. Cancer Res 26, 529-35.

Leibovitz, A., McCombs, W.M., 3rd, Johnston, D., McCoy, C.E., Stinson, J.C., 1973. New human cancer cell culture lines. I. SW-13, small-cell carcinoma of the adrenal cortex. J Natl Cancer Inst 51, 691-7.

Schteingart, D.E., Giordano, T.J., Benitez, R.S., Burdick, M.D., Starkman, M.N., Arenberg, D.A., Strieter, R.M., 2001. Overexpression of CXC chemokines by an adrenocortical carcinoma: a novel clinical syndrome. J Clin Endocrinol Metab 86, 3968-74.

Mellon, S.H., Miller, W.L., Bair, S.R., Moore, C.C., Vigne, J.L., Weiner, R.I., 1994. Steroidogenic adrenocortical cell lines produced by genetically targeted tumorigenesis in transgenic mice. Mol Endocrinol 8, 97-108.

Boissonnas, C.C., Abdalaoui, H.E., Haelewyn, V., Fauque, P., Dupont, J.M., Gut, I., Vaiman, D., Jouannet, P., Tost, J., Jammes, H., Specific epigenetic alterations of IGF2-H19 locus in spermatozoa from infertile men. Eur J Hum Genet 18, 73-80.

Dejeux, E., Audard, V., Cavard, C., Gut, I.G., Terris, B., Tost, J., 2007. Rapid identification of promoter hypermethylation in hepatocellular carcinoma by pyrosequencing of etiologically homogeneous sample pools. J Mol Diagn 9, 510-20.

Dupont, J.M., Tost, J., Jammes, H., Gut, I.G., 2004. De novo quantitative bisulfite sequencing using the pyrosequencing technology. Anal Biochem 333, 119-27.

Gicquel, C., Bertagna, X., Gaston, V., Coste, J., Louvel, A., Baudin, E., Bertherat, J., Chapuis, Y., Duclos, J.M., Schlumberger, M., Plouin, P.F., Luton, J.P., Le Bouc, Y., 2001. Molecular markers and long-term recurrences in a large cohort of patients with sporadic adrenocortical tumors. Cancer Res 61, 6762-7.

Armengol, G., Knuutila, S., Lluis, F., Capella, G., Miro, R., Caballin, M.R., 2000. DNA copy number changes and evaluation of MYC, IGF1R, and FES amplification in xenografts of pancreatic adenocarcinoma. Cancer Genet Cytogenet 116, 133-41.

Liu, L.Z., Zhou, X.D., Qian, G., Shi, X., Fang, J., Jiang, B.H., 2007. AKT1 amplification regulates cisplatin resistance in human lung cancer cells through the mammalian target of rapamycin/p70S6K1 pathway. Cancer Res 67, 6325-32.

Cohen, A.I., Furth, J., Buffett, R.F., 1957. Histologic and physiologic characteristics of hormone-secreting transplantable adrenal tumors in mice and rats. Am J Pathol 33, 631-51.

Logie, A., Boulle, N., Gaston, V., Perin, L., Boudou, P., Le Bouc, Y., Gicquel, C., 1999. Autocrine role of IGF-II in proliferation of human adrenocortical carcinoma NCI H295R cell line. J Mol Endocrinol 23, 23-32.

Constancia, M., Dean, W., Lopes, S., Moore, T., Kelsey, G., Reik, W., 2000. Deletion of a silencer element in Igf2 results in loss of imprinting independent of H19. Nat Genet 26, 203-6.

Feil, R., Walter, J., Allen, N.D., Reik, W., 1994. Developmental control of allelic methylation in the imprinted mouse Igf2 and H19 genes. Development 120, 2933-43.

Murrell, A., Heeson, S., Bowden, L., Constancia, M., Dean, W., Kelsey, G., Reik, W., 2001. An intragenic methylated region in the imprinted Igf2 gene augments transcription. EMBO Rep 2, 1101-6.

Gicquel, C., Raffin-Sanson, M.L., Gaston, V., Bertagna, X., Plouin, P.F., Schlumberger, M., Louvel, A., Luton, J.P., Le Bouc, Y., 1997. Structural and functional abnormalities at 11p15 are associated with the malignant phenotype in sporadic adrenocortical tumors: study on a series of 82 tumors. J Clin Endocrinol Metab 82, 2559-65.

Ilvesmaki, V., Kahri, A.I., Miettinen, P.J., Voutilainen, R., 1993. Insulin-like growth factors (IGFs) and their receptors in adrenal tumors: high IGF-II expression in functional adrenocortical carcinomas. J Clin Endocrinol Metab 77, 852-8.

Slater, E.P., Diehl, S.M., Langer, P., Samans, B., Ramaswamy, A., Zielke, A., Bartsch, D.K., 2006. Analysis by cDNA microarrays of gene expression patterns of human adrenocortical tumors. Eur J Endocrinol 154, 587-98.

Gabory, A., Ripoche, M.A., Yoshimizu, T., Dandolo, L., 2006. The H19 gene: regulation and function of a non-coding RNA. Cytogenet Genome Res 113, 188-93.

Matouk, I.J., DeGroot, N., Mezan, S., Ayesh, S., Abu-lail, R., Hochberg, A., Galun, E., 2007. The H19 non-coding RNA is essential for human tumor growth. PLoS One 2, e845.

Cai, X., Cullen, B.R., 2007. The imprinted H19 noncoding RNA is a primary microRNA precursor. Rna 13, 313-6.

Tsang, W.P., Ng, E.K., Ng, S.S., Jin, H., Yu, J., Sung, J.J., Kwok, T.T., Oncofetal H19-derived miR-675 regulates tumor suppressor RB in human colorectal cancer. Carcinogenesis 31, 350-8.

Pateras, I.S., Apostolopoulou, K., Niforou, K., Kotsinas, A., Gorgoulis, V.G., 2009. p57KIP2: "Kip"ing the cell under control. Mol Cancer Res 7, 1902-19.

Zhang, P., Liegeois, N.J., Wong, C., Finegold, M., Hou, H., Thompson, J.C., Silverman, A., Harper, J.W., DePinho, R.A., Elledge, S.J., 1997. Altered cell differentiation and proliferation in mice lacking p57KIP2 indicates a role in Beckwith-Wiedemann syndrome. Nature 387, 151-8.

Grandjean, V., Smith, J., Schofield, P.N., Ferguson-Smith, A.C., 2000. Increased IGF-II protein affects p57kip2 expression in vivo and in vitro: implications for Beckwith-Wiedemann syndrome. Proc Natl Acad Sci U S A 97, 5279-84.

Murrell, A., Ito, Y., Verde, G., Huddleston, J., Woodfine, K., Silengo, M.C., Spreafico, F., Perotti, D., De Crescenzo, A., Sparago, A., Cerrato, F., Riccio, A., 2008. Distinct methylation changes at the IGF2-H19 locus in congenital growth disorders and cancer. PLoS One 3, e1849.

Bird, A.P., Wolffe, A.P., 1999. Methylation-induced repression--belts, braces, and chromatin. Cell 99, 451-4.

CHAPTER 3

MODELING LOSS OF IMPRINTING OF *IGF2* LOCUS IN THE MOUSE ADRENAL CORTEX

ABSTRACT

Adrenocortical carcinoma's association with hereditary cancer syndromes and its gene expression profile implicate loss of imprinting (LOI) within the 11p15.5 chromosomal region as a major molecular aberration in ACC pathogenesis. One of the LOI manifestations in this rare but lethal disease is the strong overexpression of insulin-like growth factor 2 (*IGF2*). To examine the role of LOI in the mouse adrenal cortex, we conditionally deleted the *Igf2/H19* imprinting control region. We assessed *Igf2* expression and observed a two-fold increase in transcript levels by quantitative RT-PCR. Immunoblotting of adrenal lysates revealed increased phospho-Akt^{Ser473}, indicative of active IGF signaling. β-catenin (a mediator of canonical Wnt signaling) immunohistochemistry of LOI adrenals at 15 weeks unexpectedly displayed a stronger subcapsular staining. This observation was first confirmed with quantitative RT-PCR to show increased expression of *Axin2* (a canonical Wnt target gene) and also with immunoblotting to demonstrate increased levels of total β-catenin and unphosphorylated β-catenin (a marker of active canonical Wnt signaling). Additionally, we present evidence to suggest that this IGF-II-mediated canonical Wnt activation is achieved through an inhibitory phosphorylation on serine 9 of GSK3β. Histological examination of 30 week adrenals displayed an unexpected progression towards cortical failure. In another conditional mouse model, constitutively active canonical Wnt signaling in the mouse cortex results in dysplastic tissue that eventually progress to adenomas and, in one case, to ACC. Since activation of both IGF and Wnt signaling pathways often occur

together in human ACC, we activated both pathways simultaneously in the mouse adrenal. These double knockout adrenals possessed higher *Axin2* levels and a more severe dysplastic phenotype compared to both LOI adrenals and constitutive Wnt adrenals. This chapter posits a role for IGF-II in mediating activation of canonical Wnt signaling *in vivo* possibly through GSK3β and also proposes a new mouse model that may be prove to be useful in studying adrenocortical tumorigenesis.

INTRODUCTION

Adrenocortical carcinoma (ACC) is an aggressive and often a lethal disease, largely because its escapes diagnosis until it progresses into late stages. Its rarity compounds efforts in understanding its etiology as few clinical samples are available for laboratory studies and its inherent chemoresistence renders most cytotoxic therapies ineffective. These facts prompt the requirement to generate better mouse models of ACC in order to further understand underlying mechanisms and to develop effective targeted therapies (Barlaskar et al., 2008).

Although adrenal cortex tumors may manifest in the context of a familial cancer syndrome, such as Familial Adenomatous Polyposis (FAP) or Beckwith-Wiedemann Syndrome (BWS), the majority of pediatric ACCs, and nearly all adult cases, arise sporadically (Kirschner, 2002). Nevertheless, insights into the pathogenesis of sporadic ACC have been gained from studying these inherited cancer syndromes that include ACC - as both diseases appear to manifest similar molecular profiles (Giordano et al., 2003; Velazquez-Fernandez et al., 2005). Activation of Wnt signaling, the key molecular defect in the vast most cases of FAP (through the loss of the destruction complex member, *APC*), is also a frequent manifestation observed in sporadic cases of both adrenal adenomas and carcinomas (Tissier et al., 2005). Although adrenal tumors have been documented in ~13% of FAP patients these have rarely progressed into ACC (Marchesa et al., 1997; Ono et al., 1991; Smith et al., 2000). The genetic basis of almost all BWS cases has been mapped to the 11p15.5 locus; this same locus is implicated in 85% of sporadic ACCs (Gicquel et al., 2001). *IGF2*, a gene located in 11p15.5 that is an activator ligand in the IGF signaling pathway, is upregulated in 80-90% of ACCs but is

only increased in ~5% of adrenal adenomas (de Fraipont et al., 2005; Gicquel et al., 1997; Giordano et al., 2009; Giordano et al., 2003; West et al., 2007). These observations highlight two pathways strongly associated with adrenal tumorigenesis but also hint at a stepwise genetic order that may be necessary to induce progression of a normal adrenal into an adrenal adenoma and culminating into an adrenocortical carcinoma.

The canonical Wnt signaling pathway regulates diverse cellular processes such as proliferation, specification of cell fate, stem cell maintenance, and differentiation (Clevers, 2006; Logan and Nusse, 2004; MacDonald et al., 2009). Activation of this pathway occurs through binding of a Wnt ligand to a Frizzled/LRP receptor complex at the cell membrane. This receptor complex recruits Dishevelled and Axin to the membrane, resulting in the stabilization of cytoplasmic β-catenin, the main effector of the pathway. Without pathway activation, β-catenin is continually degraded by destruction complex consisting of the four proteins, Axin/Apc/Gsk3β/CK1. β-catenin binding to the destruction complex results in Gsk3β and CK1 to phosphorylate β-catenin. This phospho-β-catenin is now recognized by β-TrCP, an E3 ubiquitin ligase. As a result, the β-catenin is ubiquitinated and targeted for proteosomal degradation. With Wnt pathway activation, disruption of the degradation complex occurs by sequestering Axin to the receptor complex. This increases the abundance and translocation of β-catenin into the nucleus where it interacts with Tcf/Lef transcription factors to activate expression of target genes, such as *Axin2* and *Lef* (Clevers, 2006; Logan and Nusse, 2004; MacDonald et al., 2009).

The IGF signaling pathway plays a pivotal role in normal growth and development (Riedemann and Macaulay, 2006). The IGF-1R is a receptor tyrosine

kinase that is activated by IGFs (IGF-I and IGF-II) outside of the cell that may come from endocrine, paracrine or autocrine sources. IGF-1R activation results in autophosphorylation and subsequent recruitment of specific docking intermediates (e.g. IRS-1, Shc, 14-3-3). These proteins link the IGF-1R to diverse intercellular signaling pathways, which efficiently engage the cell to proliferate, differentiate, and survive. For instance, IRS-1 binding to an activated IGF-1R results in IRS-1 phosphorylation. This results in activation of both the PI3K and MAPK pathways. PI3K activation leads to the generation of PIP_3, which functions as a second messenger to activate several downstream kinases such as PDK1 and Akt. Activated Akt imparts inhibitory phosphorylation on many proteins. One such protein is GSK3β which results in glycogen synthesis among many other cellular effects (Mitsiades et al., 2004; Riedemann and Macaulay, 2006).

Our laboratory has extensively studied the role of canonical Wnt signaling pathway utilizing mouse models. When Wnt signaling is conditionally inactivated in the mouse adrenal cortex through the genetic ablation of β-catenin, two distinct phenotypes occur depending on the extent of inactivation (Kim et al., 2008a). Inactivation within all adrenocortical cells causes embryonic adrenal aplasia and post-natal lethality, emphasizing the indispensible role Wnt signaling plays in cortical development. However, inactivation affecting only ~50% of adrenocortical cells leads to an age-dependent degeneration of the adult adrenal cortex with eventual adrenal failure, which points to this pathway's role in adult cortical tissue maintenance (Kim et al., 2008a). When Wnt signaling is constitutively activated in the cortex through the genetic ablation of the destruction complex member Apc, two distinct phenotypes are also dependent on

the extent of Wnt activation. With full activation of Wnt signaling in all cortical cells, the adrenal develops abnormally and persists in the adult as a gland trapped in an embryonic state (unpublished observations). With Wnt signaling activation in only 50% of the cells, these mice aberrantly expand their cortical progenitor population that eventually results in formation of adrenocortical adenomas and one case of ACC (unpublished observations). Based on these studies characterizing a common molecular defect found in human adrenocortical tumors, we speculated whether LOI in the mouse adrenal cortex could accurately model human ACC and result in the formation of malignant tumors.

In this chapter, we explore LOI, resulting in *Igf2* overexpression, within the mouse adrenal cortex. These LOI mice display higher *Igf2* expression and possess increased IGF signaling activity. Our histological and molecular analyses reveal evidence of active canonical Wnt signaling and hint at GSK3β as a potential crosstalk mediator. Over time, these adrenals display evidence of cortical failure. Adrenals with both LOI and Wnt activation display a severe dysplastic phenotype in comparison to single transgenic mutant adrenals. These results provide evidence supporting IGF-mediated canonical Wnt signaling *in vivo* possibly through GSK3β and also describe new LOI /Wnt activation mouse model that may soon prove to be useful in studying adrenocortical tumorigenesis.

MATERIALS AND METHODS

Mice

Animals used in this study were maintained in facilities approved by the American Association for Accreditation of Laboratory Animal Care in accordance with current regulations and standards of the United States Department of Agriculture and Department of Health and Human Services. Studies were performed in accordance to an institutionally approved protocol under the auspice of the University Committee on Use and Care of Animals at the University of Michigan. Generation and genotyping of transgenic mice with loxP sites flanking the *Igf2*/*H19* ICR have been previously described (Thorvaldsen et al., 2006). Generation and genotyping of transgenic mice with loxP sites flanking exon 14 of the *Apc* gene (resulting in a frameshift mutation in *Apc*) were obtained from Bart Williams (Van Andel Instititue) and have been previously described (Shibata et al., 1997). The *Sf1-Cre* transgene targets Cre recombinase expression to the adrenal cortex and other steroidogenic cells of the mouse and the generation and genotyping of this mouse have been previously described (Bingham et al., 2006). For consistency, data in this chapter is only from male mice (except Fig 3.1 A), however female tissues and timepoints were collected and analyzed to confirm observations noted in the males.

RNA extraction and quantitative RT-PCR

Snap frozen tissues were lysed in TRIzol reagent (Invitrogen) and total RNA was collected as detailed in the manufacturer's protocol. In the case of primary liver culture cells, the total cell pellet was washed once with PBS, and then directly harvested in

Trizol reagent. Following UV quantification of RNA, one microgram was subjected to *iScript* (BioRad) cDNA synthesis and final purification with PCR purification columns (Qiagen). Quantitative RT-PCR analyses with intron-spanning primers were performed with SYBR Green PCR mix and ABI 7300 q-PCR system (Applied Biosystems). Each quantitative measurement was normalized to Rox dye as an internal standard and performed in triplicate. Transcript abundance was normalized to the average C_t value of mouse β-actin for each sample. Statistical significance between pairs of groups was performed with two-sided two sample T-tests. Primer sequences for Axin2: Fwd-5' gcaggagcctcacccttc, Rev-5' tgccagtttctttggctctt, β-actin: Fwd-5' ctaaggccaaccgtgaaaacg, Rev-5' accagaggcatacagggaca Igf2: Fwd-5'gtgctgcatcgctgcttac Igf2: Rev-5'acgtccctctcggacttgg H19: Fwd-5'gaacagaagcattctaggctgg H19: Rev-ttctaagtgaattacggtgggtg

Immunoblotting

Protein extracts from snap frozen tissues were harvested in lysis buffer (40 mM HEPES, 120 mM sodium chloride, 10 mM sodium pyrophosphate, 10 mM sodium glycerophosphate, 1 mM EDTA, 50 mM sodium fluoride, 0.5 mM sodium orthovanadate, 1% Triton X-100 and Sigma protease inhibitor cocktail) and dissociated using brief sonication pulses on ice. Lysates were cleared by high speed centrifugation, and protein concentrations were determined by Bradford protein assay (BioRad). Equal amounts of protein were separated by standard SDS-PAGE and transferred to nitrocellulose. Membranes were incubated overnight with appropriate antibodies, incubated with HRP-labeled secondary antibodies (Roche), and antigens were detected with West Dura ECL Reagent (Pierce Biotechnology).

Immunohistochemistry

Adrenal glands were collected at the indicated ages and fixed for 2 hours in 4% paraformaldehyde/PBS. Tissues were dehydrated in graded ethanol solutions and embedded in paraffin before sectioning. Sections were cut at 6 μm thickness and processed using standard procedures. Hematoxylin and eosin staining slides were deparaffinized in xylenes and rehydrated in graded ethanols followed by deionized water. Sections were stained for 5 seconds in hematoxylin solution, washed in deionized water and stained for 3 seconds in eosin solution. The sections were washed and dehydrated in graded ethanols and xylenes, and then mounted. For immunohistochemical analyses, adrenal glands were processed as above and washed in Tris-buffered saline/0.1% Tween-20 (TBST, pH 7.5). Antigen retrieval was performed by boiling rehydrated sections in 10 mM sodium citrate (pH 6.0) for 20 min, followed by one wash in deionized water and two washes in TBST at room temperature. Antibody stainings were conducted using VECTASTAIN ABC kits and Vector Mouse on Mouse (M.O.M.) kits according to manufacturer's protocol (Vector Laboratories, Burlingame, CA). Tissue sections were blocked in antibody diluent solution for 1 hour, and then incubated overnight at 4 degrees C with anti-β-catenin (610154) (1:1000, BD Biosciences), anti-β-catenin (H-102) (1:500, Santa Cruz Biotechnology), anti-tyrosine hydroxylase (1:500, Pel-Freez Biologicals), and anti-Sf1 (1:1000 dilution and generously provided by Dr. Ken Morohashi). The next day, the sections were washed, exposed to secondary antibodies, and processed for signal detection according to the manufacturer's protocols. Bands were analyzed by the ImageJ software (http://rsbweb.nih.gov/ij/).

RESULTS

Confirmation of tissue-specific LOI-mediated activation of *Igf2* expression

We previously characterized two Sf1/Cre transgenic lines (the Sf1 promoter driving Cre expression) to show one strain contained five copies of the transgene while the other had one copy. As predicted, the strain with one transgene copy is a weaker, mosaic driver of recombination (~50% of the cortical cells recombined to express the reporter gene compared to ~100% with the other strain) but, importantly, both possessed similar sites of expression (Kim et al., 2008a). For these studies, we exploited the mosaic transgenic strain with one copy of the Sf1/Cre with the rationale that modeling a true cancer milieu (with the proposed upregulation of a proto-oncogene, *Igf2*) necessitates the presence of normal, unmutated cells in addition to cells harboring the desired mutation. Notably, this mosaic transgenic mouse was used to activate Wnt signaling through loss of *Apc* and resulted in the mouse adrenocortical tumors discussed above (manuscript in preparation). In cultured cells, Cre expression alone has been shown to be toxic (Silver and Livingston, 2001). Importantly, a former graduate student in the lab (Alex Kim) has bred both strains with no floxed constructs and did not observe any histologic signs of Cre-mediated toxicity between Cre+ and Cre- littermate controls.

The conditional *Igf2/H19* ICR (LOI) strain was originally characterized in neonatal liver, through crosses with Albumin-Cre mice, to show this region is necessary for maternal allele silencing (Thorvaldsen et al., 2006). A maternally inherited ICR deletion led to expression of *Igf2* from the maternal allele (i.e. biallelic expression of *Igf2* led to ~2 fold higher expression) (Thorvaldsen et al., 2006). To characterize the loss of

imprinting in the adrenal cortex, our breeding scheme was to cross female $ICR^{loxP/loxP}$ mice with male Sf1/Cre+ mice to obtain Sf1/Cre– $ICR^{wt/loxP}$ (controls) and Sf1/Cre+ $ICR^{wt/loxP}$ (LOI experimentals) F1 progeny with an excised maternally-inherited ICR (**Fig 3.1 A-B**). We first tested the ability of the Sf1/Cre to specifically recombine and excise the ICR only in tissues where Sf1 is expressed using DNA isolated Sf1 expressing tissues (the adrenal and gonad) and non-Sf1 expressing control tissue (liver) (**Fig 3.2 A**). This DNA was PCR amplified using primers flanking each boundary of the deleted ICR and amplification confirmed excision occurred only in the Sf1+ tissues and but not in the liver. Primers designed to amplify GAPDH DNA was used as a positive control.

Next, quantitative RT-PCR for *Igf2* and *H19* transcripts were performed on 6 week adrenals harvested from maternally and paternally inherited ICR deletion mice to verify LOI- mediated *Igf2* activation (**Fig 3.2 B**). The paternal inheritance cross served as a negative control for *Igf2* expression. As previously described in the neonatal liver, there was no change in *Igf2* expression in the paternal LOI as this region is predicted to be methylated and thus, protected from CTCF binding. However, no significant *H19* expression changes were detected as previously described in the neonatal liver (Thorvaldsen et al., 1998). This result was compared to a study examining the tissue-specific expression changes observed with the loss of the paternal ICR with the following tissues analyzed: liver, tongue, kidney, heart, lung, gut and brain. Loss of imprinting was observed in all tissues but the extent of change varied widely among all tissues (e.g., 50% reduction of *H19* in liver but 95% *H19* reduction in the kidney) (Thorvaldsen et al., 2002). These results suggest the existence of many tissue-specific regulatory elements within the locus or acting upon the locus that precisely regulate the *H19* and *Igf2*

expression patterns in each tissue. However, no studies have thoroughly examined the expression changes of *Igf2* or *H19* with LOI over time. Potentially, temporal changes to regulatory regions during tissue turnover, proliferation, and/or senescence may also account for some of the expression differences observed in neonatal tissues when compared to expression profiles obtained from adult tissues at various timepoints. Another important caveat to these comparisons is the studies' use of a germline ICR knockout versus our conditional ICR knockout approach.

With the maternal LOI knockout, we saw a statistically significant 1.8 fold increase in *Igf2* expression ($p < 0.05$) which is comparable to what was described in the neonatal liver LOI (~2 fold increase). However, there was no significant change in *H19* transcript levels. This H19 expression result is also not consistent with the paradigm of CTCF binding loss leading to decreased *H19* RNA levels and to what is described in the tissue-specific ICR knockout expression study (Thorvaldsen et al., 2002). Most tissues in this study had, at minimum, a 40% reduction in *H19* levels with loss of the maternal ICR. We wanted to directly confirm this previous study and show this difference in expression patterns was due to tissue-specific regulation of *H19* expression by infecting maternal LOI primary liver cells with adenovirus-expressing Cre recombinase (**Fig 3.2 C**). This significantly increased *Igf2* and decreased *H19* transcript levels ($p < 0.05$), again suggesting some unknown tissue-specific elements (i.e. enhancers, insulators, etc.) may be playing a dominant role in sustaining *H19* expression specifically within the adrenal cortex. Although this experiment is consistent with results in the previously published study, an important caveat to note is our *in vitro* primary culture infection approach versus their germline ICR knockout characterization. Specifically, we could not

recapitulate the dosage of Cre, compare the excision efficiency or the percentage of unexcised cells, or control for any potential toxicity effect of virally-induced Cre expression (Silver and Livingston, 2001).

15 week LOI adrenals possess activated canonical Wnt signaling

Transactivation of endogenous mouse *Igf2* results in a BWS-like syndrome and postnatal overexpression of mouse *Igf2* results in significant adrenocortical hyperplasia (Sun et al., 1997; Weber et al., 1999). These and other studies led us to design our experiments to study our LOI mouse model at specific timepoints. At 15 weeks of age, the histologic architecture of the LOI adrenals versus littermate controls by hematoxylin and eosin staining were similar in four littermates (**Fig 3.3**). Two LOI adrenals did exhibit cortical expansion and displaced medullar tissue, as assessed by Sf1 (a cortical marker) and TH (a medullar marker) immunohistochemistry, respectively. There were no statistically significant differences in adrenal weights between experimental and controls (data not shown). Intriguingly, all 6 LOI adrenals displayed a stronger β-catenin staining in the cortical subcapsular area compared to controls.

We next performed quantitative RT-PCR specifically for *Axin2*, a canonical Wnt target gene, and found a statistically significant 1.76 fold increase in its transcription in the LOI adrenals ($p < 0.05$) while *Igf2* and *H19* expression levels were similar to what was described above for 6 week adrenals (**Fig 3.4 A**). We tested this potential crosstalk between IGF and Wnt signaling further by performing immunoblots for activated proteins (**Fig 3.4 B**). In the LOI adrenals, there was increased phospho-Akt^{Ser473}, indicating active IGF signaling (ImageJ estimates 47% increase). Additionally, the bands

for total β-catenin and active β-catenin were also stronger in the LOI adrenals indicating increased abundance of β-catenin and increased stabilized (i.e. transcriptionally active) β-catenin (ImageJ estimates 12% and 67% increase, respectively). Finally, phospho-GSK3β ^{Ser9} is also much stronger in the knockout. As described above, GSK3β is a serine/threonine protein kinase that participates in both IGF and Wnt signaling (Jin et al., 2008). We currently hypothesize GSK3β may be a possible link between LOI/increased *Igf2* levels and activated canonical Wnt signaling.

30 week LOI adrenals reveal a progression towards organ failure

At 30 weeks of age, we found obvious histological differences between H & E stained LOI adrenals versus controls. Two knockout adrenals are displayed to emphasize the spectrum of these defects. (**Fig 3.5 A**). The far right panel adrenal is hypocellular throughout the entire cortex. With a higher magnification picture, (**Fig 3.5 B**) the adrenal contains giant eosinophilic cells (i.e. cytomegalic) and/or deposits throughout the cortex. The middle panel adrenal displays areas of hypocellularity within the adrenal cortex, suggesting it may have been progressing towards the phenotype observed in the knockout adrenal on the far right. The far left is a representative control tissue for comparison. Also, the knockout adrenal weights at 30 weeks were similar to controls (data not shown). Immunohistochemically, the cortical deposits/cells are Sf1 positive, the medulla look intact and normal and the cortical subcapsular β-catenin staining now look similar to controls.

With the β-catenin staining equal across all samples, we again performed quantitative RT-PCR specifically for *Axin2* and found no difference in the LOI adrenals

versus controls (**Fig 3.6 A**). While *Igf2* and *H19* expression levels are somewhat higher than baseline, this difference is not statistically significant. We also immunoblotted for the same proteins and phospho-proteins and saw no differences that were apparent in the 15 week adrenals (**Fig 3.6 B**).

The histologic appearance of the knockout adrenals is very similar to another transgenic mouse we study that models a human disease called adrenal hypoplasia congenita (manuscript submitted). This occurs due to an eventual failure of the adrenal gland caused by an inactivating mutation in the gene encoding the nuclear receptor Dax1 (*NROB1*) (Mizusaki et al., 2003; Muscatelli et al., 1994). Our characterization of this adrenal phenotype has revealed these adrenals are initially hyperfunctional, as assessed by increased proliferation, enhanced expression of steroidogenic enzymes, and increased steroidogenic (i.e., corticosterone) output compared to controls. As these Dax1 knockout mice age, however, their adrenals progressively lose their hyperproliferative phenotype and eventually succumb to adrenal failure (i.e., marked decrease in proliferation, hypocellular cortex, reduced expression of steroidogenic enzymes, and diminished corticosterone output). We hypothesize this adrenal failure occurs due to Dax1's role in maintaining the tissue stem/progenitor cell population within the adrenal. In support of this hypothesis, Dax1 expression has been characterized as an essential factor in maintaining the undifferentiated/pluripotent state of embryonic stem cells (Kim et al., 2008b). We hypothesize IGF-II's established role in maintaining the niche for embryonic and tissue-specific stem/progenitor cells and Dax1's function in stem/progenitor cell maintenance could be a conceptual link between these two mechanistically different models of adrenal failure.

ACC from an *Apc* knockout mouse displays evidence of second hit

Our lab characterized mice with active canonical Wnt signaling in the cortex which resulted in dysplastic tissue that eventually progressed to adenomas and, in one case, progression to ACC. However, most mouse models of activated canonical Wnt signaling or *Apc* inactivation develop benign tumors that progress to cancer only after another mutation has been acquired (Sakatani et al., 2005). Therefore we assayed for *Igf2* levels by quantitative RT-PCR in the mouse ACC and compared its expression profile to a histologically confirmed adrenal adenoma harvested from an Apc knockout mouse and a normal wildtype adrenal (**Fig 3.7**). Our results revealed >10 fold increase in *Igf2* transcript levels when normalized to normal adrenal tissue. *Axin2* levels were also close to 50 fold higher in the ACC sample which may reflect the contribution of both higher *Igf2* levels and overactive Wnt signaling. Surprisingly, *H19* levels were extremely high (>1000 fold over normal tissue) which is contrary to what is observed in human ACCs. This could be a byproduct of another uncharacterized mutation (e.g., loss of *H19* suppressor, chromosomal translocations or duplications), a cellular response to *IGF2* overexpression, or the acquisition of additional epimutations. It could also be a consequence of the unique adrenocortical-specific *H19* expression pattern described above in Fig. 3.2 B-C. It may also underlie a fundamental difference in *H19* function between mouse and human adrenocortical carcinomas (i.e., tumor suppressor vs. oncogene, respectively). Further molecular characterization of this cancer (e.g., cytogenetics, gene expression profiling, pyrosequencing, etc.) and the possible progression of more ACAs to ACCs in this mouse model (to gain more samples for analysis) would facilitate interpretation of this intriguing result. Taken together, these

results suggest this mouse Apc knockout adrenal may have acquired an additional mutation that led to *Igf2* upregulation during its progression to ACC. However, we do not rule out, and perhaps expect other mutations to be present in this ACC sample.

Initial characterization of an adrenal cortex-specific LOI/Apc double knockout

The combination of upregulated IGF signaling and dysregulated Wnt signaling very often manifest together in human ACC. Based on this fact and combined with our data which suggests LOI was not sufficient to promote adrenal tumorigenesis and that an ACC from an Apc knockout mouse acquired an additional genetic hit resulting in *Igf2* upregulation, we proceeded to model loss of Apc and LOI together in the same mouse (Apc/LOI double knockout). At 15 weeks, quantitative RT-PCR confirmed these adrenals displayed ~3 fold higher *Axin2* levels over its littermate control adrenal (**Fig 3.8 A**). This increase is higher than what is observed in LOI adrenals at 15 weeks (a 1.76 fold increase) and Apc knockout adrenals at 15 weeks (a 1.8 fold increase – unpublished observation). At 30 weeks, the histologic architecture of the LOI adrenals versus littermate controls by H & E staining show the double knockout adrenals are larger in overall size, have a thicker capsular rim and display evidence of dysplasia (**Fig 3.8 B**). Importantly, this dysplasia is more pronounced than Apc knockout tissues at the same age. Also, the LOI phenotype of adrenal failure at 30 weeks is not present, suggesting a rescue or attenuation of the adrenal failure phenotype. Analysis of these adrenals at later timepoints will be assessed to characterize changes from these initial molecular and histologic findings and will determine if the activation of both Wnt and IGF signaling can initiate ACC formation in the mouse adrenal cortex.

DISCUSSION

The key initiating events responsible for adrenocortical tumorigenesis have yet to be convincingly characterized. In this chapter, we describe the phenotype of a transgenic mouse model harboring the upregulation of a key gene implicated in human ACC. We investigated the phenotype of adrenals with loss of imprinting in the *Igf2/H19* locus by conditionally ablating the locus imprinting control region. At earlier timepoints, these LOI mice displayed higher *Igf2* expression with increased IGF signaling activity and possessed evidence of active canonical Wnt signaling. At later timepoints, however, these adrenals progressed towards organ failure. In addition, double transgenic mice harboring LOI and constitutive Wnt signaling displayed histologic evidence of a dysplastic adrenal.

The lack of adrenocortical tumor development in the mouse with LOI was not completely unexpected. Our LOI model only led to a ~2 fold increase in *Igf2* and this is in accordance with a modest 2-3 fold increase in most human tumors displaying LOI (Woodson et al., 2004). However, profiling human ACCs confirm *IGF2* overexpression's frequency (upwards of 90% of ACC's), specificity (~5% of ACAs) and degree (50-1000 fold increase) (de Fraipont et al., 2005; Giordano et al., 2009; Giordano et al., 2003). This highlights two potential caveats in our LOI model.

First, perhaps *IGF2* only contributes in the progression of a benign tumor into a malignant state, essentially participating as a 'second hit'. This hypothesis is supported by a mouse model of intestinal tumorigenesis in which the *Min* mouse (harboring a mutation in *Apc* and a mouse model for FAP) is crossed with an LOI mouse. In comparing LOI(+)/*Min* mice to LOI(-)/*Min* mice, the addition of LOI to the *Min*

background increased the number of intestinal tumors 2.2 fold and the tumor surface area 2.4 fold (Sakatani et al., 2005). If this second hit theory holds true for our LOI mouse model, then our double knockout model may eventually progress from a dysplastic adrenal to ACC. We are currently testing this hypothesis by examining later timepoints in the double knockout mouse and also comparing age-matched single APC knockout adrenals to double knockouts.

Secondly, it is possible this 2 fold increase in *Igf2* is not enough to overcome a theoretical threshold level required for adrenal tumor formation. This hypothesis is partially tested in a mouse model where *Igf2* was overexpressed by more than 25 fold by the use of SV40 large T antigen to induce pancreatic tumors (Christofori et al., 1995). A caveat to this study is that *IGF*2 is not usually overexpressed in human pancreatic tumors but it implies a high level of *Igf2* overexpression can cause tumorigenesis. This strategy may work in regards to ACC modeling in a mouse, but would require the generation of a new transgenic strain. Also, identifying and then modeling the mechanism(s) causing *IGF2* overexpression in ACC is a more favorable approach.

The lack of adrenal tumor formation from *IGF2* overexpression may just reflect the reality that *IGF2* is not a causative mutation in ACC. This ligand has been extensively characterized as a prenatal mitogen for proliferation and survival. Perhaps, this ligand does not elicit as strong of a growth response due to the differences in the cellular milieu between fetal and adult tissues. It may also highlight the caveat of species-specific differences that are commonly encountered when attempting to model human-specific genetic alterations in model systems.

In addition to the Dax1 knockout mouse discussed above, insights can also be drawn from another conditional knockout mouse that addresses the age-dependent adrenal failure phenotype in the LOI mouse. In our conditional Wnt inactivation study through the ablation of β-catenin, we also observed a progressive failure that was not visible at 15 weeks, histologically noticeable in most adrenals by 30 weeks but completely apparent at 45 weeks (Kim et al., 2008a). This comparatively slow progression towards failure may be due to the adrenal cortex's low rates of proliferation and physiologic tissue turnover in comparison to most other organs. Pulse-chase experiments using tritiated thymidine demonstrate that ~200 days (~30 weeks) are necessary for the complete renewal of the mouse adrenal cortex (Kataoka et al., 1996). Since, in the LOI adrenals at 30 weeks, we observed a spectrum of histologically noticeable adrenal failure sections, we are currently waiting to harvest our 45 week timepoints for this study. We also plan to do an ACTH stimulation study in the 45 week cohort to functionally assess the adrenal cortex's ability to produce and secrete corticosterone (Asare, 2007).

Our observation that IGF signaling may activate canonical Wnt signaling could add to a growing body of evidence which suggests that these two pathways interact to coordinate multiple cellular functions dictated by mitogenic stimuli (Jin et al., 2008). We are planning to test whether IGF inhibition abrogates Wnt signaling to assess whether Igf-II signaling is responsible for Wnt activation. Based on our current results, we propose the following working hypothesis for a mechanism of this IGF/Wnt crosstalk: LOI-mediated biallelic production of IGF-II results in increased binding to and activation of the IGF-1R. This receptor communicates its activation to several signal transduction

pathways but the two most prominent being the PI3K/Akt and the MAPK/ERK pathways. Activated phospho-Akt^{Ser473} promotes cell metabolism through an inhibitory phosphorylation of GSK3β on its Ser9, thus promoting the conversion of glucose to glycogen through phospho-GSK3β^{Ser9}'s inability to inhibit glycogen synthase. Phosphorylated GSK3β^{Ser9} now cannot phosphorylate β-catenin in the destruction complex to direct β-catenin's degradation by the proteosome. Unphosphorylated β-catenin (i.e. active β-catenin) can now translocate into the nucleus and transcribe its target genes through binding the Tcf/Lef family of transcription factors.

Although several groups support this model of IGF-mediated Wnt activation (Morali et al., 2001; Satyamoorthy et al., 2001; Weston and Davis, 2001) there are other growth factors (e.g., HGF and EGF) that can signal through the same PI3K/Akt signal transduction pathway (Lu et al., 2003; Muller et al., 2002). Interestingly, there is evidence for direct Akt phosphorylation of β-catenin at its C-terminal Ser552 that induces direct nuclear localization of β-catenin in addition to Akt's indirect regulation through GSK3β inhibition (Fang et al., 2007). Finally, there is also evidence that the MAPK/ERK (through downstream Ras activation) arm of IGF-1R signaling also stimulates Tcf/Lef-dependent transcription (Desbois-Mouthon et al., 2001). We are currently performing experiments to test whether direct Akt activation at Ser552 and Ras activation are inputs for IGF-dependent Wnt activation in our LOI adrenals. Conceivably, identifying where this crosstalk mechanism is occurring could provide new insights for ACC treatment as two activated pathways can be inhibited with one novel therapeutic drug.

ACKNOWLEDGEMENTS

Author Contributions: Ferdous Barlaskar performed all experiments and analysis.

The authors acknowledge funding support from the U.S. National Institutes of Health/NIDDKD DK 062027 (Gary Hammer) and the American Cancer Society RSG-04-236 (Gary Hammer). Ferdous Barlaskar is supported through a pre-doctoral fellowship from NIH/Training Program for Organogenesis, T-32-HD007505. We thank Dr. David E. Schteingart and Kristen Stevens for technical support.

Figure 3.1 Loss of imprinting schematic. (A) Gender-specific mouse breeding strategy employed for the informative cross. (B) Depiction of ICR allele before and after the the Cre-mediated excision event.

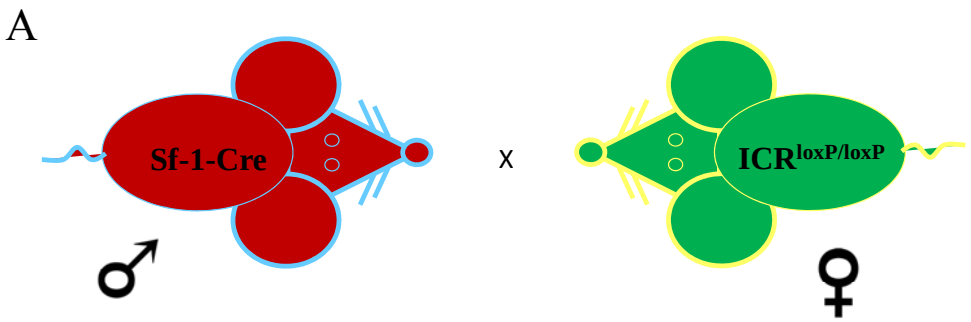
A
Sf-1-Cre
X
ICR loxP/loxP

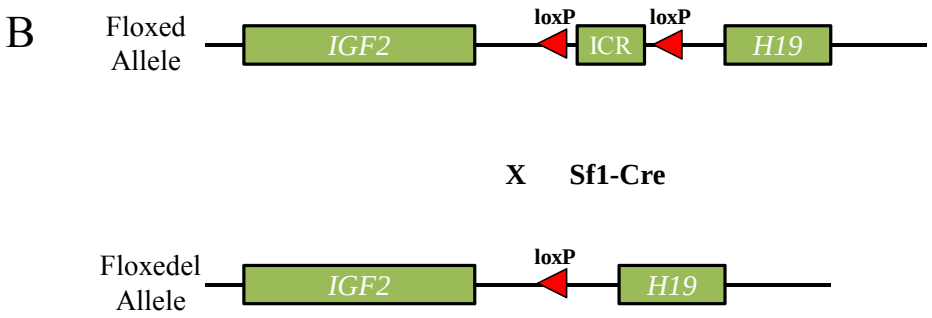
B
Floxed Allele
IGF2
loxP
ICR
loxP
H19
X Sf1-Cre
Floxedel Allele
IGF2
loxP
H19

Figure 3.2 Confirmatory analyses of LOI tissues. (**A**) DNA isolated from the adrenal, ovary and liver of 6 week old Sf1/Cre – and Sf1/Cre + mice were PCR amplified using primers flanking the proximal and distal loxP sites surrounding the ICR to assess tissue-specific recombination. (**B**) Quantitative RT-PCR for *Igf2* and *H19* transcripts were performed on 6 week adrenals from 1) Sf1/Cre– maternal LOI 2) Sf1/Cre+ maternal LOI 3) Sf1/Cre– paternal LOI and 4) Sf1/Cre+ paternal LOI. The y-axis represents relative message levels normalized to each sample's β-actin transcript levels and then normalized to Sf1/Cre– control levels. Data shown represent the mean +/- S.D. of triplicate samples from one representative experiment. (**C**) Quantitative RT-PCR for *Igf2* and *H19* transcripts were performed on primary liver cultures isolated from a 6 week maternal LOI mouse followed by Adeno-Cre viral infection (or sham infection). The y-axis represents relative message levels normalized to each sample's β-actin transcript levels and then normalized to sham infected control levels. Data shown represent the mean +/- S.D. of triplicate samples from one representative experiment.

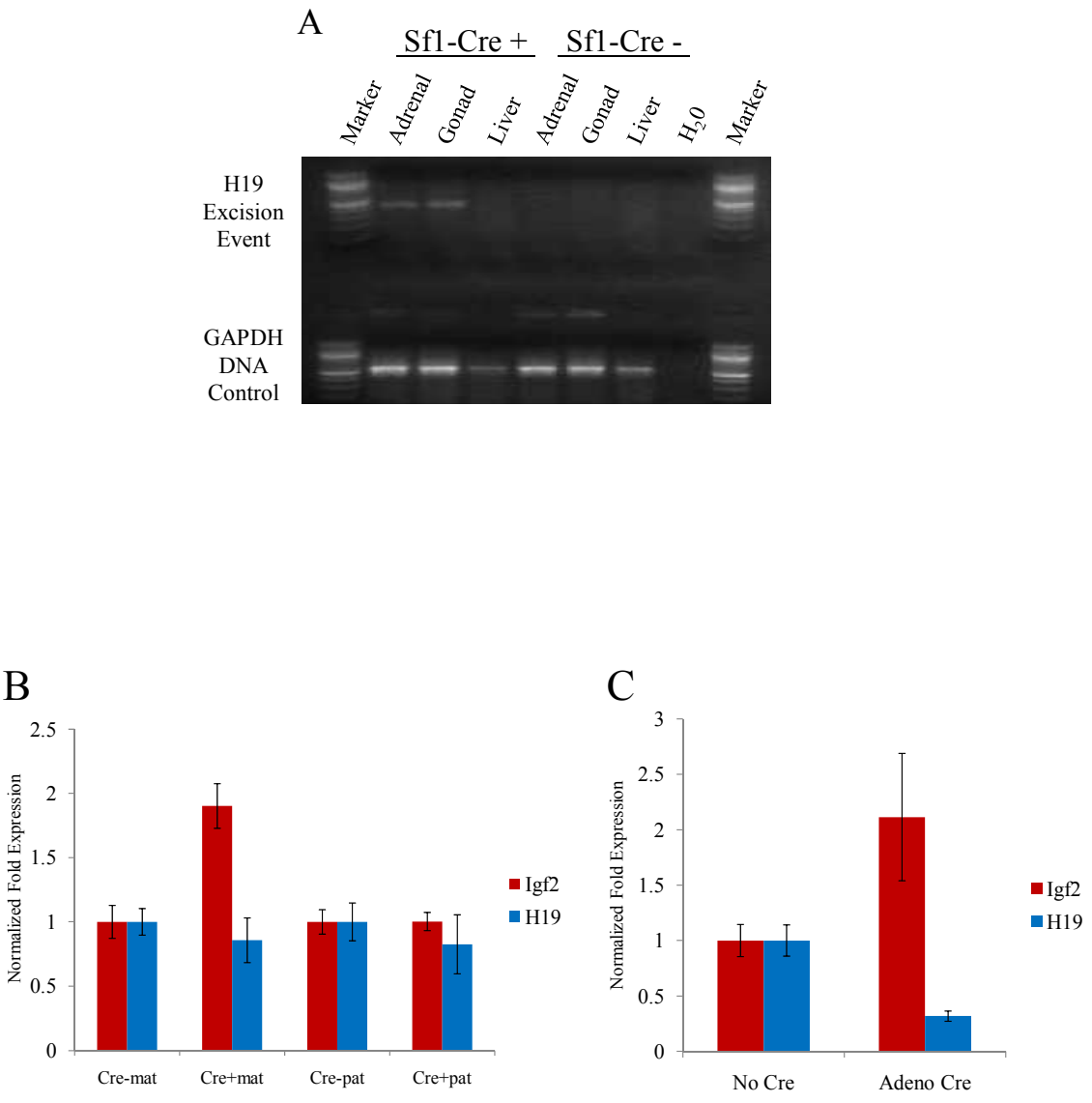
A
Sf1-Cre +
Sf1-Cre -
Marker
Adrenal
Gonad
Liver
Adrenal
Gonad
Liver
H20
Marker
H19
Excision
Event
GAPDH
DNA
Control
B
Normalized Fold Expression
2.5
2
1.5
1
0.5
0
Cre-mat
Cre+mat
Cre-pat
Cre+pat
Igf2
H19
C
Normalized Fold Expression
3
2.5
2
1.5
1
0.5
0
No Cre
Adeno Cre
Igf2
H19

Figure 3.3 Histologic examination of 15 week LOI adrenals. Sectioned adrenal tissues from 15 week old Sf1/Cre– and Sf1/Cre+ maternal LOI littermates were stained by hematoxylin and eosin (H & E). Immunohistochemical analyses were performed with α-Sf1 (adrenal cortex marker), α-TH (adrenal medulla marker) and α-β-catenin (subcapsular adrenal cortex marker) antibodies.

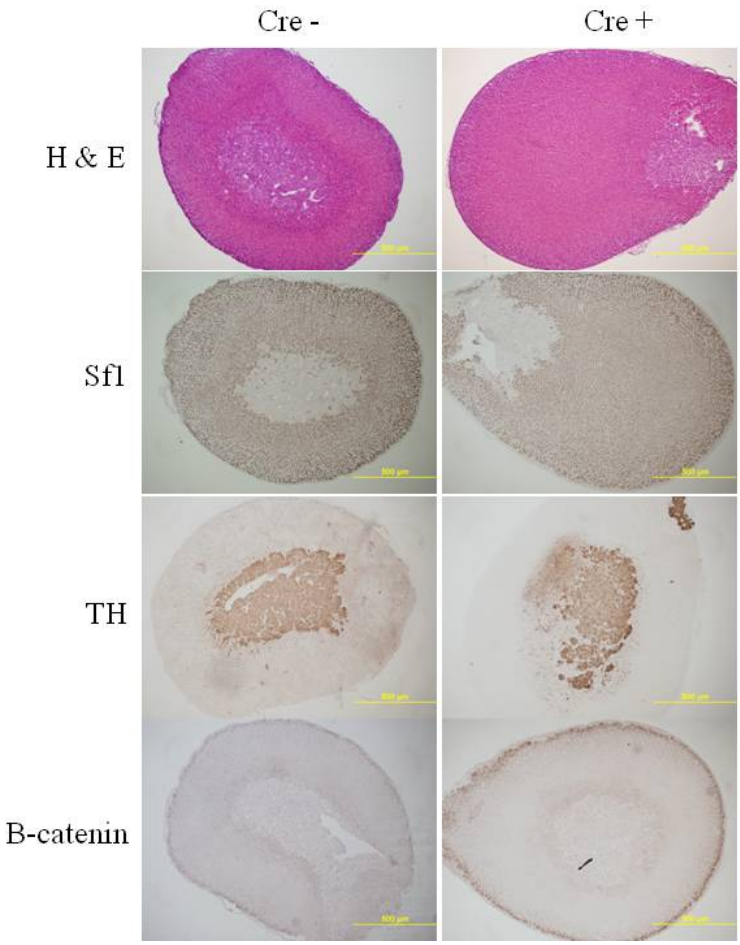
Cre -
Cre +
H & E
Sfl
TH
B-catenin

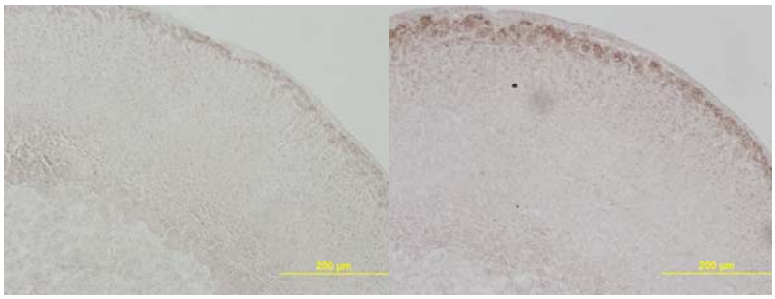
B-catenin
High Mag

Figure 3.4 Biochemical analyses of 15 week knockout adrenals. (**A**) Quantitative RT-PCR for *Igf2*, *H19* and *Axin2* transcripts were performed on 15 week adrenals from Sf1/Cre– and Sf1/Cre+ maternal LOI littermates. The y-axis represents relative message levels normalized to each sample's β-actin transcript levels and then normalized to Sf1/Cre– control levels. Data shown represent the mean +/- S.D. of triplicate samples from one representative experiment. (**B**) Immunoblot analysis were performed on 15 week adrenals from Sf1/Cre– and Sf1/Cre+ maternal LOI littermates using α-Akt, α-phospho-Akt^{Ser473} (indicative of active IGF signaling), α-β-catenin, α-active β-catenin (indicative of active canonical Wnt signaling), α-β-actin, α-GSK3β and α-phospho-GSK3β^{Ser9} (indicative of active destruction complex) antibodies.

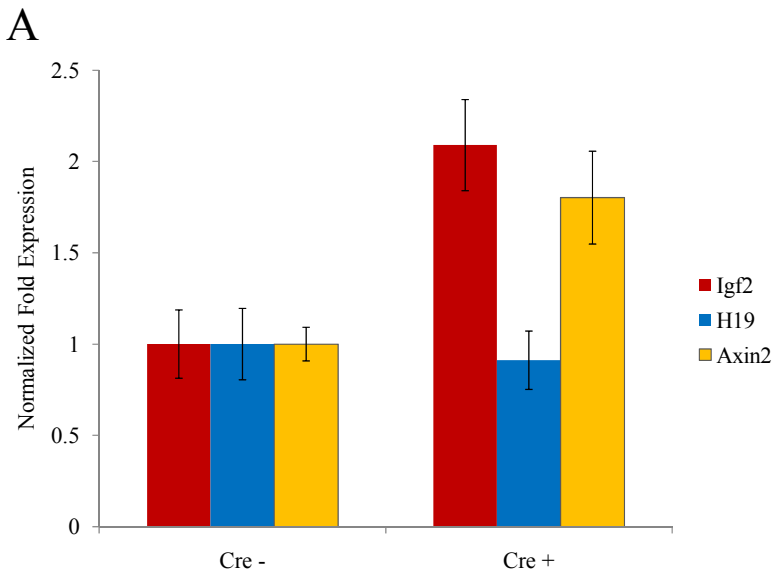
A
2.5
2
1.5
1
0.5
0
Normalized Fold Expression
Cre -
Cre +
Igf2
H19
Axin2

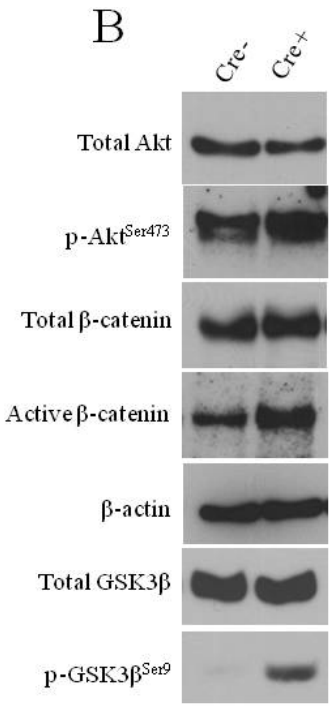
B
Cre-
Cre+
Total Akt
p-Akt Ser473
Total β-catenin
Active β-catenin
β-actin
Total GSK3β
p-GSK3β Ser9

Figure 3.5 Histologic examination of 30 week LOI adrenals. (**A**) Sectioned adrenal tissues from one 30 week old Sf1/Cre– and two Sf1/Cre+ maternal LOI littermates were stained by H & E. Immunohistochemical analyses were performed with α-Sf1 (adrenal cortex marker), α-TH (adrenal medulla marker) and α-β-catenin (subcapsular adrenal cortex marker) antibodies. (**B**) Adrenals from above were photographed at high magnification to illustrate cellularity differences between control and knockout tissues.

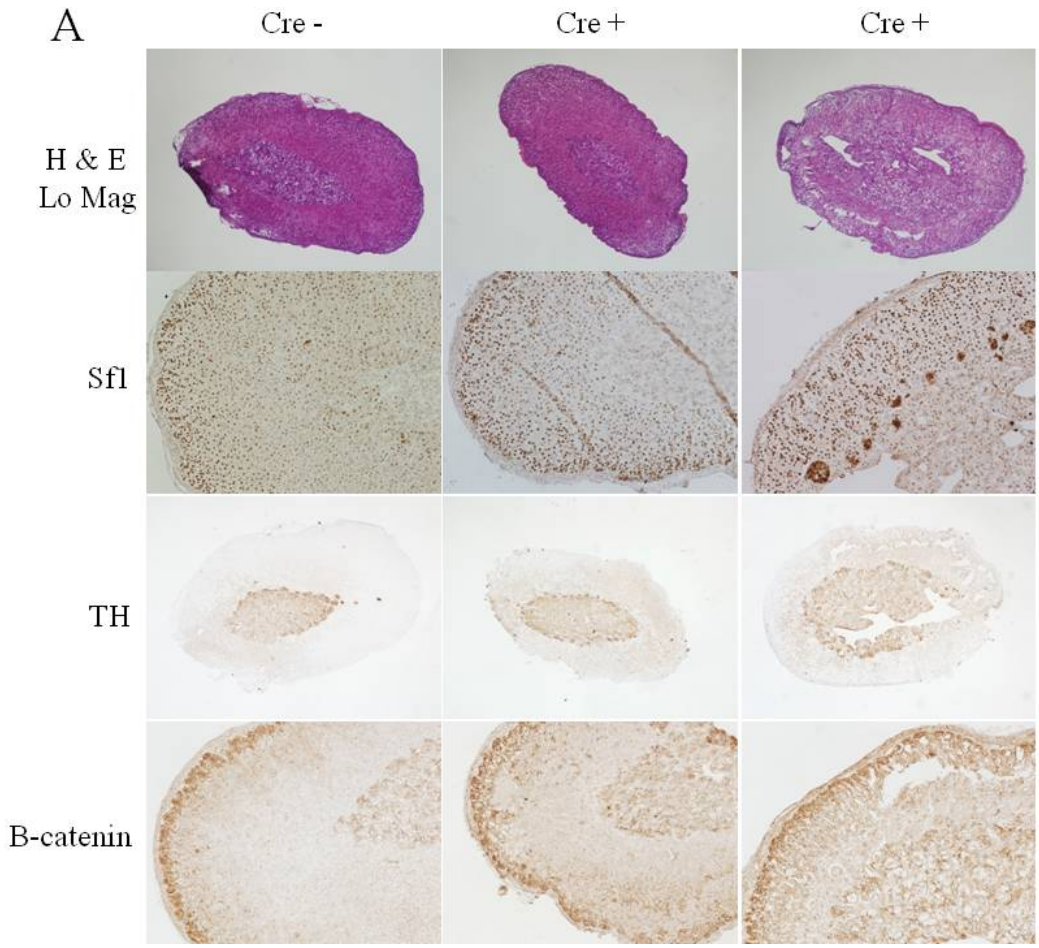
A
Cre -
Cre +
Cre +
H & E
Lo Mag
Sf1
TH
B-catenin

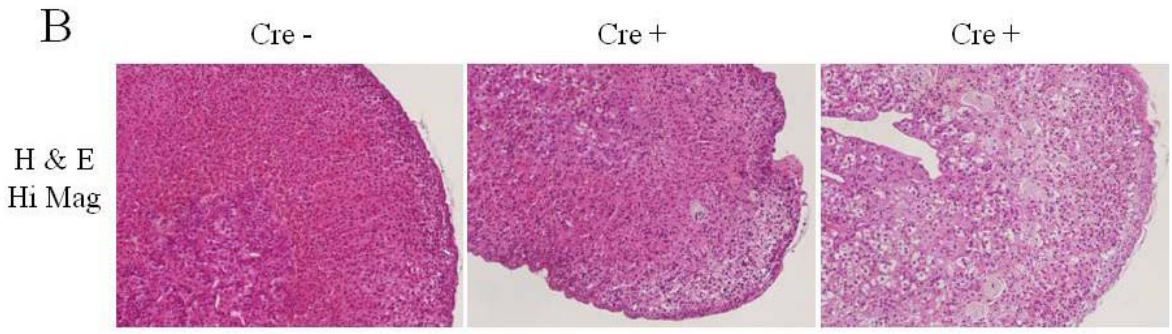
B
Cre -
Cre +
Cre +
H & E
Hi Mag

Figure 3.6 Biochemical analyses of 30 week knockout adrenals. (**A**) Quantitative RT-PCR for *Igf2*, *H19* and *Axin2* transcripts were performed on 30 week adrenals from Sf1/Cre– and Sf1/Cre+ maternal LOI littermates. The y-axis represents relative message levels normalized to each sample's β-actin transcript levels and then normalized to Sf1/Cre– control levels. Data shown represent the mean +/- S.D. of triplicate samples from one representative experiment. (**B**) Immunoblot analysis were performed on 30 week adrenals from Sf1/Cre– and Sf1/Cre+ maternal LOI littermates using α-Akt, α-phospho-Akt^{Ser473} (indicative of active IGF signaling), α-β-catenin, α-active β-catenin (indicative of active canonical Wnt signaling), α-β-actin, α-GSK3β and α-phospho-GSK3β^{Ser9} (indicative of active destruction complex) antibodies.

A

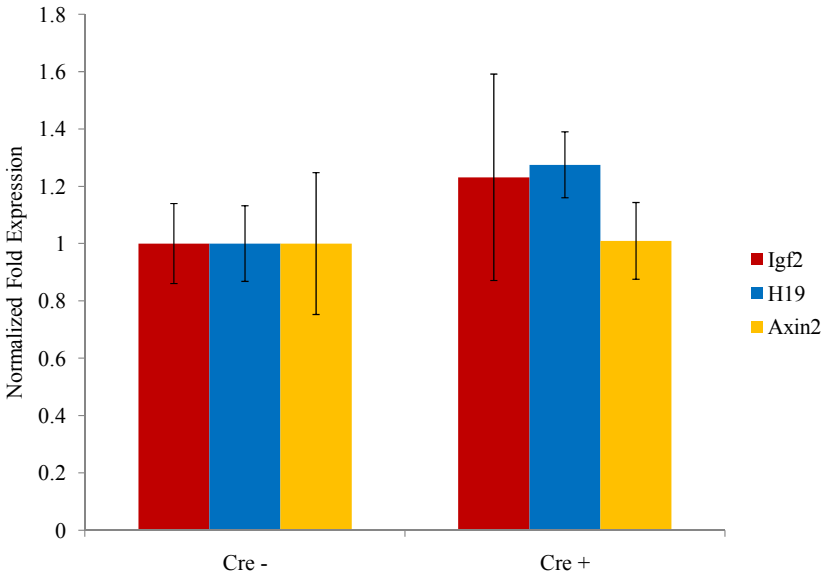
1.8
1.6
1.4
1.2
1
0.8
0.6
0.4
0.2
0
Normalized Fold Expression
Cre -
Cre +
Igf2
H19
Axin2

B

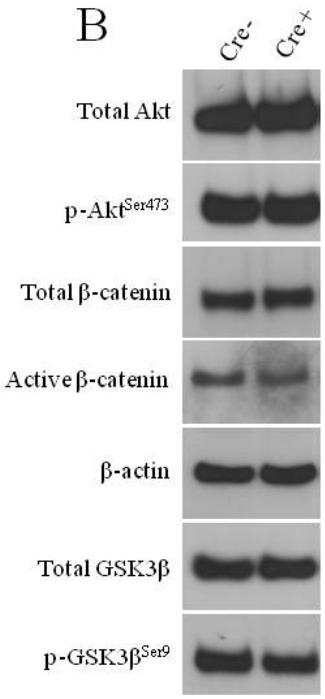
Cre-
Cre+
Total Akt
p-Akt Ser473
Total β-catenin
Active β-catenin
β-actin
Total GSK3β
p-GSK3β Ser9

Figure 3.7 Gene expression analysis of normal and *Apc* knockout mouse adrenals. Quantitative RT-PCR for *Igf2*, *H19* and *Axin2* transcripts were performed on a histologically confirmed normal adrenal tissue (NAT), adrenocortical adenoma (ACA) and an adrenocortical carcinoma (ACC). The NAT was from a Sf1/Cre– mouse and the ACA and ACC were from Sf1/Cre+ Apc knockout mice. The y-axis represents relative message levels normalized to each sample's β-actin transcript levels and then normalized to Sf1/Cre– control levels. Data shown represent the mean +/- S.D. of triplicate samples from one representative experiment.

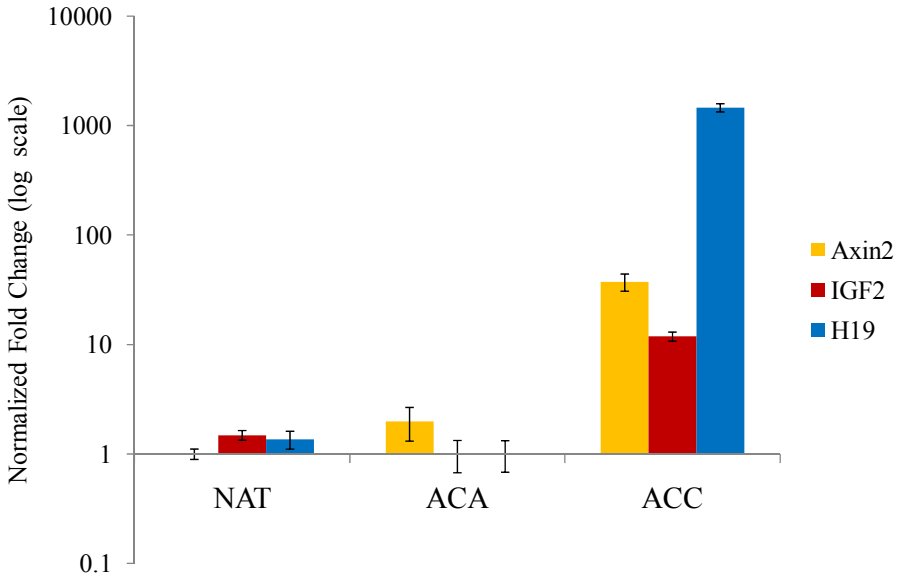
10000
1000
100
10
1
0.1
Normalized Fold Change (log scale)
NAT
ACA
ACC
Axin2
IGF2
H19

Figure 3.8 Biochemical and histologic analysis of Apc/LOI double knockout adrenals. (**A**) Quantitative RT-PCR for *Igf2*, *H19* and *Axin2* transcripts was performed on 15 week adrenals from Sf1/Cre– and Sf1/Cre+ Apc/LOI double knockout (2KO) littermates. The y-axis represents relative message levels normalized to each sample's β-actin transcript levels and then normalized to Sf1/Cre– control levels. Data shown represent the mean +/- S.D. of triplicate samples from one representative experiment. (**B**) Sectioned adrenal tissues from 30 week Sf1/Cre– and Sf1/Cre+ Apc/LOI double knockout (2KO) littermates were stained by H & E.

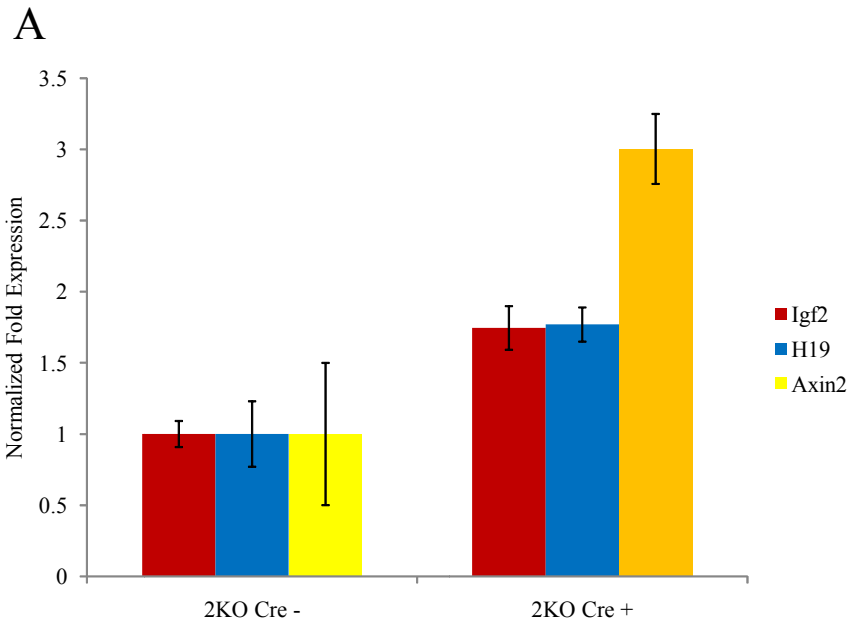
A
3.5
3
2.5
2
1.5
1
0.5
0
Normalized Fold Expression
2KO Cre -
2KO Cre +
Igf2
H19
Axin2

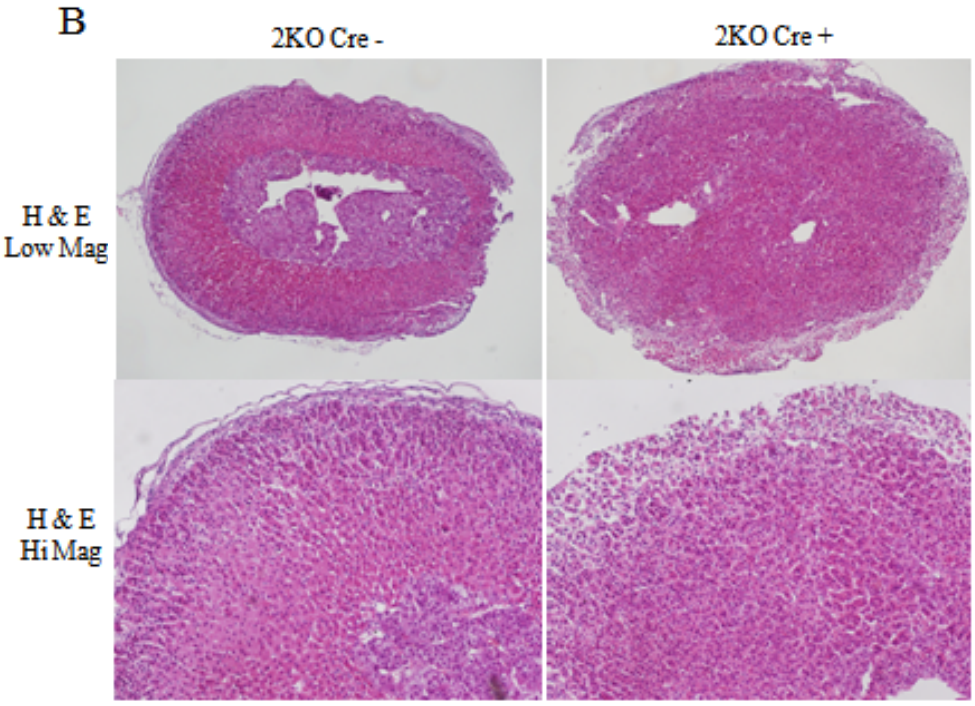
B
2KO Cre -
2KO Cre +
H & E
Low Mag
H & E
Hi Mag

BIBLIOGRAPHY

Barlaskar, F.M., Spalding, A.C., Heaton, J.H., Kuick, R., Kim, A.C., Thomas, D.G., Giordano, T.J., Ben-Josef, E., Hammer, G.D., 2008. Preclinical Targeting of the Type 1 Insulin-like Growth Factor Receptor in Adrenocortical Carcinoma. J Clin Endocrinol Metab.

Kirschner, L.S., 2002. Signaling pathways in adrenocortical cancer. Ann N Y Acad Sci 968, 222-39.

Giordano, T.J., Thomas, D.G., Kuick, R., Lizyness, M., Misek, D.E., Smith, A.L., Sanders, D., Aljundi, R.T., Gauger, P.G., Thompson, N.W., Taylor, J.M., Hanash, S.M., 2003. Distinct transcriptional profiles of adrenocortical tumors uncovered by DNA microarray analysis. Am J Pathol 162, 521-31.

Velazquez-Fernandez, D., Laurell, C., Geli, J., Hoog, A., Odeberg, J., Kjellman, M., Lundeberg, J., Hamberger, B., Nilsson, P., Backdahl, M., 2005. Expression profiling of adrenocortical neoplasms suggests a molecular signature of malignancy. Surgery 138, 1087-94.

Tissier, F., Cavard, C., Groussin, L., Perlemoine, K., Fumey, G., Hagnere, A.M., Rene-Corail, F., Jullian, E., Gicquel, C., Bertagna, X., Vacher-Lavenu, M.C., Perret, C., Bertherat, J., 2005. Mutations of beta-catenin in adrenocortical tumors: activation of the Wnt signaling pathway is a frequent event in both benign and malignant adrenocortical tumors. Cancer Res 65, 7622-7.

Marchesa, P., Fazio, V.W., Church, J.M., McGannon, E., 1997. Adrenal masses in patients with familial adenomatous polyposis. Dis Colon Rectum 40, 1023-8.

Ono, C., Iwama, T., Mishima, Y., 1991. A case of familial adenomatous polyposis complicated by thyroid carcinoma, carcinoma of the ampulla of vater and adrenocortical adenoma. Jpn J Surg 21, 234-40.

Smith, T.G., Clark, S.K., Katz, D.E., Reznek, R.H., Phillips, R.K., 2000. Adrenal masses are associated with familial adenomatous polyposis. Dis Colon Rectum 43, 1739-42.

Gicquel, C., Bertagna, X., Gaston, V., Coste, J., Louvel, A., Baudin, E., Bertherat, J., Chapuis, Y., Duclos, J.M., Schlumberger, M., Plouin, P.F., Luton, J.P., Le Bouc, Y., 2001. Molecular markers and long-term recurrences in a large cohort of patients with sporadic adrenocortical tumors. Cancer Res 61, 6762-7.

de Fraipont, F., El Atifi, M., Cherradi, N., Le Moigne, G., Defaye, G., Houlgatte, R., Bertherat, J., Bertagna, X., Plouin, P.F., Baudin, E., Berger, F., Gicquel, C., Chabre, O., Feige, J.J., 2005. Gene expression profiling of human adrenocortical tumors using complementary deoxyribonucleic Acid microarrays identifies several candidate genes as markers of malignancy. J Clin Endocrinol Metab 90, 1819-29.

Gicquel, C., Raffin-Sanson, M.L., Gaston, V., Bertagna, X., Plouin, P.F., Schlumberger, M., Louvel, A., Luton, J.P., Le Bouc, Y., 1997. Structural and functional abnormalities at 11p15 are associated with the malignant phenotype in sporadic adrenocortical tumors: study on a series of 82 tumors. J Clin Endocrinol Metab 82, 2559-65.

Giordano, T.J., Kuick, R., Else, T., Gauger, P.G., Vinco, M., Bauersfeld, J., Sanders, D., Thomas, D.G., Doherty, G., Hammer, G., 2009. Molecular classification and prognostication of adrenocortical tumors by transcriptome profiling. Clin Cancer Res 15, 668-76.

West, A.N., Neale, G.A., Pounds, S., Figueredo, B.C., Rodriguez Galindo, C., Pianovski, M.A., Oliveira Filho, A.G., Malkin, D., Lalli, E., Ribeiro, R., Zambetti, G.P., 2007. Gene expression profiling of childhood adrenocortical tumors. Cancer Res 67, 600-8.

Clevers, H., 2006. Wnt/beta-catenin signaling in development and disease. Cell 127, 469-80.

Logan, C.Y., Nusse, R., 2004. The Wnt signaling pathway in development and disease. Annu Rev Cell Dev Biol 20, 781-810.

MacDonald, B.T., Tamai, K., He, X., 2009. Wnt/beta-catenin signaling: components, mechanisms, and diseases. Dev Cell 17, 9-26.

Riedemann, J., Macaulay, V.M., 2006. IGF1R signalling and its inhibition. Endocr Relat Cancer 13 Suppl 1, S33-43.

Mitsiades, C.S., Mitsiades, N., Koutsilieris, M., 2004. The Akt pathway: molecular targets for anti-cancer drug development. Curr Cancer Drug Targets 4, 235-56.

Kim, A.C., Reuter, A.L., Zubair, M., Else, T., Serecky, K., Bingham, N.C., Lavery, G.G., Parker, K.L., Hammer, G.D., 2008a. Targeted disruption of {beta}-catenin in Sf1-expressing cells impairs development and maintenance of the adrenal cortex. Development 135, 2593-602.

Thorvaldsen, J.L., Fedoriw, A.M., Nguyen, S., Bartolomei, M.S., 2006. Developmental profile of H19 differentially methylated domain (DMD) deletion alleles reveals multiple roles of the DMD in regulating allelic expression and DNA methylation at the imprinted H19/Igf2 locus. Mol Cell Biol 26, 1245-58.

Shibata, H., Toyama, K., Shioya, H., Ito, M., Hirota, M., Hasegawa, S., Matsumoto, H., Takano, H., Akiyama, T., Toyoshima, K., Kanamaru, R., Kanegae, Y., Saito, I., Nakamura, Y., Shiba, K., Noda, T., 1997. Rapid colorectal adenoma formation initiated by conditional targeting of the Apc gene. Science 278, 120-3.

Bingham, N.C., Verma-Kurvari, S., Parada, L.F., Parker, K.L., 2006. Development of a steroidogenic factor 1/Cre transgenic mouse line. Genesis 44, 419-24.

Silver, D.P., Livingston, D.M., 2001. Self-excising retroviral vectors encoding the Cre recombinase overcome Cre-mediated cellular toxicity. Mol Cell 8, 233-43.

Thorvaldsen, J.L., Duran, K.L., Bartolomei, M.S., 1998. Deletion of the H19 differentially methylated domain results in loss of imprinted expression of H19 and Igf2. Genes Dev 12, 3693-702.

Thorvaldsen, J.L., Mann, M.R., Nwoko, O., Duran, K.L., Bartolomei, M.S., 2002. Analysis of sequence upstream of the endogenous H19 gene reveals elements both essential and dispensable for imprinting. Mol Cell Biol 22, 2450-62.

Sun, F.L., Dean, W.L., Kelsey, G., Allen, N.D., Reik, W., 1997. Transactivation of Igf2 in a mouse model of Beckwith-Wiedemann syndrome. Nature 389, 809-15.

Weber, M.M., Fottner, C., Schmidt, P., Brodowski, K.M., Gittner, K., Lahm, H., Engelhardt, D., Wolf, E., 1999. Postnatal overexpression of insulin-like growth factor II in transgenic mice is associated with adrenocortical hyperplasia and enhanced steroidogenesis. Endocrinology 140, 1537-43.

Jin, T., George Fantus, I., Sun, J., 2008. Wnt and beyond Wnt: multiple mechanisms control the transcriptional property of beta-catenin. Cell Signal 20, 1697-704.

Mizusaki, H., Kawabe, K., Mukai, T., Ariyoshi, E., Kasahara, M., Yoshioka, H., Swain, A., Morohashi, K., 2003. Dax-1 (dosage-sensitive sex reversal-adrenal hypoplasia congenita critical region on the X chromosome, gene 1) gene transcription is regulated by wnt4 in the female developing gonad. Mol Endocrinol 17, 507-19.

Muscatelli, F., Strom, T.M., Walker, A.P., Zanaria, E., Recan, D., Meindl, A., Bardoni, B., Guioli, S., Zehetner, G., Rabl, W., et al., 1994. Mutations in the DAX-1 gene give rise to both X-linked adrenal hypoplasia congenita and hypogonadotropic hypogonadism. Nature 372, 672-6.

Kim, J., Chu, J., Shen, X., Wang, J., Orkin, S.H., 2008b. An extended transcriptional network for pluripotency of embryonic stem cells. Cell 132, 1049-61.

Sakatani, T., Kaneda, A., Iacobuzio-Donahue, C.A., Carter, M.G., de Boom Witzel, S., Okano, H., Ko, M.S., Ohlsson, R., Longo, D.L., Feinberg, A.P., 2005. Loss of imprinting of Igf2 alters intestinal maturation and tumorigenesis in mice. Science 307, 1976-8.

Woodson, K., Flood, A., Green, L., Tangrea, J.A., Hanson, J., Cash, B., Schatzkin, A., Schoenfeld, P., 2004. Loss of insulin-like growth factor-II imprinting and the presence of screen-detected colorectal adenomas in women. J Natl Cancer Inst 96, 407-10.

Christofori, G., Naik, P., Hanahan, D., 1995. Deregulation of both imprinted and expressed alleles of the insulin-like growth factor 2 gene during beta-cell tumorigenesis. Nat Genet 10, 196-201.

Kataoka, Y., Ikehara, Y., Hattori, T., 1996. Cell proliferation and renewal of mouse adrenal cortex. J Anat 188 (Pt 2), 375-81.

Asare, K., 2007. Diagnosis and treatment of adrenal insufficiency in the critically ill patient. Pharmacotherapy 27, 1512-28.

Morali, O.G., Delmas, V., Moore, R., Jeanney, C., Thiery, J.P., Larue, L., 2001. IGF-II induces rapid beta-catenin relocation to the nucleus during epithelium to mesenchyme transition. Oncogene 20, 4942-50.

Satyamoorthy, K., Li, G., Vaidya, B., Patel, D., Herlyn, M., 2001. Insulin-like growth factor-1 induces survival and growth of biologically early melanoma cells through both the mitogen-activated protein kinase and beta-catenin pathways. Cancer Res 61, 7318-24.

Weston, C.R., Davis, R.J., 2001. Signal transduction: signaling specificity- a complex affair. Science 292, 2439-40.

Lu, Z., Ghosh, S., Wang, Z., Hunter, T., 2003. Downregulation of caveolin-1 function by EGF leads to the loss of E-cadherin, increased transcriptional activity of beta-catenin, and enhanced tumor cell invasion. Cancer Cell 4, 499-515.

Muller, T., Bain, G., Wang, X., Papkoff, J., 2002. Regulation of epithelial cell migration and tumor formation by beta-catenin signaling. Exp Cell Res 280, 119-33.

Fang, D., Hawke, D., Zheng, Y., Xia, Y., Meisenhelder, J., Nika, H., Mills, G.B., Kobayashi, R., Hunter, T., Lu, Z., 2007. Phosphorylation of beta-catenin by AKT promotes beta-catenin transcriptional activity. J Biol Chem 282, 11221-9.

Desbois-Mouthon, C., Cadoret, A., Blivet-Van Eggelpoel, M.J., Bertrand, F., Cherqui, G., Perret, C., Capeau, J., 2001. Insulin and IGF-1 stimulate the beta-catenin pathway through two signalling cascades involving GSK-3beta inhibition and Ras activation. Oncogene 20, 252-9.

CHAPTER 4

PRECLINICAL TARGETING OF THE TYPE 1 INSULIN-LIKE GROWTH FACTOR RECEPTOR IN ADRENOCORTICAL CARCINOMA

ABSTRACT

Drug therapy for adrenocortical carcinoma (ACC), a rare and lethal malignancy, is largely empirical and ineffective. New treatments directed at molecular targets critical to the pathophysiology of ACC may prove more efficacious. We examined the efficacy of two IGF receptor (IGF-1R) antagonists both *in vitro* and *in vivo*. We show both antagonists cause significant dose-dependent growth inhibition in ACC cell lines. Furthermore, we observe that mitotane, the first-line adrenolytic drug used for ACC treatment in patients, results in enhanced growth inhibition when used in combination with the IGF-1R antagonists. We next examined the activity of these IGF-1R antagonists against human ACC xenografts in athymic mice. IGF inhibition markedly reduced tumor growth greater than that observed with mitotane treatment and combination therapy with mitotane significantly enhanced tumor growth suppression. Importantly, this anti-proliferative effect is dependent upon the expression of IGF-II and its receptor, thus identifying a potential biomarker to select patients who may benefit from this treatment. These findings establish the critical role of IGF signaling in ACC pathophysiology and provide rationale for the use of targeted IGF-1R antagonists to treat adrenocortical carcinoma in future clinical trials.

INTRODUCTION

Adrenocortical carcinoma (ACC) is a rare endocrine malignancy characterized by a limited understanding of its development and pathophysiology, a dismal clinical prognosis, and a lack of efficacious therapeutic regimens. The annual incidence of ACC ranges from 0.5 to 2 cases per million (Wajchenberg et al., 2000). While complete operative resection remains the only potentially curative option for ACC, approximately half of all patients present with metastatic disease (Allolio and Fassnacht, 2006; Wajchenberg et al., 2000). This results in a 5 year survival rate of less than 10% (Icard et al., 2001; Wajchenberg et al., 2000). ACCs are highly resistant to cytotoxic therapies, thus when complete surgical resection is not possible, therapy with mitotane in combination with other chemotherapies has response rates of only 20-33% (Kirschner, 2006). A better understanding of the etiology and pathogenesis of this devastating disease could lead to more effective drug designs and the development of molecularly targeted treatments.

ACC's association with a select number of genetic syndromes such as Beckwith-Wiedemann Syndrome (BWS) has provided insights into its pathophysiology. BWS arises from a loss of heterozygosity and/or a loss of imprinting of the 11p15.5 chromosomal region. In patients, this mutation clinically manifests with gigantism, macroglossia and a concomitant predisposition to cancers such as ACC. The 11p15.5 locus includes the mitogenic hormone, insulin-like growth factor-2 gene (*IGF2*), and locus dysregulation results in its significant overexpression. Transcriptional profiling of sporadic ACC tissues provides additional support for this hormone's pathogenic role. We and others have shown *IGF2* as the single most up-regulated transcript in 80-90% of

ACCs (Giordano et al., 2003; Velazquez-Fernandez et al., 2005; West et al., 2007). IGF-II mainly elicits its cellular effects through the ubiquitously expressed type 1 IGF receptor (IGF-1R). Importantly, human ACCs have also shown elevated levels of IGF-1R mRNA and protein (Weber et al., 1997). Taken together, these observations suggest that activation of the IGF pathway is a common pathologic mechanism employed by tumor cells during adrenocortical tumorigenesis.

The IGF-1R receptor tyrosine kinase has garnered increasing attention in tumor biology as numerous studies in a diverse set of cancers have demonstrated its critical role in cell proliferation, anti-apoptosis, angiogenesis, invasion and metastasis (Tao et al., 2007). IGF-1R inhibition has been a concept long sought after for its potential in cancer therapeutics. Previous generations of IGF-1R inhibitors failed in preclinical studies and clinical trials, as they caused significant side effects (such as hyperglycemia) due to IGF-1R's 84% sequence homology with the insulin receptor (Bahr and Groner, 2005). However, newer generation IGF-1R kinase inhibitors have been developed that specifically target IGF-1R with much lower cross-reactivity to insulin receptor. Recently, several monoclonal antibodies have also been developed to target human IGF-1R (Sachdev and Yee, 2007).

In this study, we used a small molecule inhibitor (Novartis NVP-AEW541) and a fully human monoclonal antibody (ImClone Systems IMC-A12), both targeting IGF-1R, to demonstrate specific abrogation of IGF-mediated signaling and concomitant inhibition of proliferation. Only ACC lines with increased IGF signaling responded to both agents. Synergistic anti-proliferative effects were observed when IGF-1R inhibition was combined with mitotane in culture. *In vivo*, both IGF-1R antagonists markedly

attenuated human ACC xenograft growth in athymic nude mice. Moreover, IGF inhibition combined with mitotane significantly enhanced single agent tumor growth inhibition. Our results validate IGF-1R as an important target in ACC and provide rationale for the testing of IGF-1R antagonists as a novel and promising therapeutic agent in clinical trials.

Materials and Methods

Reagents

IMC-A12, a fully human monoclonal antibody directed against the human IGF-1R, has been previously described and was provided by ImClone Systems (Burtrum et al., 2003). NVP-AEW541, a pyrrolo (2,3-d)pyrimidine derivative small molecule inhibitor designed to target the kinase domain of IGF-1R, has been described previously and was generously provided by Novartis (Garcia-Echeverria et al., 2004). Recombinant human IGF-I and IGF-II ligands were purchased from Peprotech. Mitotane, lectin-FITC, and anti-β-actin were purchased from Sigma. Anti-IGF-1Rβ was obtained from Santa Cruz Biotechnology while anti-Akt, anti-phospho-Akt^{Ser473} were purchased from Cell Signaling Technology. Anti-phospho-tyrosine (4G10) was purchased from Millipore Bioscience.

Cell lines and cell culture

All standard cell culture reagents were purchased from Invitrogen Life Technologies. The cell lines NCI-H295 (Gazdar et al., 1990), Y1 (Cohen et al., 1957), and SW13 (Leibovitz et al., 1973) were obtained from American Type Culture Collection. The RL251 cell line (Schteingart et al., 2001) was previously described and was generously provided by Dr. David Schteingart (University of Michigan) while the ST5 (Mellon et al., 1994) cell line was generated and provided by Dr. Synthia Mellon (University of California at San Francisco). The Y1 and ST5 cell lines were maintained in DMEM supplemented with 7.5% horse serum and 2.5% calf serum. H295 cells were cultured DMEM/F12 media containing 2.5% calf serum supplemented with transferrin,

insulin and selenium. RL251 and SW13 cells were maintained in DMEM with 10% FCS. Log phase cells were treated and analyzed as described above and were maintained for no longer than 15 weeks after recovery from frozen stocks.

Cell proliferation assay

Depending on individual cell lines, 2500 to 10,000 cells were seeded on 96-well plates in 100 μl of total media. Twenty-four hours after plating, increasing concentrations of the compounds were added in triplicate wells and incubation continued for 72 hours (for NVP-AEW541 treatment) or 7 days (for IMC-A12 treatment). To measure the number of metabolically active cells in each well an MTS assay was performed. Briefly, Promega Cell Titer 96 reagent was added to each well, plates were incubated for 1 hour at 37°C, followed by measurement of absorbance levels at 490 nm with a microplate reader. A dose response index was calculated by dividing the average absorbance for each condition by the average untreated control absorbance.

RNA extraction and RT-PCR

Total RNA was isolated from tissue culture cells and snap frozen xenograft tissues using TRIzol reagent (Invitrogen) as detailed in the manufacturer's protocol. Following UV quantification of RNA, one microgram was subjected to *iScript* (BioRad) cDNA synthesis and final purification with PCR purification columns (Qiagen). RT-PCR for mRNA expression for *IGF2* and *GAPDH* genes was carried out in a standard thermocycler with primer sequences as follows: mIGF2 Fwd TTCTCATCTCTTTGGCCTTCGCCT, mIGF2 Rev ACGATGACGTTTGGCCTCTCTGAA, hIGF2 Fwd TGGCATCGTTGAGGAGTGCTGTTT, hIGF2 Rev

GTTTGAAGATGCTGCTGTGCTTCCTC, mIGF1 Fwd

ACCTCAGACAGGCATTGTGGATGA, mIGF1 Rev

AGCTTAGTGAGGACTGCCTTGCTT, hIGF1 Fwd

GCCTGCGCAATGGAATAAAGTCCT, hIGF1 Rev

TGCACTCCCTCTACTTGCGTTCTT. Quantitative RT-PCR analyses with intron-spanning primers were performed with SYBR Green PCR mix and ABI 7300 q-PCR system (Applied Biosystems). Primer sequences include: hVEGF Fwd GCACCCATGGCAGAAGG, hVEGF Rev CTCGATTGGATGGCAGTAGCT, hGAPDH Fwd CCAACCGCGAGAAG, hGAPDH Rev TCCATCACGATGCC.

Immunoblot analysis

Protein extracts from cells and snap frozen xenograft tissues were harvested in lysis buffer (40 mM HEPES, 120 mM sodium chloride, 10 mM sodium pyrophosphate, 10 mM sodium glycerophosphate, 1 mM EDTA, 50 mM sodium fluoride, 0.5 mM sodium orthovanadate, 1% Triton X-100 and Sigma protease inhibitor cocktail) and dissociated using brief sonication pulses on ice. Lysates were cleared by high speed centrifugation, and protein concentrations were determined by Bradford protein assay (BioRad). Proteins (15-30 micrograms per lane) were separated by standard SDS-PAGE and transferred to nitrocellulose. Membranes were incubated overnight with appropriate antibodies, incubated with HRP-labeled secondary antibodies (Roche), and antigens were detected with West Dura ECL Reagent (Pierce Biotechnology). IGF-1R tyrosine phosphorylation levels were assessed by overnight incubation of 500 μg cell lysate with 5 μg IGF-1Rβ antibody, immunoprecipitation with 50 μL Protein A-Agarose (Invitrogen), three lysis buffer washes and SDS-PAGE/immunoblotting with anti-phospho-tyrosine antibody.

Mice

Animals used in this study were maintained in facilities approved by the American Association for Accreditation of Laboratory Animal Care in accordance with current regulations and standards of the United States Department of Agriculture and Department of Health and Human Services. Studies were performed in accordance to an institutionally approved protocol under the auspice of the University Committee on Use and Care of Animals at the University of Michigan. Tumor xenografts (2-4 per animal) were established by subcutaneous injection of $1x10^6$ RL251 or $2.5x10^6$ H295 cells into flank regions of four to six week old female athymic (CD-1 nu/nu) mice. Grafts were measured every other day and randomized into respective treatment or control groups after average tumor sizes reached 100-150 mm^3. Tumor volume (TV) was calculated according to the equation $TV = (\pi \times a \times b^2)/6$, where a and b are the longer and shorter dimensions of the tumor, respectively. Animals treated with IMC-A12 diluted in PBS received an initial 15 mg/kg loading dose via intraperitoneal injection and a 5 mg/kg maintenance dose every two days for the duration of the study. NVP-AEW541 treated mice were dosed twice daily by oral gavage with 50 mg/kg of compound dissolved in 0.2 mL of 25 mM L(+)-tartaric acid for the entire study. Mitotane was reformulated in 10% Tween-80/0.9% normal saline and administered by intraperitoneal injection once daily at 300 mg/kg. Weights of all mice were monitored closely for possible drug-induced toxicities. At the end of the three week treatment period mice were euthanized, examined for metastases, and their xenografts and adrenal glands were collected for analysis. Each tumor was dissected, cleared of surrounding tissue and divided into three parts. Two

sections were snap-frozen for protein and RNA analysis and the third section was fixed with 4% paraformaldehyde overnight, ethanol dehydrated, and paraffin embedded for routine H & E staining and immunohistochemical analysis.

Immunohistochemistry

Paraffin-embedded tissue sections on slides were rehydrated and stained with hematoxylin & eosin for examining morphology. Immunohistochemistry was performed as described previously (Looyenga and Hammer, 2007). Briefly, slides were rehydrated, boiled in 0.01M sodium citrate for antigen retrieval, incubated with respective antibodies overnight, and detected with DAB-Peroxidase (Sigma). Primary antibody dilutions (in TBS-T + 5% goat serum) for IGF-1R (1:250), Akt (1:100), and phospho-Akt^{Ser473} (1:100) were used. In Figure 6c, Lectin-FITC (1:100) was used.

Statistical analysis

Numerical differences between two groups were tested for significance with 2-tailed Student's t-test. ANOVA and was used when making multiple statistical comparisons. The xenograft studies were powered at 80% to detect a 30% difference in AGD between the 12 tumors per group. We used Calcusyn software to determine combination indices with *in vitro* mitotane and NVP-AEW541 MTS assay.

RESULTS

Inhibition of IGF signaling by IGF-1R antagonists

IMC-A12, a fully human IgG_1 monoclonal antibody engineered to selectively bind to the ligand binding domain of IGF-1R, was provided by ImClone Systems for these studies (Burtrum et al., 2003; Rowinsky et al., 2007). NVP-AEW541, a pyrrolo-(2,3-d)-pyrimidine derivative small molecule IGF-1R inhibitor that is 27-fold more selective for IGF-1R than insulin receptor, was provided by Novartis (Garcia-Echeverria et al., 2004). To assess the ability of both IGF antagonists to specifically inhibit IGF-II/IGF-1R mediated signaling, log phase H295 cells were cultured to ~80% confluency and subjected to increasing amounts of IMC-A12 or NVP-AEW541 in the presence of 10 nM IGF-I/ IGF-II (**Fig 4.1**). Immunoblotting of cell lysates incubated with increasing concentrations of IMC-A12 resulted in a dose-dependent reduction of IGF-1R levels, with an ~80% receptor decrease achieved at 100 nM concentrations of antibody (**Fig 4.1 A**). This decrease may be attributed to antibody-mediated receptor internalization and degradation, a phenomenon not seen when IGF ligands are incubated alone (Burtrum et al., 2003). IMC-A12 attenuated phospho-Akt^{Ser473} in a dose-dependent manner, indicating targeted decrease of IGF signaling. We also found NVP-AEW541 inhibited IGF-1R signaling in H295 cells (**Fig 4.1 B**). At 5 μM NVP-AEW541 concentrations, receptor phospho-tyrosine levels were undetectable and phospho-Akt^{Ser473} levels were also completely abrogated. No change in total IGF-1R or Akt levels was observed with treatment. Similar dose-dependent responses were obtained in Y1 and SW13 cell lines

(data not shown). Taken together, these results indicate that both pharmacologic agents are able to specifically target and inhibit IGF-mediated signaling in ACC cell lines.

IGF-1R antagonists inhibit the proliferative potential of ACC cell lines

As discussed previously, IGF signaling regulates several aspects of cellular function including the enhancement of proliferation. To test the functional consequence of IGF-1R inhibition, MTS proliferation assays were performed on H295 cells with IMC-A12 and NVP-AEW541 (**Fig 4.2**). We used the RL251 cell line as a negative control in these assays because it lacks similar expression levels of IGF-1R protein in comparison to other ACC lines. As predicted, increasing doses of IMC-A12 had no substantial effect on the RL251 cells, while H295 cells exhibited anti-proliferative effects at high concentrations of the antibody (left panel). The IMC-A12 IC_{50} value for the H295 cells was 90 nM, while RL251 cells were never close to achieving inhibition at maximal IMC-A12 doses ($p<0.001$ at 100 nM A12). The NVP-AEW541 IC_{50} value for H295 cells was 2.7 μM while RL251 cells had an IC_{50} of 36 μM ($p<0.001$ at 3 μM NVP-AEW541), again demonstrating targeted suppression of the H295 cell line's ability to proliferate due to the presence of IGF-1R.

Targeting of IGF-1R delays tumor xenograft growth

In light of IGF-1R inhibition resulting in a significant decrease of downstream signaling and proliferation *in vitro*, its *in vivo* activity was assessed using human ACC cell lines. Using the rationale discussed above, we chose to utilize the RL251 cell line as an additional control in these assays to assess growth differences resulting from the

presence of IGF-1R. The H295 and RL251 cell lines were inoculated subcutaneously into athymic nude mice which were subsequently randomized into three treatment groups (n = 8 tumors per group for H295 and n = 10 for RL251): placebo, IMC-A12 treatment, and NVP-AEW541 treatment. Growth curves were generated from tumor volume measurements taken three times a week for 21 days (**Fig 4.3**). RL251 xenografts had a higher tumor engraftment rate than H295 xenografts (94% vs. 75%, data not shown) and grew over 2.5 times faster than H295 xenografts, illustrated by the difference in the two control tumor growth curves. The left panel of Figure 5a reveals that treating H295 tumors with IMC-A12 for 21 days resulted in a 55% reduction in tumor size over untreated controls ($p = 0.019$). IMC-A12 was well tolerated in treated mice with no substantial adverse effects or weight changes observed between groups (data not shown). NVP-AEW541 treatment of H295 xenografts also displayed anti-tumor activity, resulting in a 34% reduction in tumor burden ($p = 0.10$) (**Fig 4.4**). As shown in the right panel of Figure 5a, similar IMC-A12 treatment in RL251 xenografts resulted in a 28% reduction in tumor volume after 21 days of treatment ($p = 0.047$). This growth inhibition, although statistically significant, was of considerably less magnitude than H295 xenografts, presumably due to low levels of IGF-1R expression in RL251 tumor cells. Additionally, IGF-1R expression within the supporting stromal tissue of xenografts may also account for a share of this observed growth effect. NVP-AEW541 treatment of mice harboring RL251 xenografts had an insignificant 20% reduction of tumor volume ($p = 0.16$) (**Fig 4.4**). To determine whether blocking IGF-1R resulted in decreased IGF signaling *in vivo*, H295 xenografts were subjected to immunoblot analysis (**Fig 4.4 B**). Lysates prepared from two separate samples of tumors from control and IMC-A12-treated mice were

immunoblotted for Akt and phospho-Akt^{Ser473} levels. Although total Akt expression levels were similar in both treatment arms, phospho-Akt^{Ser473} levels were decreased in the tumors of mice treated with IMC-A12, thus revealing a targeted decrease in IGF signaling. IGF-1R and β-actin levels were expressed at similar levels in all samples. Taken together, these results indicate *in vivo* IGF-1R inhibition caused significant and targeted tumor growth delay of human ACC xenografts and underscores the importance of IGF signaling in ACC pathophysiology.

Inhibition of IGF-1R enhances the inhibitory effects of mitotane

Mitotane therapy is the standard-of-care medication used for treatment of ACC because of its specific cellular inhibition of the adrenal cortex. To evaluate whether this response could be enhanced by additional IGF inhibition, we investigated the effect of combining mitotane with IGF antagonists in culture and *in vivo* tumor growth. First, MTS proliferation assays were performed on H295 and RL251 cells with increasing concentrations of NVP-AEW541 and mitotane (**Fig 4.5 A**). Both H295 and RL251 cells incubated with mitotane displayed reduced proliferation but the presence of IGF-1R in H295 cells enhanced the anti-proliferative response of NVP-AEW541. This is qualitatively represented by the leftward shift of the growth curves. Analysis of these data using Calcusyn software to directly quantitate combined drug effects, confirmed a synergistic relationship of mitotane and NVP-AEW541 *in vitro* (**Fig 4.6**). To further evaluate this effect, H295 xenografts were again established in nude mice (n = 20 tumors per treatment group) which were treated with mitotane or IMC-A12 as either single agents or in combination (**Fig 4.5 B**). Treatment with antibody alone resulted in a 51% reduction in tumor size ($p < 0.001$), comparable to 55% reduction observed previously in

the earlier experiment. Mitotane treatment was not as effective as IMC-A12 but did lead to a 25% decrease in tumor volume ($p = 0.038$). The highest growth inhibition was achieved with the combination of IMC-A12 and mitotane, which caused a 70% decrease in tumor burden ($p < 0.001$) and effectively halted H295 xenograft growth. A statistically significant synergistic interaction between both compounds *in vivo* could not be demonstrated ($p = 0.22$) however, tumors were approximately 20% smaller than what would be expected under an additive model. After 21 days, xenograft specimens were collected for histochemical analysis (**Fig 4.5 C**). Interestingly, hematoxylin and eosin staining revealed treatment results in a clear decrease in vascularity compared to control sections. We investigated this further by immunohistochemically evaluating microvessel density using a FITC conjugated lectin molecule that binds specifically to endothelial cells. Dense areas of lectin-positive endothelial cells are observed throughout control xenograft sections but IMC-A12-treated xenograft sections display a marked decrease in endothelial cell density. The greatest decrease was observed in xenografts treated with the combination of IMC-A12 and mitotane. We hypothesized IGF inhibition may reduce the angiogenic potential imparted by the expression of IGF-II via induction of vascular endothelial growth factor (VEGF) expression, seen in other systems (Beppu et al., 2005; Kwon et al., 2004). Therefore, we generated cDNA from xenografts for q-PCR to assess human VEGF expression utilizing PCR primers designed to recognize all four isoforms of VEGF transcripts (Hata et al., 2004) (**Fig 4.5 D**). Results demonstrate a 1.6 fold decrease in human VEGF expression in IMC-A12-treated samples ($p = 0.044$) and a 2.2 fold decrease when antibody is combined with mitotane ($p = 0.008$). Mitotane treatment alone results in a small and statistically insignificant decrease ($p = 0.46$). Thus, inhibition

of IGF signaling is the major factor causing the decreased VEGF transcript levels in these tumors. These results, taken together, demonstrate that IGF signaling inhibition with IMC-A12 leads to a larger suppression of ACC tumor growth in comparison to mitotane and that the combining both agents can specifically decrease ACC xenograft growth greater than either agent alone.

DISCUSSION

Current therapy for adrenocortical cancer consists of surgical resection and adjuvant mitotane treatment or, in non-resectable disease, mitotane in combination with other cytotoxic chemotherapies (Kirschner, 2006). A recent retrospective study evaluating the efficacy mitotane following radical resection as adjuvant therapy in adrenocortical cancer revealed that mitotane may indeed prolong recurrence-free survival to two or three times that of untreated patients (Schteingart, 2007; Terzolo et al., 2007). However, mitotane, a structural isomer of the pesticide DDT, is associated with significant toxicity due to the high doses required for its adrenolytic effects. Unfortunately, a large number of ACC patients present with metastatic disease which precludes surgery and carries a dismal prognosis (Ng and Libertino, 2003). These outcomes underscore the need for new treatment strategies for this fatal disease based on identification of specific pathways critical for ACC pathogenesis.

Imprinting is an epigenetic mechanism by which cells regulate gene expression in a parent-of-origin-specific manner in about 1% of genes so that one allele, whether maternally or paternally inherited, is expressed while the other is stably and efficiently silenced through DNA methylation. In pathologic situations, as in the case in the majority of patients with Beckwith-Wiedemann Syndrome, this process goes awry and results in aberrant expression of imprinted genes (Feinberg, 2007). Individuals with BWS often have a form of loss of heterozygosity, uniparental paternal isodisomy – loss of the maternal locus with an accompanying gain of the paternal allele. Less frequently, there is a loss of imprinting (LOI) phenomenon leading to excessive transcriptional activation of the paternal allele (Feinberg, 2007). Our gene expression profiling of

sporadic human adrenal tumors revealed a dysregulation of the 11p15.5 locus that is not limited to IGF-II overexpression but also dysregulation of other 11p15.5 genes including *CDKN1C* and *H19*. Additionally, the 11p15.5 expression profile is reminiscent of that commonly observed in BWS, suggesting ACC encompasses similar imprinting defects. Not surprisingly, 11p15 LOH holds a higher prognostic value than IGF-II overexpression alone, suggesting *CDKN1C* and *H19* genes, in addition to IGF-II, are important contributors to ACC pathogenesis (Gicquel et al., 2001). Whether this epigenetic defect is causative or associative in ACC pathogenesis is yet to be determined.

ACC has long been recognized to be a malignancy highly resistant to several structurally unrelated chemotherapeutic agents. Although the exact mechanism of resistance has not been defined, normal adrenal tissues express high levels of the ATP binding cassette transporter family member, multidrug resistance 1 (MDR1), and ACCs retain this expression (Cordon-Cardo et al., 1990). Recently, phase II clinical trials of MDR1 inhibition in adrenocortical cancers have been initiated (Kirschner, 2006). Because IGF signaling is known to mediate resistance to chemotherapy and is activated as a survival mechanism in response to ionizing radiation (Cosaceanu et al., 2007), inhibition of the IGF pathway increases the sensitivity of both standard cytotoxic chemotherapies and radiation (Allen et al., 2007; Warshamana-Greene et al., 2005). Therefore, we hypothesized that IGF-1R inhibition may enhance the efficacy of mitotane in ACC cells where IGF-1R overexpression and/or activation is evident. Indeed, the combination of IGF inhibition and mitotane resulted in greater anti-proliferative effects *in vitro* and in xenograft growth inhibition *in vivo* over single agent treatment. These results raise the prospect of utilizing targeted disruption of IGF-1R signaling to attain a therapeutic

advantage when used as an adjuvant in mitotane therapy or possibly other chemotherapeutics in ACC patients.

In summary, this preclinical study implicates aberrant IGF signaling in adrenocortical carcinoma pathogenesis. We used two IGF-1R antagonists with differing mechanisms of receptor-mediated signaling inhibition to validate IGF-1R as a specific molecular target in human tumor xenografts. Antagonizing this pathway with each pharmacologic agent resulted in inhibition of growth *in vitro* and *in vivo*. Furthermore, this targeted inhibition was more potent than mitotane treatment in decreasing xenograft growth. Importantly, the IGF-1R antagonists enhanced the established adrenolytic effects of mitotane. These results suggest a new paradigm in the treatment of patients with ACC and provide the rationale for the new clinical trials targeting this important growth factor pathway.

ACKNOWLEDGEMENTS

Author Contributions: Ferdous Barlaskar is the first author on this study, conducted the majority of experiments and wrote the manuscript represented in this chapter. Aaron Spalding provided substantial technical advice, analyzed data, and revised the manuscript. Joanne Heaton performed the VEGF q-PCR, aided with xenograft studies, and revised the manuscript. Edgar Ben-Josef and Gary Hammer obtained the targeted reagents, directed the project, and revised the manuscript. This work was published in *The Journal of Clinical Endocrinology and Metabolism*, 2009 Jan;94(1):204-12.

The authors acknowledge funding support from the U.S. National Institutes of Health/NIDDKD DK 062027 (Gary Hammer) and the American Cancer Society RSG-04-236 (Gary Hammer). Ferdous Barlaskar is supported through a pre-doctoral fellowship from NIH/Training Program for Organogenesis, T-32-HD007505. We also thank ImClone Systems and Novartis for generously providing their respective targeted reagents. Finally, we thank Dr. David E. Schteingart for technical support and Julie Pepera for assistance with xenograft measurements.

Figure 4.1 IGF-1R antagonist treatments decrease IGF-mediated signaling. (**A**) H295 cells were pretreated with increasing nanomolar concentrations of IMC-A12 for one hour before addition of 10 nM IGF-I/II ligand mix for 10 minutes. Cells were subsequently harvested and immunoblotted for IGF-1Rβ, Akt, phospho-Akt^{Ser473}, or β-actin. (**B**) H295 cells were pretreated with increasing micromolar concentrations of NVP-AEW541 for 30 minutes before addition of 10 nM IGF-I/II ligand mix for 10 minutes. Cells were then harvested and either immunoprecipitated with an anti-IGF-1Rβ antibody and immunoblotted for phospho-tyrosine residues or directly immunoblotted for IGF-1Rβ, Akt, phospho-Akt^{Ser473}, or β-actin.

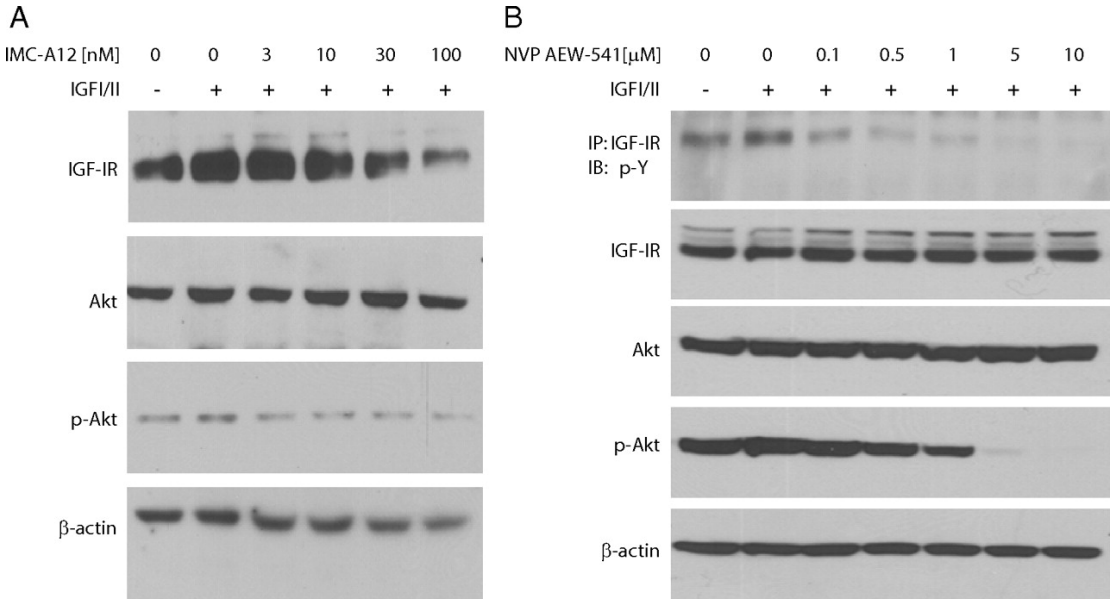
A
IMC-A12 [nM] 0 0 3 10 30 100
IGFI/II - + + + + +
IGF-IR
Akt
p-Akt
β-actin
B
NVP AEW-541[μM] 0 0 0.1 0.5 1 5 10
IGFI/II - + + + + + +
IP: IGF-IR
IB: p-Y
IGF-IR
Akt
p-Akt
β-actin

Figure 4.2 Anti-proliferative effects of IGF-1R antagonist treatments *in vitro*. H295 and RL251 cells were incubated with increasing micromolar concentrations of NVP-AEW541 (right panel) or nanomolar concentrations of IMC-A12 (left panel) and proliferation was assessed with MTS reagent. Squares (■) represent the mean of quadruplicate wells of RL251 cells while diamonds (♦) represent quadruplicate wells of H295 cells with error bars indicating +/- S.D. Data is representative of at least four independent experiments. Asterisks indicate a p value < 0.05.

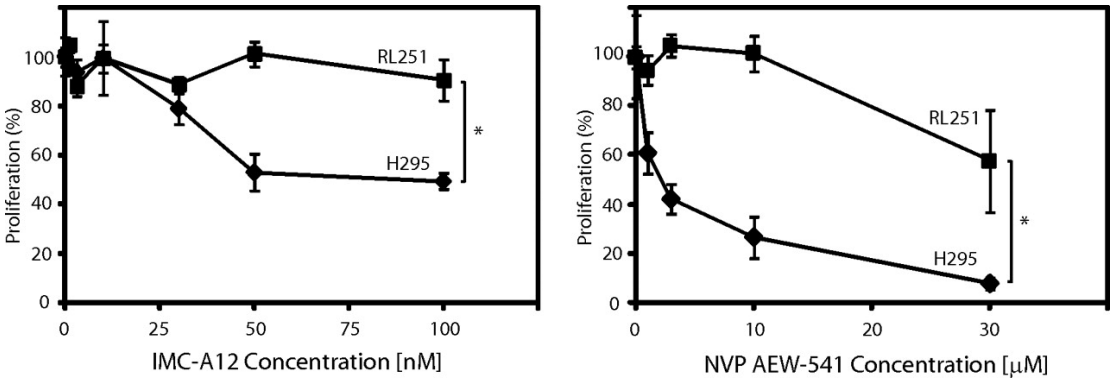
Proliferation (%)
100
80
60
40
20
0
0
25
50
75
100
IMC-A12 Concentration [nM]
RL251
H295
*
Proliferation (%)
100
80
60
40
20
0
0
10
20
30
NVP AEW-541 Concentration [μM]
RL251
H295
*

Figure 4.3 Targeted inhibition of tumor growth *in vivo*. (**A**) H295 (left panel) and RL251 (right panel) cells were injected subcutaneously into athymic nude mice and mice were randomized into treatment groups (n = 8 for H295 and n = 10 for RL251). Groups were treated with vehicle or IMC-A12 every other day. Tumor dimensions on control (♦) mice or IMC-A12-treated (■) mice were measured three times a week for the duration of the 21 day study and data are shown as the log ratios of tumor size to initial tumor size means +/- S.E. (B) To confirm *in vivo* targeting of IGF inhibition, harvested H295 tumors were lysed and two tumors from each treatment arm were subjected to immunoblotting for IGF-1Rβ, Akt, phospho-Akt^{Ser473}, and β-actin.

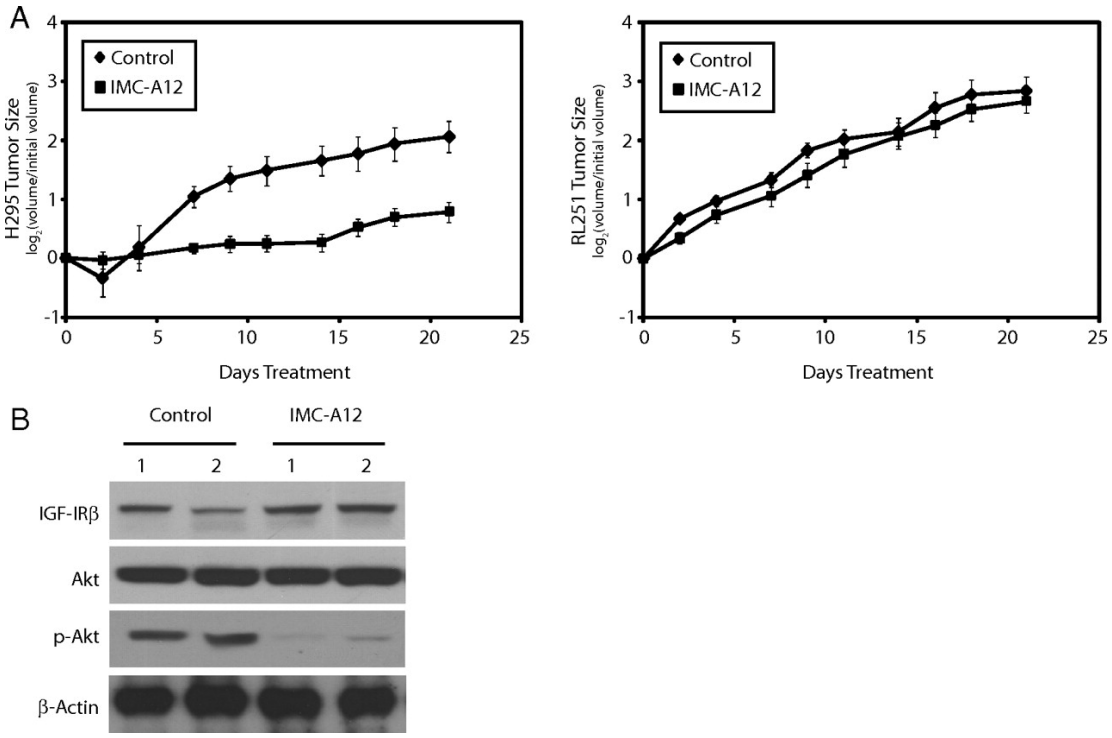
A
Control
IMC-A12
H295 Tumor Size
log2(volume/initial volume)
Days Treatment
RL251 Tumor Size
log2(volume/initial volume)
Days Treatment
B
Control
IMC-A12
1
2
1
2
IGF-IRβ
Akt
p-Akt
β-Actin

Figure 4.4 NVP-AEW541 mediated growth inhibition of ACC xenografts *in vivo.* (**A**) H295 (left panel) and RL251 (right panel) cells were injected subcutaneously into athymic nude mice and tumors were allowed to grow to ~200mm^3. Mice were randomized into treatment groups (n = 8 for H295 and n = 10 for RL251). Groups were treated with vehicle or NVP-AEW541 twice daily. Tumor dimensions on control (♦) mice or NVP-AEW541 treated mice (■) mice were measured three times a week for the duration of the 21 day study and data are represented as mean +/- S.E. (**B**) H295 tumor xenograft sections stained with hematoxylin and eosin in NVP-AEW541 treated (right panel) and control tissues (left panel).

A

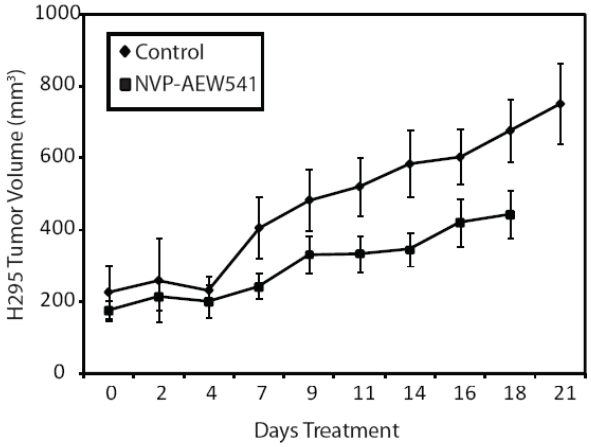
Control
NVP-AEW541
H295 Tumor Volume (mm³)
1000
800
600
400
200
0
0 2 4 7 9 11 14 16 18 21
Days Treatment

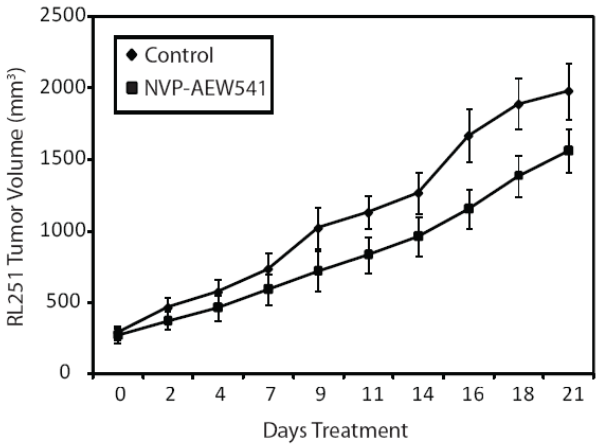
Control
NVP-AEW541
RL251 Tumor Volume (mm³)
2500
2000
1500
1000
500
0
0 2 4 7 9 11 14 16 18 21
Days Treatment

B

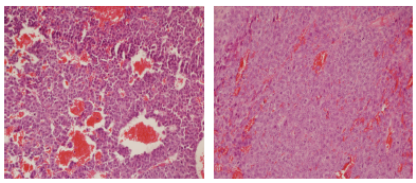
Control
NVP-AEW541

Figure 4.5 IGF-1R antagonists enhance the inhibitory effects of mitotane. (**A**) RL251 (left panel) and H295 (right panel) cells were incubated in triplicate with a combination of mitotane and increasing concentrations of NVP-AEW541. Proliferation was assessed with MTS reagent. Data are representative of three independent experiments and displayed as mean +/- S.D. (**B**) Mice harboring H295 xenografts were randomized into 4 groups (n = 20 per treatment arm) and treated with vehicle or IMC-A12 every other day and/or mitotane once daily for the duration of the experiment. Tumor volumes were measured 3 times a week. Data are presented as log ratios of tumor size over initial tumor size means +/- S.E. (**C**) Hematoxylin and eosin stained section of H295 tumor xenografts (left panels) at 40X magnification. Lectin-FITC immunohistochemical analysis (right panels) was performed to detect relative levels of endothelial cells. (**D**) Quantitative RT-PCR of 3 or 4 tumors from each treatment arm with primers detecting all four isoforms of human vascular endothelial growth factor (VEGF). The y-axis represents relative VEGF levels normalized to glyceraldehyde 3-phosphate dehydrogenase (GAPDH) transcript levels followed by normalization to control tissue values. Each value represents the average of triplicates of two independent experiments and data are presented as the mean +/- S.E. Asterisks indicate a p value < 0.05.

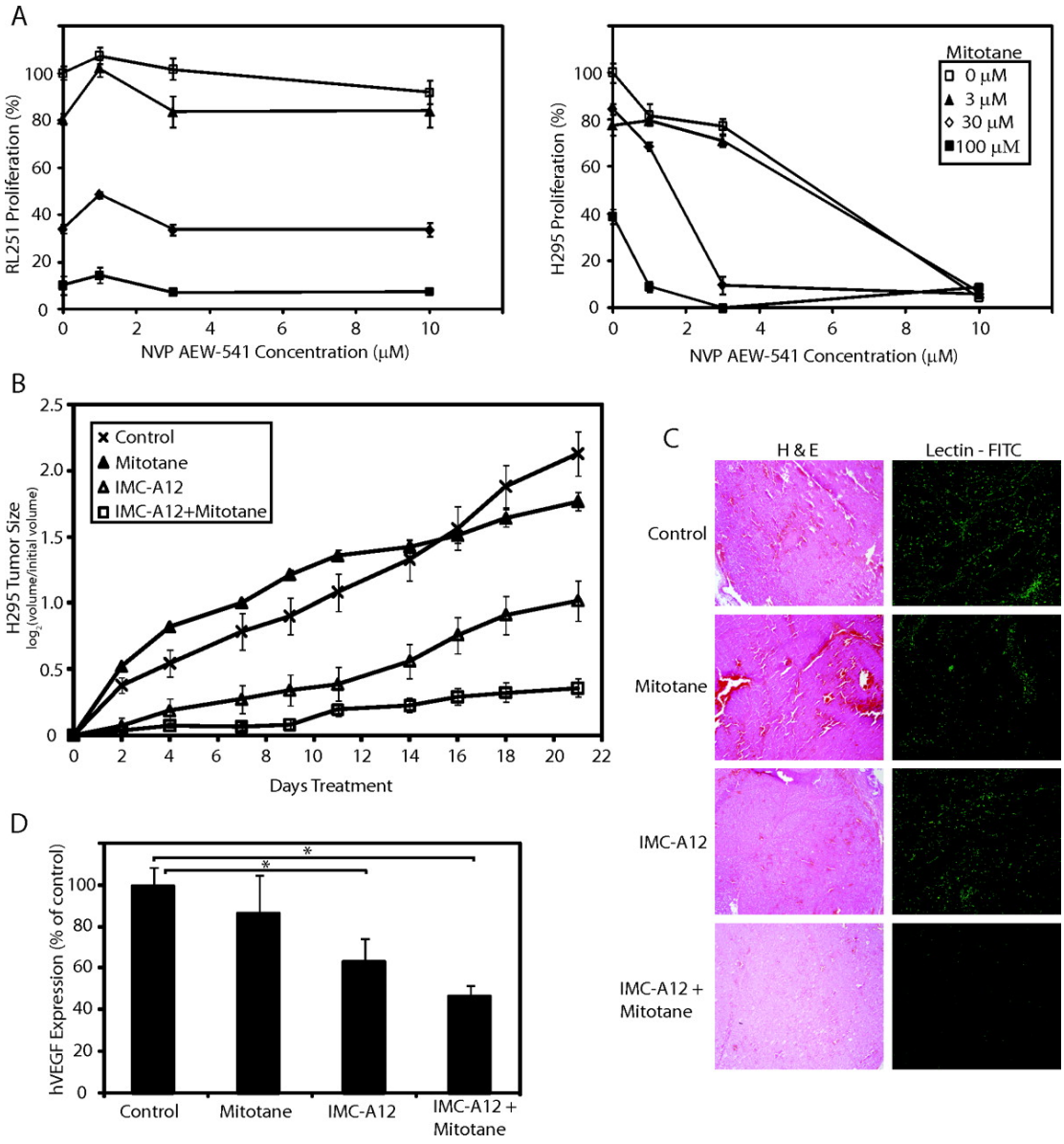
A
RL251 Proliferation (%)
NVP AEW-541 Concentration (μM)
H295 Proliferation (%)
NVP AEW-541 Concentration (μM)
Mitotane
0 μM
3 μM
30 μM
100 μM
B
H295 Tumor Size
log2 (volume/initial volume)
Days Treatment
Control
Mitotane
IMC-A12
IMC-A12+Mitotane
C
H & E
Lectin - FITC
Control
Mitotane
IMC-A12
IMC-A12 + Mitotane
D
hVEGF Expression (% of control)
Control
Mitotane
IMC-A12
IMC-A12 + Mitotane

Figure 4.6 NVP-AEW541 and mitotane synergistically inhibit ACC cell proliferation. The combined drug effects of NVP-AEW541 and mitotane on H295 (left panel) and RL251 (right panel) cell proliferation (data presented in Figure 4.5 A) is quantitatively represented here using Calcusyn software. A combination index (CI) of less than one indicates a greater than predicted effect from the individual agents (synergy). A CI greater than one is consistent with an antagonistic effect and indicates the likelihood of synergy is very low.

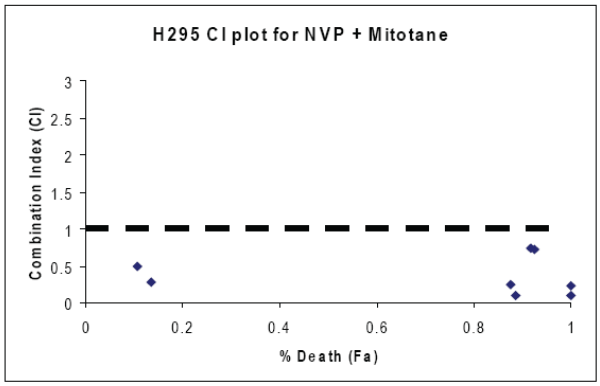
H295 CI plot for NVP + Mitotane
Combination Index (CI)
3
2.5
2
1.5
1
0.5
0
0
0.2
0.4
0.6
0.8
1
% Death (Fa)

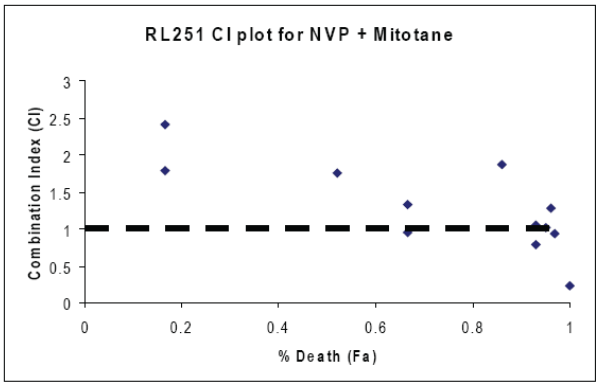
RL251 CI plot for NVP + Mitotane
Combination Index (CI)
3
2.5
2
1.5
1
0.5
0
0
0.2
0.4
0.6
0.8
1
% Death (Fa)

BIBLIOGRAPHY

Wajchenberg, B.L., Albergaria Pereira, M.A., Medonca, B.B., Latronico, A.C., Campos Carneiro, P., Alves, V.A., Zerbini, M.C., Liberman, B., Carlos Gomes, G., Kirschner, M.A., 2000. Adrenocortical carcinoma: clinical and laboratory observations. Cancer 88, 711-36.

Allolio, B., Fassnacht, M., 2006. Clinical review: Adrenocortical carcinoma: clinical update. J Clin Endocrinol Metab 91, 2027-37.

Icard, P., Goudet, P., Charpenay, C., Andreassian, B., Carnaille, B., Chapuis, Y., Cougard, P., Henry, J.F., Proye, C., 2001. Adrenocortical carcinomas: surgical trends and results of a 253-patient series from the French Association of Endocrine Surgeons study group. World J Surg 25, 891-7.

Kirschner, L.S., 2006. Emerging treatment strategies for adrenocortical carcinoma: a new hope. J Clin Endocrinol Metab 91, 14-21.

Giordano, T.J., Thomas, D.G., Kuick, R., Lizyness, M., Misek, D.E., Smith, A.L., Sanders, D., Aljundi, R.T., Gauger, P.G., Thompson, N.W., Taylor, J.M., Hanash, S.M., 2003. Distinct transcriptional profiles of adrenocortical tumors uncovered by DNA microarray analysis. Am J Pathol 162, 521-31.

Velazquez-Fernandez, D., Laurell, C., Geli, J., Hoog, A., Odeberg, J., Kjellman, M., Lundeberg, J., Hamberger, B., Nilsson, P., Backdahl, M., 2005. Expression profiling of adrenocortical neoplasms suggests a molecular signature of malignancy. Surgery 138, 1087-94.

West, A.N., Neale, G.A., Pounds, S., Figueredo, B.C., Rodriguez Galindo, C., Pianovski, M.A., Oliveira Filho, A.G., Malkin, D., Lalli, E., Ribeiro, R., Zambetti, G.P., 2007. Gene expression profiling of childhood adrenocortical tumors. Cancer Res 67, 600-8.

Weber, M.M., Auernhammer, C.J., Kiess, W., Engelhardt, D., 1997. Insulin-like growth factor receptors in normal and tumorous adult human adrenocortical glands. Eur J Endocrinol 136, 296-303.

Tao, Y., Pinzi, V., Bourhis, J., Deutsch, E., 2007. Mechanisms of disease: signaling of the insulin-like growth factor 1 receptor pathway--therapeutic perspectives in cancer. Nat Clin Pract Oncol 4, 591-602.

Bahr, C., Groner, B., 2005. The IGF-1 receptor and its contributions to metastatic tumor growth-novel approaches to the inhibition of IGF-1R function. Growth Factors 23, 1-14.

Sachdev, D., Yee, D., 2007. Disrupting insulin-like growth factor signaling as a potential cancer therapy. Mol Cancer Ther 6, 1-12.

Burtrum, D., Zhu, Z., Lu, D., Anderson, D.M., Prewett, M., Pereira, D.S., Bassi, R., Abdullah, R., Hooper, A.T., Koo, H., Jimenez, X., Johnson, D., Apblett, R., Kussie, P.,

Bohlen, P., Witte, L., Hicklin, D.J., Ludwig, D.L., 2003. A fully human monoclonal antibody to the insulin-like growth factor I receptor blocks ligand-dependent signaling and inhibits human tumor growth in vivo. Cancer Res 63, 8912-21.

Garcia-Echeverria, C., Pearson, M.A., Marti, A., Meyer, T., Mestan, J., Zimmermann, J., Gao, J., Brueggen, J., Capraro, H.G., Cozens, R., Evans, D.B., Fabbro, D., Furet, P., Porta, D.G., Liebetanz, J., Martiny-Baron, G., Ruetz, S., Hofmann, F., 2004. In vivo antitumor activity of NVP-AEW541-A novel, potent, and selective inhibitor of the IGF-IR kinase. Cancer Cell 5, 231-9.

Gazdar, A.F., Oie, H.K., Shackleton, C.H., Chen, T.R., Triche, T.J., Myers, C.E., Chrousos, G.P., Brennan, M.F., Stein, C.A., La Rocca, R.V., 1990. Establishment and characterization of a human adrenocortical carcinoma cell line that expresses multiple pathways of steroid biosynthesis. Cancer Res 50, 5488-96.

Cohen, A.I., Furth, J., Buffett, R.F., 1957. Histologic and physiologic characteristics of hormone-secreting transplantable adrenal tumors in mice and rats. Am J Pathol 33, 631-51.

Leibovitz, A., McCombs, W.M., 3rd, Johnston, D., McCoy, C.E., Stinson, J.C., 1973. New human cancer cell culture lines. I. SW-13, small-cell carcinoma of the adrenal cortex. J Natl Cancer Inst 51, 691-7.

Schteingart, D.E., Giordano, T.J., Benitez, R.S., Burdick, M.D., Starkman, M.N., Arenberg, D.A., Strieter, R.M., 2001. Overexpression of CXC chemokines by an adrenocortical carcinoma: a novel clinical syndrome. J Clin Endocrinol Metab 86, 3968-74.

Mellon, S.H., Miller, W.L., Bair, S.R., Moore, C.C., Vigne, J.L., Weiner, R.I., 1994. Steroidogenic adrenocortical cell lines produced by genetically targeted tumorigenesis in transgenic mice. Mol Endocrinol 8, 97-108.

Looyenga, B.D., Hammer, G.D., 2007. Genetic removal of Smad3 from inhibin-null mice attenuates tumor progression by uncoupling extracellular mitogenic signals from the cell cycle machinery. Mol Endocrinol 21, 2440-57.

Rowinsky, E.K., Youssoufian, H., Tonra, J.R., Solomon, P., Burtrum, D., Ludwig, D.L., 2007. IMC-A12, a human IgG1 monoclonal antibody to the insulin-like growth factor I receptor. Clin Cancer Res 13, 5549s-5555s.

Beppu, K., Nakamura, K., Linehan, W.M., Rapisarda, A., Thiele, C.J., 2005. Topotecan blocks hypoxia-inducible factor-1alpha and vascular endothelial growth factor expression induced by insulin-like growth factor-I in neuroblastoma cells. Cancer Res 65, 4775-81.

Kwon, Y.W., Kwon, K.S., Moon, H.E., Park, J.A., Choi, K.S., Kim, Y.S., Jang, H.S., Oh, C.K., Lee, Y.M., Kwon, Y.G., Lee, Y.S., Kim, K.W., 2004. Insulin-like growth factor-II regulates the expression of vascular endothelial growth factor by the human keratinocyte cell line HaCaT. J Invest Dermatol 123, 152-8.

Hata, K., Osaki, M., Dhar, D.K., Nakayama, K., Fujiwaki, R., Ito, H., Nagasue, N., Miyazaki, K., 2004. Evaluation of the antiangiogenic effect of Taxol in a human epithelial ovarian carcinoma cell line. Cancer Chemother Pharmacol 53, 68-74.

Schteingart, D.E., 2007. Adjuvant mitotane therapy of adrenal cancer - use and controversy. N Engl J Med 356, 2415-8.

Terzolo, M., Angeli, A., Fassnacht, M., Daffara, F., Tauchmanova, L., Conton, P.A., Rossetto, R., Buci, L., Sperone, P., Grossrubatscher, E., Reimondo, G., Bollito, E., Papotti, M., Saeger, W., Hahner, S., Koschker, A.C., Arvat, E., Ambrosi, B., Loli, P., Lombardi, G., Mannelli, M., Bruzzi, P., Mantero, F., Allolio, B., Dogliotti, L., Berruti, A., 2007. Adjuvant mitotane treatment for adrenocortical carcinoma. N Engl J Med 356, 2372-80.

Ng, L., Libertino, J.M., 2003. Adrenocortical carcinoma: diagnosis, evaluation and treatment. J Urol 169, 5-11.

Feinberg, A.P., 2007. Phenotypic plasticity and the epigenetics of human disease. Nature 447, 433-40.

Gicquel, C., Bertagna, X., Gaston, V., Coste, J., Louvel, A., Baudin, E., Bertherat, J., Chapuis, Y., Duclos, J.M., Schlumberger, M., Plouin, P.F., Luton, J.P., Le Bouc, Y., 2001. Molecular markers and long-term recurrences in a large cohort of patients with sporadic adrenocortical tumors. Cancer Res 61, 6762-7.

Cordon-Cardo, C., O'Brien, J.P., Boccia, J., Casals, D., Bertino, J.R., Melamed, M.R., 1990. Expression of the multidrug resistance gene product (P-glycoprotein) in human normal and tumor tissues. J Histochem Cytochem 38, 1277-87.

Cosaceanu, D., Budiu, R.A., Carapancea, M., Castro, J., Lewensohn, R., Dricu, A., 2007. Ionizing radiation activates IGF-1R triggering a cytoprotective signaling by interfering with Ku-DNA binding and by modulating Ku86 expression via a p38 kinase-dependent mechanism. Oncogene 26, 2423-34.

Allen, G.W., Saba, C., Armstrong, E.A., Huang, S.M., Benavente, S., Ludwig, D.L., Hicklin, D.J., Harari, P.M., 2007. Insulin-like growth factor-I receptor signaling blockade combined with radiation. Cancer Res 67, 1155-62.

Warshamana-Greene, G.S., Litz, J., Buchdunger, E., Garcia-Echeverria, C., Hofmann, F., Krystal, G.W., 2005. The insulin-like growth factor-I receptor kinase inhibitor, NVP-ADW742, sensitizes small cell lung cancer cell lines to the effects of chemotherapy. Clin Cancer Res 11, 1563-71.

CHAPTER 5

CONCLUSION

A universal characteristic of most cancers is their ability to arise by acquiring a genetic or epigenetic hit that imparts a selective growth or survival advantage for a particular cell, and through clonal evolution, ultimately result in cancer. The challenge lies in trying to decipher this genetic/epigenetic code accumulated for each type and subtype of cancer, with the hope of gaining that one rare insight that could translate into therapeutic value. This is particularly true of cancers that are rare, specifically of adrenocortical carcinoma. To gain some insight we tested one of our hypotheses in this thesis: *IGF2* plays a critical role in the pathogenesis of ACC pathogenesis.

In chapter 2, we posed a few questions regarding the upregulation of *IGF2* in ACC. Is *IGF2* high in our ACC samples as others have independently reported? Is IGF-II functionally active and efficiently signaling? How and why is *IGF2* so high in these particular cancers? Through our gene expression analysis we confirmed and extended findings of previous groups (de Fraipont et al., 2005; Giordano et al., 2009; Giordano et al., 2003). For instance, using a mathematical model called principal component analysis (PCA) to cluster samples that have similar expression patterns, the normal adrenal tissue samples and adrenal adenoma samples are close to one another and displayed very little intragroup variation. The ACC samples revealed much greater variation in gene expression, highlighting their molecular heterogeneity. Very interestingly, PCA revealed the two ACC clusters had a statistically significant difference in survival by Kaplan-Meier analysis (Giordano et al., 2009).

We also demonstrated IGF signaling is more active in ACC samples by tissue microarray immunohistochemistry. However, knowing that approximately 90% of ACC samples possess very high levels of *IGF2* mRNA, the immunohistochemistry should reflect stronger staining intensities of phospho-IGR-1R and phospho-Akt^{Ser473} in a larger proportion of these tumor samples. Due to the sheer abundance of IGF-II ligand that would be predicted to be produced by ACCs, we currently speculate questions about the quality of the *IGF2* mRNA, the efficiency of protein translation, the quality of the protein product, the presence or absence of IGF binding proteins in the adrenal milieu that could sequester IGF-II, or protein clearance by endocytosis (mediated by IGF2R (Fottner et al., 2004)) via adrenocortical cells.

To date, there is still no unified hypothesis explaining why and how *IGF2* is so abundantly upregulated. LOI of *IGF2* results in biallelic expression of *IGF2* and therefore, only a doubling of the *IGF2* transcript levels (McCann et al., 1996). Injecting mice with a global demethylating agent (5-aza-C) leads to only a 2 fold increase in *Igf2* mRNA levels (Hu et al., 1997). This speculates existence of other regulatory elements besides methylation that may modulate *IGF2* levels in ACC. Or chromosomal microdeletions/microexpansions of this locus that result in potent upregulation of a gene or complete absence of another (Enklaar et al., 2006).

Current directions for this project include completing methylation analysis of the ICR and the DMR0 in our adrenal tumor samples as these may play a role in *IGF2* upregulation and they have been shown to be differentially methylated in cancers (Murrell et al., 2008). Increasing the tested sample size of adrenal tumors is another aspect we are currently addressing, as a few of these current tumor DNAs do not pass the

quality control steps in the pyrosequencing analysis and hence, cannot be used for these assays.

Future directions for the lab include using allele-specific methylation. This recent technology is now linked to the pyrosequencing technology so parental alleles can be distinguished based on the single nucleotide polymorphisms. Although this is a superior way to assess differentially methylated regions than our current methodology, there is a considerably longer troubleshooting/optimizing step (Wong et al., 2006). Another potentially interesting project would be to perform their comprehensive high-throughput arrays for relative methylation (CHARM). This is a genome-wide methylation analysis to decipher the entire methylome of a sample. Understanding how small or big a role epigenetics play in ACC would be very insightful. In closing, this chapter holds the greatest potential of all three chapters. Understanding this locus (among others *CDKN1C* and *IGF2R*) in ACCs may uncover the molecular underpinnings of this disease.

In chapter 3, we modeled LOI to upregulate *IGF2* expression tissue-specifically in the mouse adrenal cortex. Adrenal LOI did not result in ACC but rather, the gland displayed evidence of organ failure. IGF-II is a developmentally critical hormone that promotes proliferation during embryogenesis and, within the adrenal, it is uniquely expressed in the capsule (Han et al., 1992), the site where stem/progenitors reside (Kim et al., 2009). IGF-II is also expressed by ES fibroblasts within the stem cell niche and it alone was sufficient to maintain the stem cell niche (Bendall et al., 2007). In the developing adrenal, IGF-II responds to ACTH stimulation to promote growth of the fetal adrenal gland through gestation (Fottner et al., 2004). These data highlight the important role IGF-II plays in development and it would be interesting to examine how the LOI

fetal adrenals would look through the embryonic stages. Could there possibly be an expansion of undifferentiated stem/progenitor cells due to increased IGF-II-mediated signaling? If this held true, stem cell exhaustion may be a potential cause for why these adrenals progress towards failure at 30 weeks of age. An example of stem cell exhaustion is in the hair follicle model system with constitutively active canonical Wnt signaling in the hair follicle bud. Persistent activation led to initial rapid growth of follicles, but was soon followed by senescence and progression towards follicular failure (i.e., hair loss) (Castilho et al., 2009). Of note now, is the histologic appearance of the LOI adrenal gland at 15 weeks in which 2 out of 6 mice displayed displaced medullar tissue. This phenotype typically occurs when the cortex is perturbed. This is speculation, but a very testable hypothesis within our current mouse breeding scheme by examining earlier timepoints from the embryonic stages on and assessing whether there evidence of a stepwise progression from hyperactivity to hypofunction.

Our identification of GSK3β as the potential mediator of IGF-mediated Wnt activation will also be thoroughly tested with readily available GSK3β inhibitors and IGF-1R antagonists, as this interaction is a controversial idea (Ng et al., 2009). Additionally, we await the LOI/Apc double knockout mice timepoints, so we can begin to fully characterize their adrenal phenotype. Additionally, other important genes associated in ACC pathology have yet to be modeled (*TP53*, *CDKN1C*). In closing, this chapter's project has the potential to burgeon if there is formation of ACCs with the LOI/Apc double knockouts.

In Chapter 4, we targeted constitutively active IGF signaling by using antagonists to IGF-1R in H295 cells as they best recapitulated ACC *in vitro*. Targeting resulted in

specific growth inhibition *in vitro* and also *in vivo* using xenografted H295 tumors. The project in this chapter was the most satisfying, retrospectively. Performing a preclinical drug targeting study and then realizing a clinical trial is based that data creates desire to develop better mouse models of ACC. Xenografted nude mice are not the best models for targeting studies. The cells we used had constitutive IGF overexpression but we don't know what other mutations were present in the cell. The mice also lack a competent immune system. Feasibility with time and money is always an issue in developing a mouse model.

Future directions with this project may include drug targeting in a transgenic mouse harboring an ACC. If GSK3β proves to be a bona fide crosstalk mediator, its potential for use in trials would be high. In this research project, we identified and validated a potential mutation, examined the mutation in a mouse, and targeted the mutation's action. To conclude, more ideas have been generated to test our working hypothesis elaborated in this in thesis.

‘**BIBLIOGRAPHY**

de Fraipont, F., El Atifi, M., Cherradi, N., Le Moigne, G., Defaye, G., Houlgatte, R., Bertherat, J., Bertagna, X., Plouin, P.F., Baudin, E., Berger, F., Gicquel, C., Chabre, O., Feige, J.J., 2005. Gene expression profiling of human adrenocortical tumors using complementary deoxyribonucleic Acid microarrays identifies several candidate genes as markers of malignancy. J Clin Endocrinol Metab 90, 1819-29.

Giordano, T.J., Kuick, R., Else, T., Gauger, P.G., Vinco, M., Bauersfeld, J., Sanders, D., Thomas, D.G., Doherty, G., Hammer, G., 2009. Molecular classification and prognostication of adrenocortical tumors by transcriptome profiling. Clin Cancer Res 15, 668-76.

Giordano, T.J., Thomas, D.G., Kuick, R., Lizyness, M., Misek, D.E., Smith, A.L., Sanders, D., Aljundi, R.T., Gauger, P.G., Thompson, N.W., Taylor, J.M., Hanash, S.M., 2003. Distinct transcriptional profiles of adrenocortical tumors uncovered by DNA microarray analysis. Am J Pathol 162, 521-31.

Fottner, C., Hoeflich, A., Wolf, E., Weber, M.M., 2004. Role of the insulin-like growth factor system in adrenocortical growth control and carcinogenesis. Horm Metab Res 36, 397-405.

McCann, A.H., Miller, N., O'Meara, A., Pedersen, I., Keogh, K., Gorey, T., Dervan, P.A., 1996. Biallelic expression of the IGF2 gene in human breast disease. Hum Mol Genet 5, 1123-7.

Hu, J.F., Nguyen, P.H., Pham, N.V., Vu, T.H., Hoffman, A.R., 1997. Modulation of Igf2 genomic imprinting in mice induced by 5-azacytidine, an inhibitor of DNA methylation. Mol Endocrinol 11, 1891-8.

Enklaar, T., Zabel, B.U., Prawitt, D., 2006. Beckwith-Wiedemann syndrome: multiple molecular mechanisms. Expert Rev Mol Med 8, 1-19.

Murrell, A., Ito, Y., Verde, G., Huddleston, J., Woodfine, K., Silengo, M.C., Spreafico, F., Perotti, D., De Crescenzo, A., Sparago, A., Cerrato, F., Riccio, A., 2008. Distinct methylation changes at the IGF2-H19 locus in congenital growth disorders and cancer. PLoS One 3, e1849.

Wong, H.L., Byun, H.M., Kwan, J.M., Campan, M., Ingles, S.A., Laird, P.W., Yang, A.S., 2006. Rapid and quantitative method of allele-specific DNA methylation analysis. Biotechniques 41, 734-9.

Han, V.K., Lu, F., Bassett, N., Yang, K.P., Delhanty, P.J., Challis, J.R., 1992. Insulin-like growth factor-II (IGF-II) messenger ribonucleic acid is expressed in steroidogenic cells of the developing ovine adrenal gland: evidence of an autocrine/paracrine role for IGF-II. Endocrinology 131, 3100-9.

Kim, A.C., Barlaskar, F.M., Heaton, J.H., Else, T., Kelly, V.R., Krill, K.T., Scheys, J.O., Simon, D.P., Trovato, A., Yang, W.H., Hammer, G.D., 2009. In search of adrenocortical stem and progenitor cells. Endocr Rev 30, 241-63.

Bendall, S.C., Stewart, M.H., Menendez, P., George, D., Vijayaragavan, K., Werbowetski-Ogilvie, T., Ramos-Mejia, V., Rouleau, A., Yang, J., Bosse, M., Lajoie, G., Bhatia, M., 2007. IGF and FGF cooperatively establish the regulatory stem cell niche of pluripotent human cells in vitro. Nature 448, 1015-21.

Castilho, R.M., Squarize, C.H., Chodosh, L.A., Williams, B.O., Gutkind, J.S., 2009. mTOR mediates Wnt-induced epidermal stem cell exhaustion and aging. Cell Stem Cell 5, 279-89.

Ng, S.S., Mahmoudi, T., Danenberg, E., Bejaoui, I., de Lau, W., Korswagen, H.C., Schutte, M., Clevers, H., 2009. Phosphatidylinositol 3-kinase signaling does not activate the wnt cascade. J Biol Chem 284, 35308-13.